

Supporting Information  
©Wiley-VCH 2021  
69451 Weinheim, Germany

## Tacticity Control of Cyclic Poly(3-Thiobutyrate) Prepared by Ring-Opening Polymerization of Racemic $\beta$ -Thiobutyrolactone

Hui Li, Jérôme Ollivier, Sophie M. Guillaume,\* Jean-François Carpentier\*

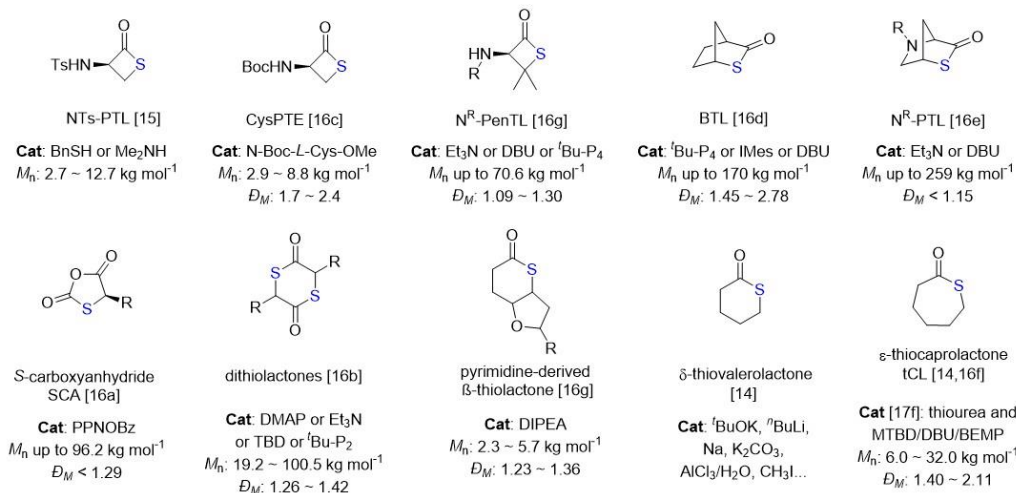
**Abstract:** We report here on the ring-opening polymerization (ROP) of racemic  $\beta$ -thiobutyrolactone (*rac*-TBL), as the first chemical synthesis of poly(3-thiobutyrolactone) (P3TB), the thioester analogue of the ubiquitous poly(3-hydroxybutyrate) (P3HB). The ROP reactions proceed very fast (TOF > 12,000 h<sup>-1</sup> at r.t.) in the presence of various metal-based catalysts. Remarkably, catalyst systems based on non-chiral yttrium complexes stabilized by tetradentate amino alkoxy- or diamino-bis(phenolate) ligands {ONXO<sup>R1,R2</sup>}<sup>2-</sup> (X = O, N) provide access to cyclic P3TB with either high isoselectivity ( $P_m$  up to 0.90) or high syndiotactic bias ( $P_r$  up to 0.70). The stereoselectivity can be controlled by manipulation of the substituents on the ligand platform and adequate choice of the reaction solvent and temperature as well. The cyclic polymer topology is evidenced by MALDI-ToF MS, NMR and TGA. Highly isotactic P3TB is a semi-crystalline material as revealed by DSC.

DOI: 10.1002/anie.2021XXXXX

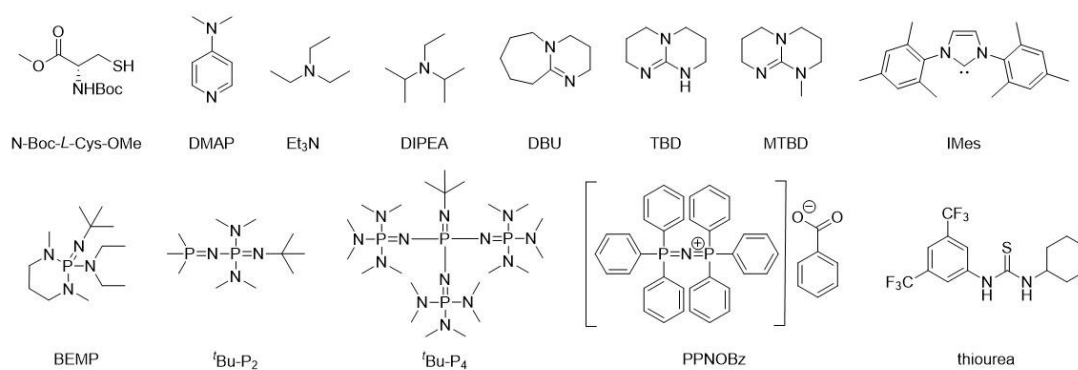
**Table of Contents**

- p. S3: Scheme S1: Thiolactones and organocatalysts reported for the ROP chemical synthesis of various polythioesters (PTEs).
- p. S4: Experimental Section – General considerations
- p. S5: Synthesis of *rac*- $\beta$ -thiobutyrolactone (*rac*-TBL)
- p. S8: Synthesis of (*S*)- $\beta$ -thiobutyrolactone ((*S*)-TBL)
- p. S11: General Polymerization Procedure
- p. S12:  $^1\text{H}$  and  $^{13}\text{C}$  NMR spectra of isolated P3TBs
- p. S13: MALDI-ToF mass spectra of isolated P3TBs
- p. S21: Representative SEC traces of P3TBs
- p. S26: Table S1. Influence of the solvent on the stereoselective ROP of *rac*-TBL promoted by complex **5k** without a co-initiator
- p. S27: Table S2. Influence of the solvent on the stereoselective ROP of *rac*-TBL promoted by the system **5c**/PrOH (1:1)
- p. S28: Determination of tacticity of P3TB by  $^{13}\text{C}$  NMR spectroscopy; representative carbonyl and methyl regions of the  $^{13}\text{C}$  NMR spectra of isotactic-enriched, atactic and syndiotactic-enriched P3TBs
- p. S50: Propagation statistics
- p. S51: Representative TGA thermograms and DSC curves of P3TBs
- p. S55: Structural parameters of  $\beta$ -thiobutyrolactone vs.  $\beta$ -butyrolactone

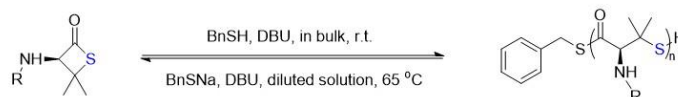
**Thiolactones:**



**Catalysts:**



ROP of a β-thiolactone and degradation back to the original monomer (Xiong *et. al.*, 2020, [17h]):



**Scheme S1.** Thiolactones and organocatalysts reported for the ROP chemical synthesis of various polythioesters (PTEs) (see references mentioned).

## Experimental Section

**General Considerations.** All syntheses and manipulations of air- and moisture-sensitive materials were carried out in flame-dried Schlenk-type glassware on a vacuum dual-manifold Schlenk line or in an argon-filled glovebox. HPLC-grade organic solvents were first purged extensively with nitrogen during filling 20-L solvent reservoirs, and then dried by passage through activated alumina [for dichloromethane] and through Q-5 supported copper catalyst [for toluene] stainless steel columns. *n*-Hexane, 1,4-dioxane, 2-methyl-tetrahydrofuran (2-MeTHF), tetrahydrofuran (THF), acetonitrile and toluene were degassed and dried over sodium/benzophenone followed by distillation under argon. *iso*-Propanol (*i*PrOH), benzyl alcohol (BnOH), isopropyl mercaptan (*i*PrSH), benzyl mercaptan (BnSH) were purified by distillation from CaH<sub>2</sub>. (SalBinam)AlO<sup>i</sup>Pr {SalBinam = *N,N*-bis(salicylidene)-1,1'-binaphthyl-2,2'-diamine} (**1**), (BDI)ZnN(SiMe<sub>3</sub>)<sub>2</sub> (**2a**), {Zn{N(SiMe<sub>3</sub>)<sub>2</sub>}<sub>2</sub> (**2b**), the amido yttrium-salan complex **4**, bisphenol {ONXO<sup>R2</sup>}H<sub>2</sub> proligands **a-I** and yttrium amide precursors were synthesized according to the methods reported in the literature.<sup>[1,2]</sup>

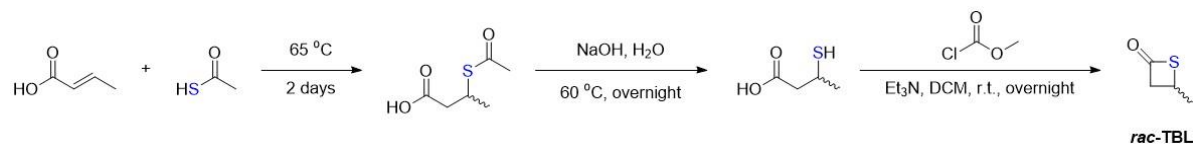
<sup>1</sup>H (500, 400 and 300 MHz), <sup>13</sup>C{<sup>1</sup>H} (125 and 100 MHz) and two-dimensional (2D) NMR spectra were recorded on Bruker Avance III HD 500, Av III 400 or Av III 300 spectrometers at 25 °C, fitted with direct broadband 5 mm probe heads (BBO/BBFO) carefully tuned on both <sup>1</sup>H and <sup>13</sup>C channels. 1D <sup>13</sup>C NMR spectra were acquired using Bruker standard zgpg30 sequence, acquisition time was 1.05 s and relaxation delay D1 5.00 s. Two-dimensional NMR experiments were acquired using standard pulse sequences (hsqcetdgtppisp2.3 with a selective <sup>13</sup>C refocussing pulse for band-selective HSQC experiments; shmbcctetgpl2nd for band-selective HMBC experiments), 2D spectra were processed using Topspin software (Bruker Biospin, Billerica, MA, USA) and analyzed in MestReNova 14.2.1 (Mestrelab Research S.L). The <sup>13</sup>C projections were prepared in Topspin software by summing F1 traces from the 2D HMBC and HSQC spectra across the region of interest.

Number and weight average molar mass ( $M_{n,SEC}$  and  $M_{w,SEC}$ ) and dispersity ( $D_M = M_w/M_n$ ) values of the polymers were determined by size-exclusion chromatography (SEC) in THF at 30 °C (flow rate = 1.0 mL min<sup>-1</sup>) on a Polymer Laboratories PL50 apparatus equipped with a refractive index detector and a set of two ResiPore PLgel 3 μm MIXED-D 300 × 7.5 mm columns. The polymer samples were dissolved in THF (2 mg mL<sup>-1</sup>). All elution curves were calibrated with polystyrene standards ( $M_n$  range = 580–126,000 g mol<sup>-1</sup>); the  $M_{n,SEC}$  values of the P3TB reported in all Tables are uncorrected for the possible difference in hydrodynamic radius *versus* that of polystyrene.

High resolution Matrix Assisted Laser Desorption Ionization – Time of Flight (MALDI-ToF) mass spectra were recorded using an ULTRAFLEX III TOF/TOF spectrometer (Bruker Daltonik GmbH, Bremen, Germany) in positive ionization mode at Centre Régional de Mesures Physiques de l'Ouest (CRMPO, ScanMAT UAR 2025 CNRS, Université de Rennes 1). Spectra were recorded using reflectron mode and an accelerating voltage of 25 kV. A mixture of a freshly prepared solution of the polymer in CH<sub>2</sub>Cl<sub>2</sub> (HPLC grade) and DCTB (*trans*-2-(3-(4-*tert*-butylphenyl)-2-methyl-2-propenylidene) malononitrile in CH<sub>2</sub>Cl<sub>2</sub> (HPLC grade, 10 mg mL<sup>-1</sup>), and a MeOH or CH<sub>2</sub>Cl<sub>2</sub>/CH<sub>3</sub>CN (50:50, *v/v*) solution of the cationizing agent (NaI, 10 mg mL<sup>-1</sup>) were prepared. The solutions were combined in a 1:1:1 (*v/v/v*) ratio of matrix-to-sample-to-cationizing agent. The resulting solution (0.25–0.5 μL) was deposited onto the sample target (Prespotted AnchorChip PAC II 384/96 HCCA) and air or vacuum dried. High resolution mass spectrum of *rac*-TBL (Figure S5) was performed using a time-of-flight Maxis 4G (Bruker Daltonik GmbH, Bremen, Germany) in ASAP (direct introduction, desorption temperature: 45 °C) positive mode at the Centre Régional de Mesures Physiques de l'Ouest (CRMPO, ScanMAT, Université de Rennes1).

Melting-transition ( $T_m$ ) and glass-transition ( $T_g$ ) temperatures were measured by differential scanning calorimetry (DSC) on a DSC2500, TA Instrument. All  $T_m$  and  $T_g$  values were obtained from the second heating run. The first heating rate was 10 °C min<sup>-1</sup>, while the cooling rate was 10 °C min<sup>-1</sup> and the second heating rate was 10 °C min<sup>-1</sup>. The onset decomposition temperatures ( $T_d$ , defined as the temperature for 5% weight loss) of the polymers were measured by thermal gravimetric analysis (TGA) on a Mettler-Toledo TGA-DSC-1 apparatus under dry nitrogen flow. Polymer samples were heated from ambient temperatures to 500 °C at a rate of 10 °C min<sup>-1</sup>.

**Synthesis of *rac*- $\beta$ -thiobutyrolactone (*rac*-TBL).** The synthesis of *rac*-TBL relies on the cyclization of  $\beta$ -thiobutyric acid, initially prepared by the addition reaction of crotonic acid with thioacetic acid (Scheme S2), following optimization of literature procedures (see below).



**Scheme S2.** Synthesis of *rac*- $\beta$ -TBL.

**Synthesis of 3-thiobutyric acid.**<sup>[3]</sup> Crotonic acid (Thermo Fisher Scientific, 84 g, 1.0 mol) and thioacetic acid (TCI, 83.6 g, 1.1 mol) were placed in a round-bottom flask (1 L). The resulting mixture was heated up to 65 °C for 2 days. The crude product containing 3-acetylthiobutyric acid was treated with NaOH (500 mL of a 3 M aqueous solution, 1.5 mol) overnight. The resulting solution was acidified with HCl (ca. 300 mL of a 2.5 M aqueous solution, 0.75 mol) until pH = 3 and extracted with diethyl ether (2  $\times$  500 mL). The organic phase was dried over anhydrous Na<sub>2</sub>SO<sub>4</sub>, the solvent was removed under reduced pressure, and the residue was purified by distillation under vacuum (ca. 400 mTorr) at 95 °C, to give 3-thiobutyric acid, as a yellowish liquid (96.9 g, 81% yield). <sup>1</sup>H NMR (300 MHz, CDCl<sub>3</sub>, 25 °C, Figure S1):  $\delta$  (ppm) 11.35 (s, 1H, COOH), 3.30–3.44 (dq,  $J$  = 14 and 7 Hz, 1H, CH), 2.58–2.73 (m, 2H, CH<sub>2</sub>), 1.86 (d,  $J$  = 7 Hz, 1H, SH), 1.41 (d,  $J$  = 7 Hz, 3H, CH<sub>3</sub>). <sup>13</sup>C{<sup>1</sup>H} NMR (101 MHz, CDCl<sub>3</sub>, 25 °C, Figure S2):  $\delta$  (ppm) 177.83 (CO), 45.72 (CH<sub>2</sub>), 30.97 (CH), 24.92 (CH<sub>3</sub>).

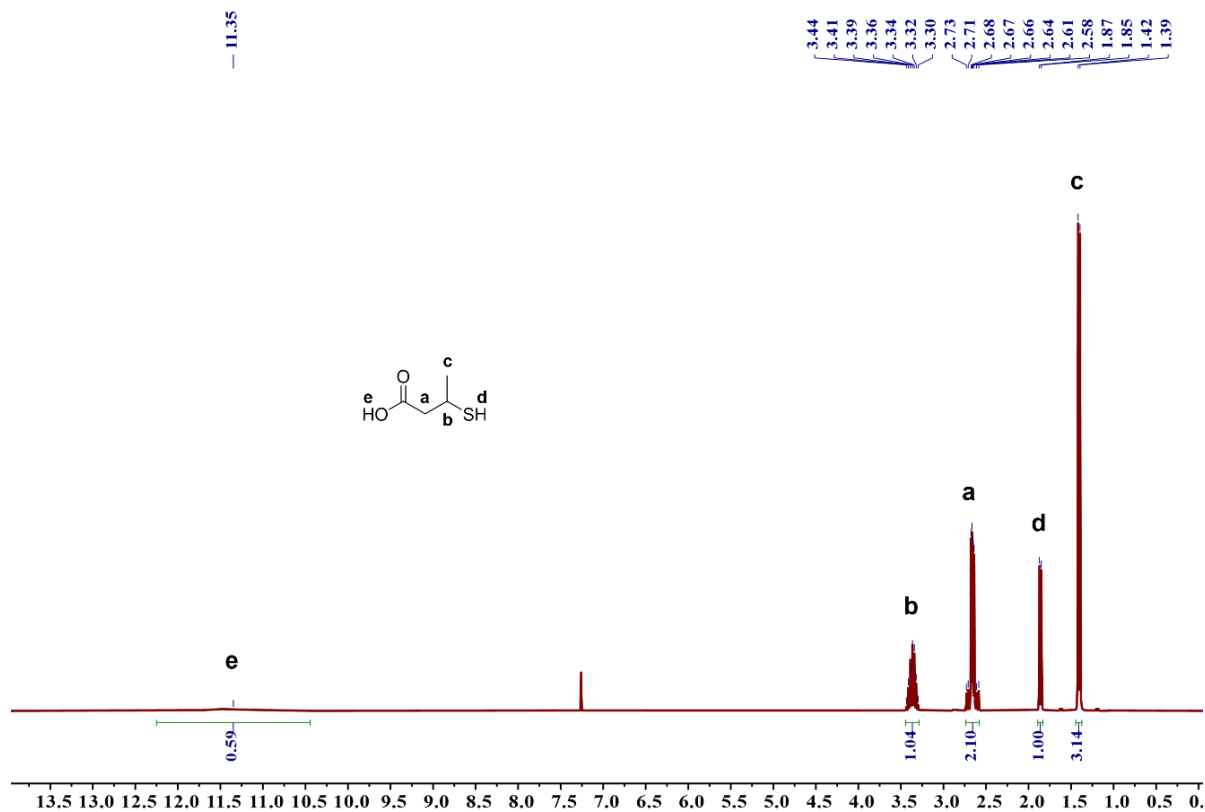


**Figure S1.** <sup>1</sup>H NMR spectrum (300 MHz, CDCl<sub>3</sub>, 25 °C) of 3-thiobutyric acid.

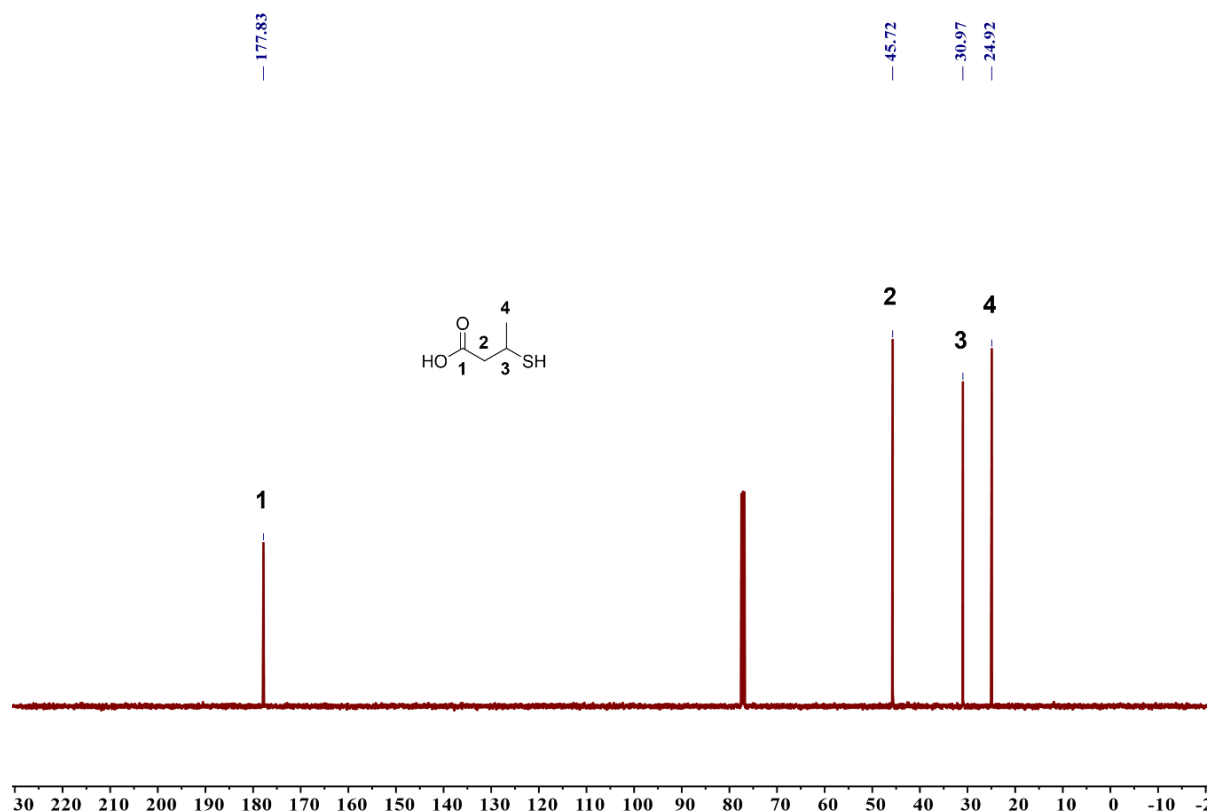


**Figure S2.**  $^{13}\text{C}\{^1\text{H}\}$  NMR spectrum (100 MHz,  $\text{CDCl}_3$ , 25 °C) of 3-thiobutyric acid.

**Synthesis of *rac*- $\beta$ -thiobutyrolactone (*rac*-TBL).** Racemic  $\beta$ -thiobutyrolactone (*rac*-TBL) was then synthesized using a modified (optimization of the purification procedure) literature procedure.<sup>[4]</sup> Methyl chloroformate (21.5 mL, 0.275 mmol) was added dropwise at 0 °C to a solution of 3-thiobutyric acid (26.4 mL, 0.25 mol) and triethylamine (38.4 mL, 0.275 mol) in dry dichloromethane (350 mL). Once the addition was completed, the reaction mixture was warmed to room temperature and stirred until evolution of  $\text{CO}_2$  ceased. The resulting mixture was washed with water (2  $\times$  100 mL), saturated  $\text{NaHCO}_3$  (250 mL), brine (250 mL) and the separated organic layer was dried over  $\text{MgSO}_4$  and rotavapored under reduced pressure. The residue was purified by distillation using the Glass Oven B-585 under vacuum twice (35 °C, 500 mTorr) to give pure *rac*-TBL as a colorless liquid (6.5 g, 26% yield, Caution: *rac*-TBL will degrade or polymerize spontaneously if purified by column chromatography on silica or neutral alumina).  $^1\text{H}$  NMR (400 MHz,  $\text{CDCl}_3$ , 25 °C, Figure S3):  $\delta$  (ppm) 4.10 (dd,  $J = 17$  and 7 Hz, 1H, *CHH*), 3.72 (pd,  $J = 7$  and 4 Hz, 1H, *CH*), 3.52 (dd,  $J = 17$  and 4 Hz, 1H, *CHH*), 1.67 (d,  $J = 7$  Hz, 3H, *CH*<sub>3</sub>).  $^{13}\text{C}\{^1\text{H}\}$  NMR (125 MHz,  $\text{CDCl}_3$ , 25 °C, Figure S4):  $\delta$  (ppm) 190.43 (CO), 62.88 (*CH*<sub>2</sub>), 28.10 (*CH*), 23.78 (*CH*<sub>3</sub>). HRMS (ESI, Figure S5): calculated for  $\text{C}_4\text{H}_6\text{SO}$  [ $\text{M}$ ]<sup>+</sup>  $m/z = 103.0212$ ; found: 103.0212.

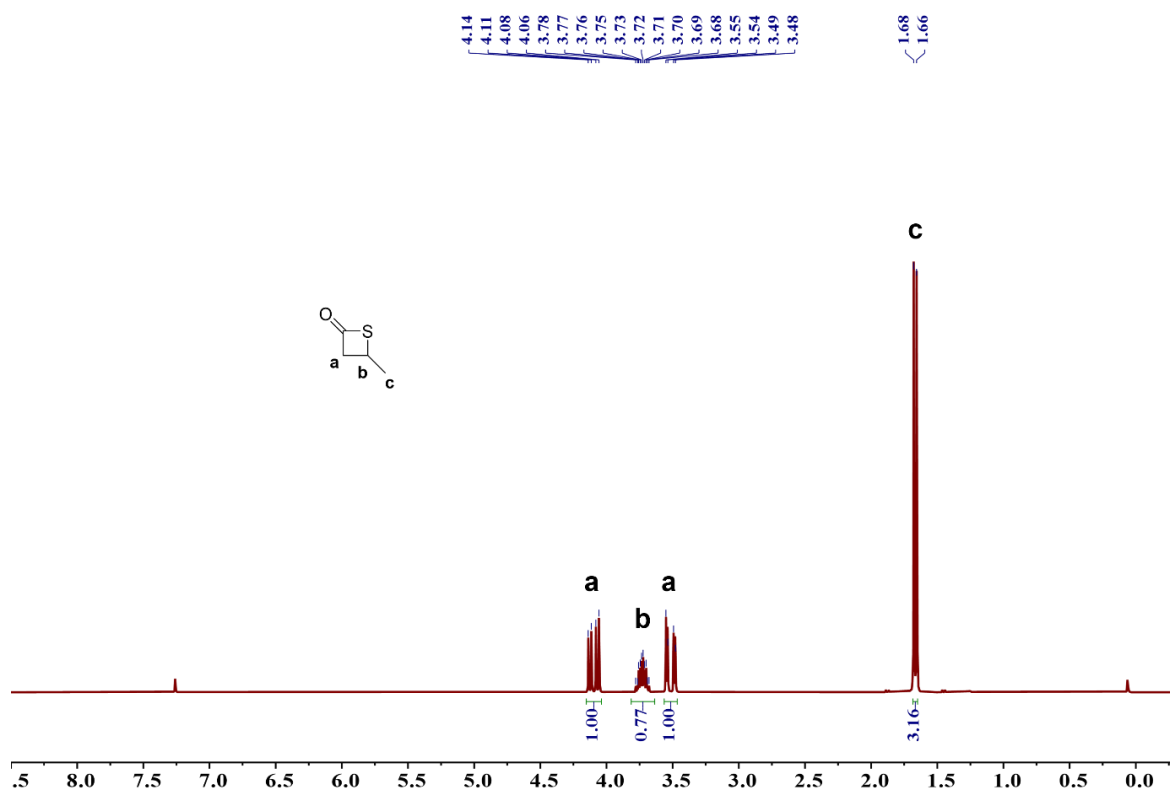


**Figure S3.**  $^1\text{H}$  NMR spectrum (300 MHz,  $\text{CDCl}_3$ , 25  $^\circ\text{C}$ ) of *rac*- $\beta$ -thiobutyrolactone (*rac*-TBL); the weak signal at 0.06 ppm is silicone grease.

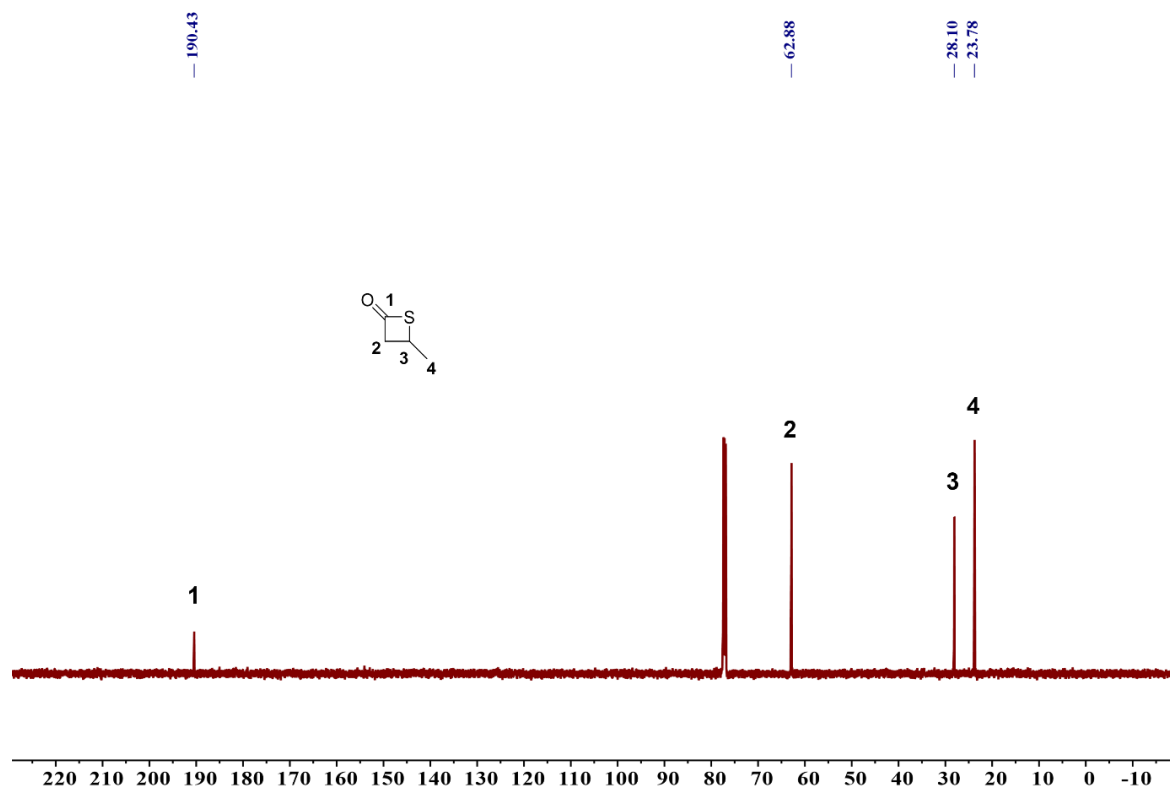


**Figure S4.**  $^{13}\text{C}\{^1\text{H}\}$  NMR spectrum (125 MHz,  $\text{CDCl}_3$ , 25  $^\circ\text{C}$ ) of *rac*- $\beta$ -thiobutyrolactone (*rac*-TBL).

Centre régional de mesures physiques de l'Ouest (CRMPO) - RAPPORT D'ANALYSE

Analysis Info

Analysis Name D:\Data\CRMPO\ASAP\_11061\_MS\_01.d  
 Method ASAP\_CRMPO\_tune\_low.m  
 Sample Name HL 270  
 Comment H. LI HL 270 Température : 45°C

Acquisition Date 7/16/2020 8:27:16 PM

Operator Philippe JÉHAN  
 Instrument maXis

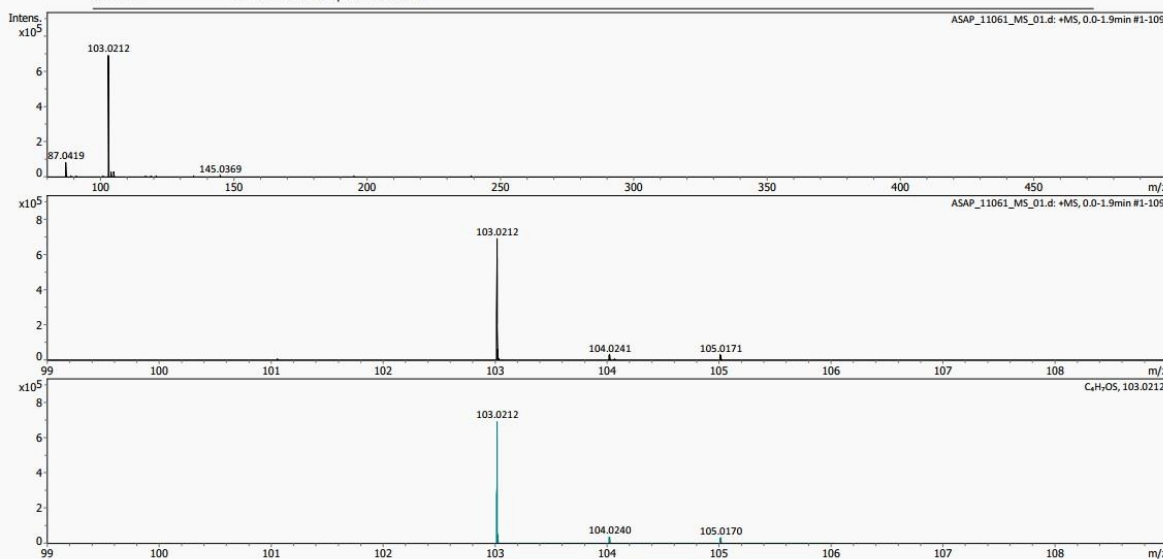
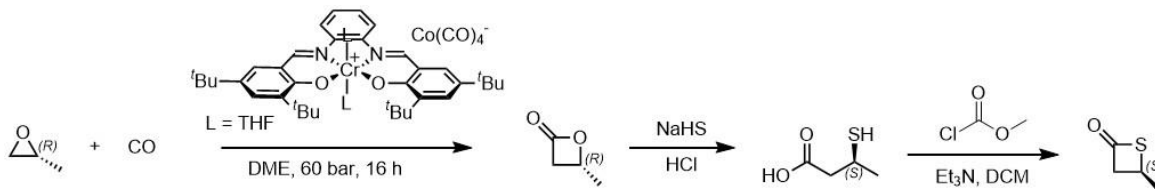


**Figure S5.** HRMS spectra of *rac*-TBL. Top: ESI mass spectrum of *rac*-TBL; middle: zoomed spectrum of top spectrum (ca. 104 *m/z*); bottom: simulated spectrum of *rac*-TBL.

**Synthesis of (S)- $\beta$ -thiobutyrolactone ((S)-TBL).** The fundamental steps involved in the synthesis of monomer (S)-TBL are depicted in Scheme S3. It relies on the cyclization of enantiomerically pure  $\beta$ -thiobutyric acid, initially prepared from (*R*)- $\beta$ -butyrolactone.



**Scheme S3.** Synthesis of enantiomerically pure (S)-TBL.

**Synthesis of (*R*)- $\beta$ -butyrolactone ((*R*)-BL):** (*R*)- $\beta$ -Butyrolactone was synthesized using a modified literature procedure (reaction conducted at higher pressure, i.e. 60 bars instead of 1 bar).<sup>[5]</sup> In the glovebox, a Schlenk flask was charged with [salph(Cr(THF)<sub>2</sub>)]<sup>+</sup>[Co(CO)<sub>4</sub>]<sup>-</sup> (520 mg, 0.57 mmol). On a Schlenk line, dry DME (10 mL) was syringed into the reaction flask and the resulting solution was cannulated into a degassed high-pressure reactor which was then pressurized with carbon monoxide to 30 bars, followed by stirring for 15 min before depressurization. A solution of (*R*)-propylene oxide (Acros Organics, 98% ee, 15 mL, 0.22 mol) in dry DME (5 mL) was then transferred into the reactor which was then pressurized with CO to 60 bars. The reaction mixture was stirred overnight at 23 °C. The reactor was vented to atmospheric pressure, volatiles were removed under vacuum and the crude product was purified by distillation at 40 °C to afford (*R*)-BL as a colorless viscous liquid (4.6 g, 26% yield). <sup>1</sup>H NMR (400 MHz, CDCl<sub>3</sub>, 25 °C, Figure S6):  $\delta$  (ppm) 4.74–4.67 (m, 1H, CH), 3.60–3.54 (m, 1H, CHH), 3.06 (dd, *J* = 16 and 4 Hz, 1H, CHH), 1.57 (d, *J* = 6 Hz, 3H, CH<sub>3</sub>). <sup>13</sup>C{<sup>1</sup>H} NMR (100 MHz, CDCl<sub>3</sub>, 25 °C, Figure S7):  $\delta$  (ppm) 168.17 (CO), 68.02 (CH<sub>2</sub>), 44.43 (CH), 20.71 (CH<sub>3</sub>).



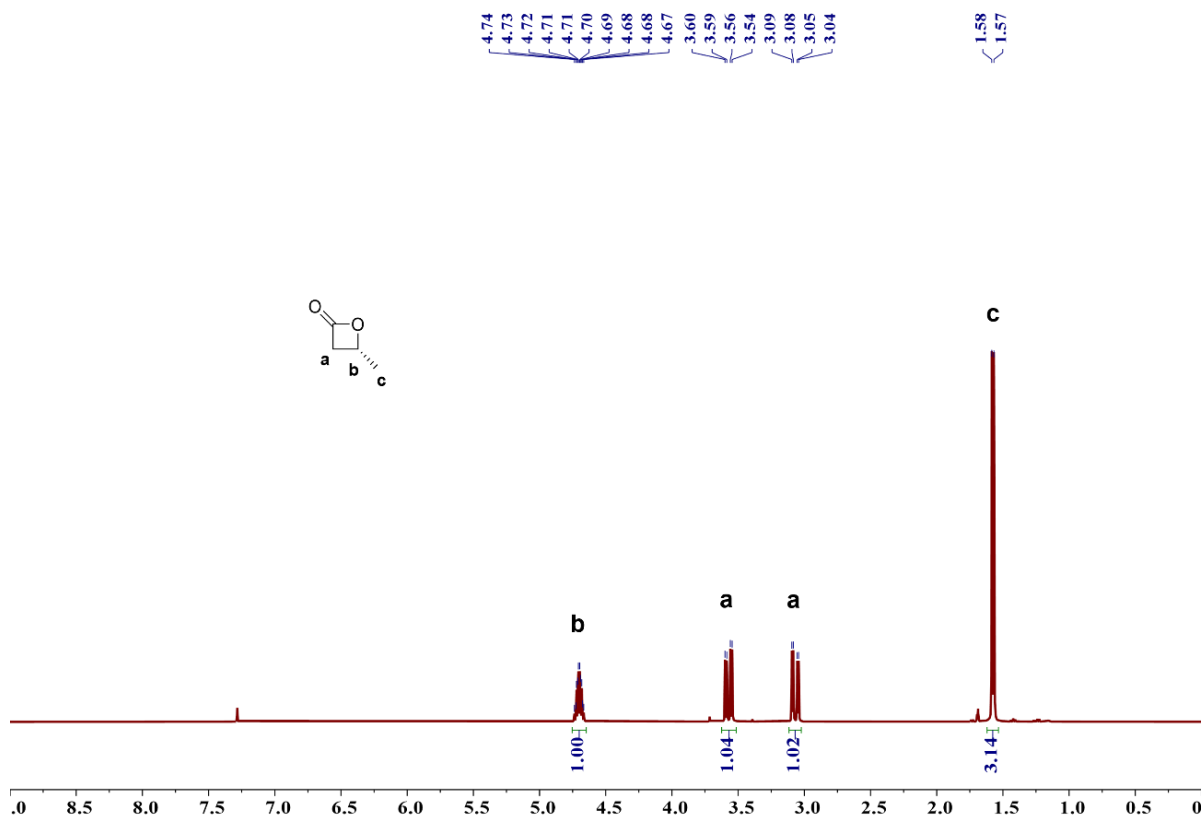


**Figure S6.** <sup>1</sup>H NMR spectrum (400 MHz, CDCl<sub>3</sub>, 25 °C) of (R)-β-butyrolactone.

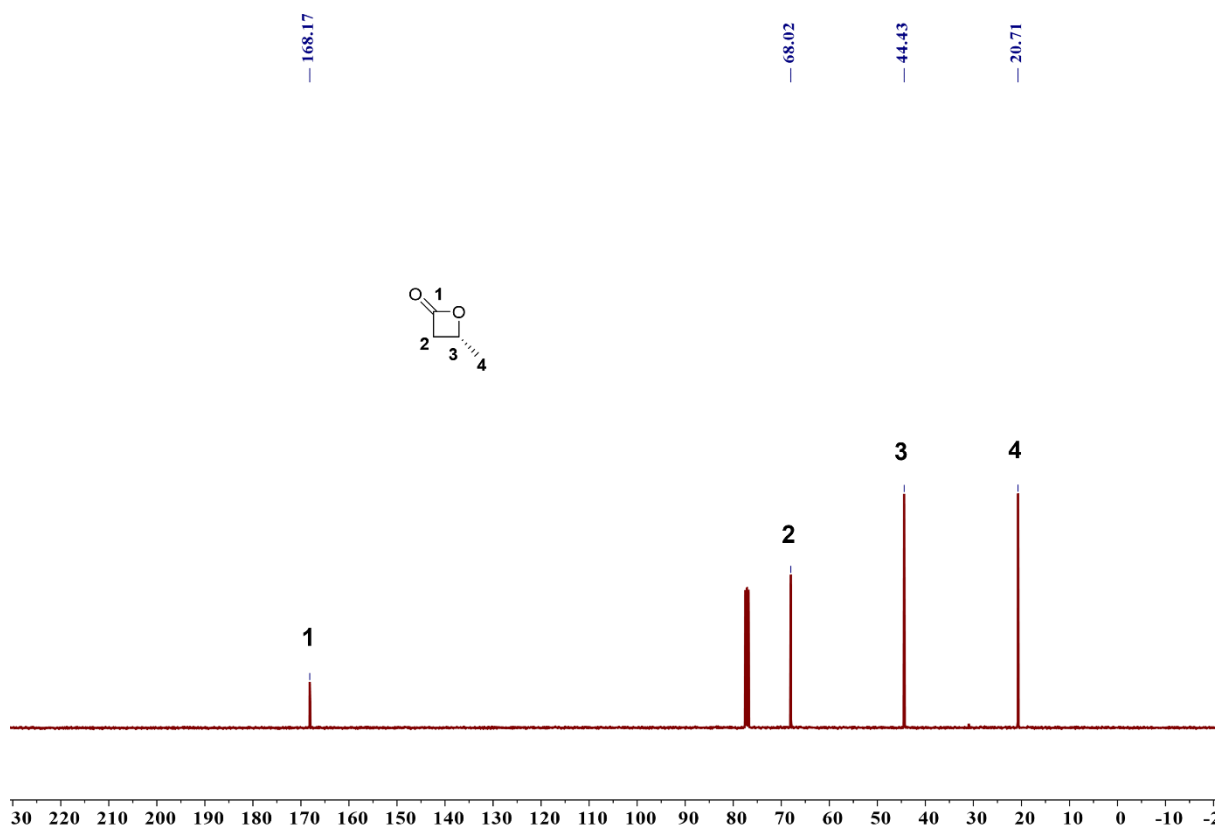


**Figure S7.** <sup>13</sup>C{<sup>1</sup>H} NMR spectrum (100 MHz, CDCl<sub>3</sub>, 25 °C) of (R)-β-butyrolactone.

**Synthesis of (S)- $\beta$ -thiobutyrolactone ((S)-TBL).** (S)-3-Thiobutyric acid was synthesized using a literature procedure.<sup>[6]</sup> (R)-BL (7.54 g, 87.6 mmol) was added dropwise at 0 °C to a solution of NaSH·H<sub>2</sub>O (5.06 g, 90.2 mmol) in water (90 mL). The mixture was then stirred for 1 h at 0 °C and for 24 h at 23 °C. Then, HCl (2.4 N aqueous solution) was added to adjust the pH  $\approx$  2 and the mixture was extracted with Et<sub>2</sub>O (3  $\times$  150 mL). The resulting organic phase was dried over MgSO<sub>4</sub>, the solvent was removed under reduced pressure and the residue was distilled to give a ca. 2:1 mixture of (S)-3TBA and (R)-3HBA isolated as a colorless liquid (3.90 g, ca. 38% yield). This mixture of the two compounds was dissolved in a solution of triethylamine (3.6 mL, 0.036 mol) in dry dichloromethane (50 mL), and methyl chloroformate (2.8 mL, 0.036 mol) was then added dropwise at 0 °C. Once the addition was completed, the reaction mixture was warmed to room temperature and stirred until evolution of CO<sub>2</sub> ceased. The resulting mixture was washed with water (2  $\times$  30 mL), saturated NaHCO<sub>3</sub> (50 mL), brine (50 mL); the separated organic layer was dried over MgSO<sub>4</sub> and rotavapored under reduced pressure. Ultimately, (S)-TBL was isolated as described above for *rac*-TBL and recovered as a colorless liquid (335 mg, 3.3 mmol, 10% yield); NMR characteristics are identical to those of *rac*-TBL. <sup>1</sup>H NMR (500 MHz, CDCl<sub>3</sub>, 25 °C, Figure S8):  $\delta$  (ppm) 4.10 (dd, *J* = 17 and 7 Hz, 1H, *CHH*), 3.72 (pd, *J* = 7 and 4 Hz, 1H, *CH*), 3.52 (dd, *J* = 17 and 4 Hz, 1H, *CHH*), 1.67 (d, *J* = 7 Hz, 3H, CH<sub>3</sub>).

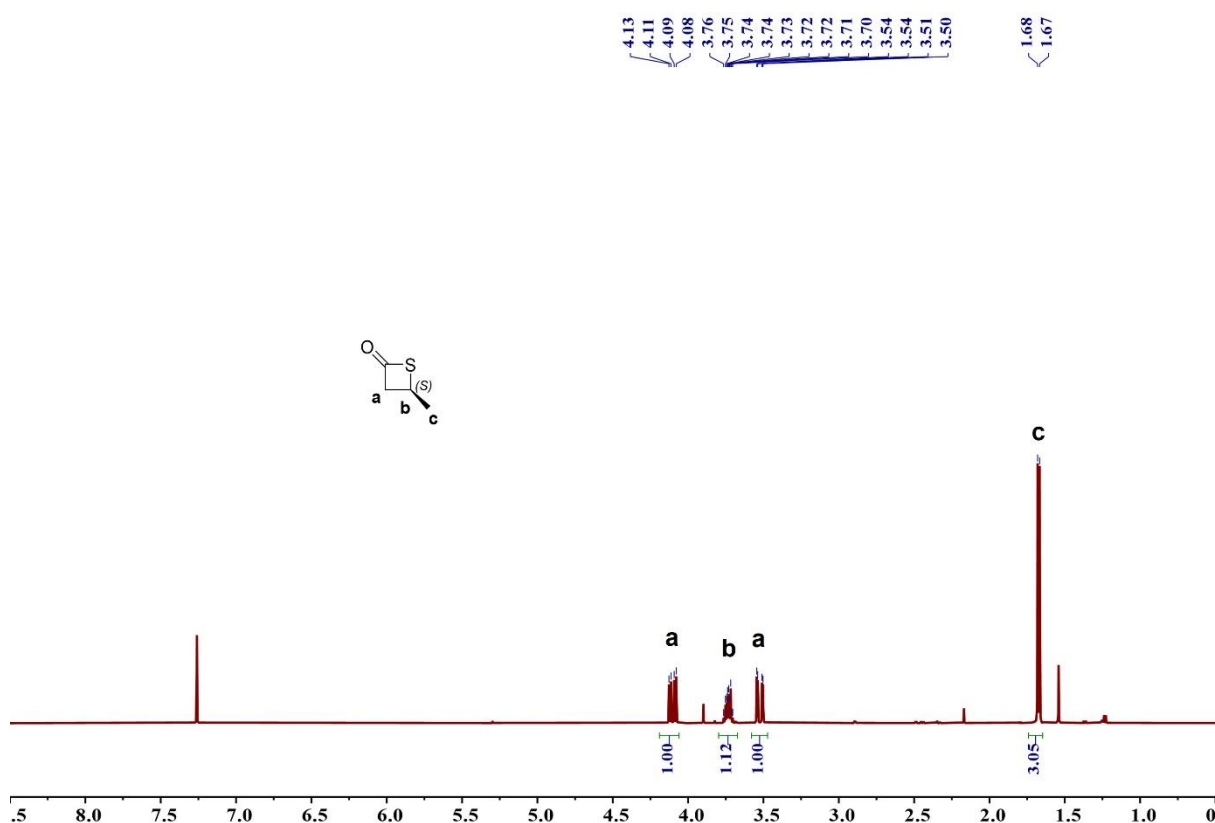


**Figure S8.** <sup>1</sup>H NMR spectrum (500 MHz, CDCl<sub>3</sub>, 25 °C) of (S)-TBL; the weak signals at  $\delta$  2.18 and 1.56 ppm correspond to residual acetone and water, respectively.

**General Polymerization Procedure.** In the glovebox, a Schlenk flask was charged with  $[\text{Y}(\text{N}(\text{SiHMe}_2)_2)_3](\text{THF})_2$  (6.3 mg, 10  $\mu\text{mol}$ ) and the desired  $\{\text{ONXO}^{\text{R}2}\}_2\text{H}_2$  proligand (10  $\mu\text{mol}$ ), and toluene (0.88 mL) was added. To this solution, in the glove box,  $i\text{PrOH}$  (10  $\mu\text{mol}$ , 38  $\mu\text{L}$  of a 2% (*v/v*) solution in toluene) was added under stirring at 14 °C. After 5 min, *rac*-TBL (102 mg, 1.0 mmol, 100 *equiv.* vs.  $\text{Y}$ ) was added rapidly. After the desired period, the polymerization was quenched by addition of benzoic acid (0.5 mL of 10 mg  $\text{mL}^{-1}$  solution in  $\text{CHCl}_3$ ). An aliquot (0.1 mL) of the reaction mixture was used to determine the monomer conversion by  $^1\text{H}$  NMR analysis. The resulting mixture was then concentrated to dryness under vacuum, and the resulting crude polymer was subsequently dissolved in  $\text{CH}_2\text{Cl}_2$  (*ca.* 2 mL) and precipitated in pentane (*ca.* 50 mL, not cooled), filtered, and dried in a vacuum oven at room temperature till constant weight. The P3TB polymer was recovered as a white powder, and analyzed by NMR spectroscopy and SEC. Pure isotactic P3TB was prepared from ROP of (*S*)-TBL (50 *equiv.*) with the **5a**/ $i\text{PrOH}$  (1:1) system in toluene at room temperature ( $P_m > 0.95$ ,  $M_n = 3.2 \text{ kg mol}^{-1}$ ,  $D_M = 1.52$ ).

**$^1\text{H}$  and  $^{13}\text{C}$  NMR spectra of isolated P3TBs**

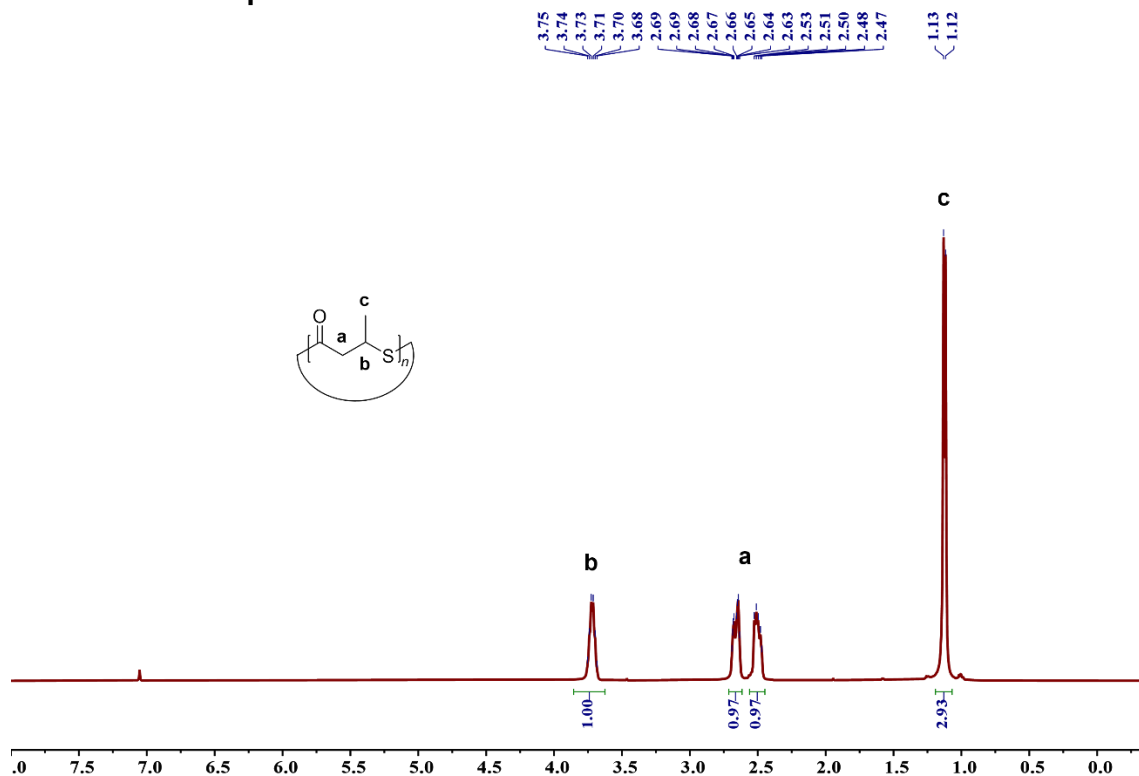


**Figure S9.**  $^1\text{H}$  NMR spectrum (500 MHz,  $\text{CDCl}_3$ , 25  $^\circ\text{C}$ ) of an isolated cyclic P3TB produced by the system **5a**/PrOH (100:1:1, r.t., toluene, entry 17).

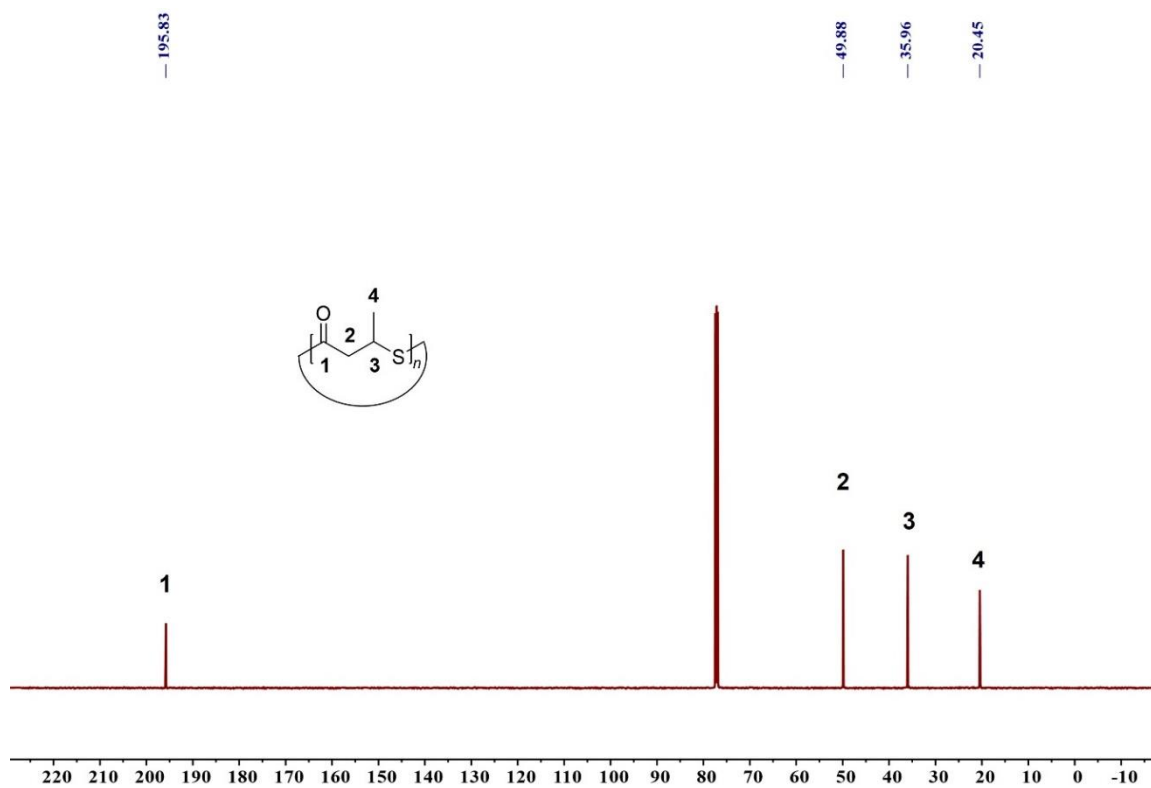


**Figure S10.**  $^{13}\text{C}\{^1\text{H}\}$  NMR spectrum (125 MHz,  $\text{CDCl}_3$ , 25  $^\circ\text{C}$ ) of an isolated cyclic P3TB produced by the system **5a**/PrOH (100:1:1, r.t., toluene, entry 17).

## MALDI-ToF mass spectra of isolated P3TBs

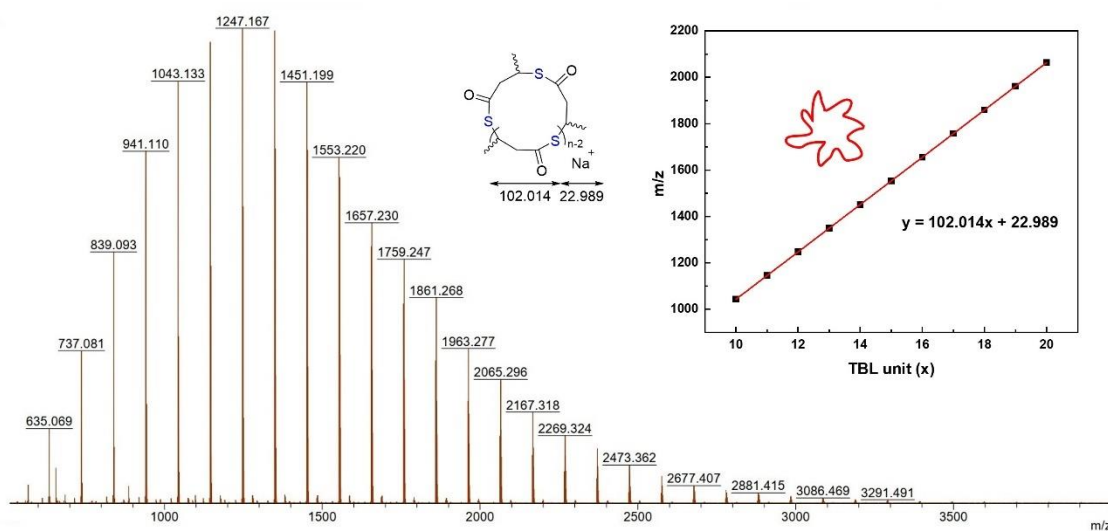


**Figure S11.** MALDI-ToF mass spectrum of a cyclic P3TB produced by the system  $Y\{ONNO^{Bu_2}\}\{N(SiHMe_2)_2\}(THF)$  (**5a**) /  $^iPrOH$  (1:1) in toluene (Table 1, entry 12), with a plot of experimental  $m/z$  values vs. theoretical number of TBL repeat units. For  $n = 12$ ,  $m/z$  exp = 1247.167 vs.  $m/z$  theo = 1247.156 for  $\{[C_4H_6OS]_{12}+Na\}^+$ .

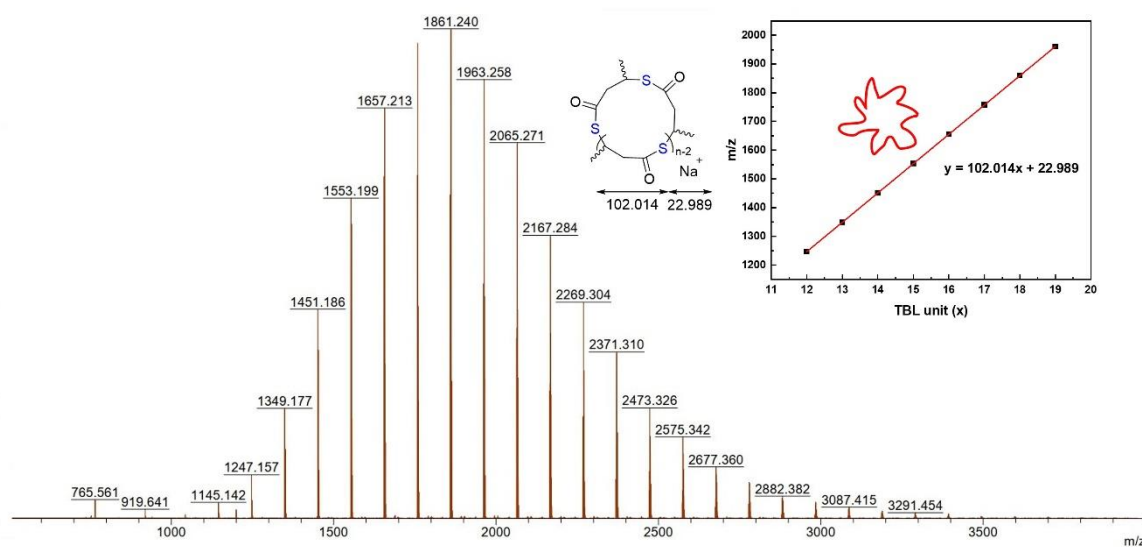


**Figure S12.** MALDI-ToF mass spectrum of a cyclic P3TB produced by the system  $Y\{ONNO^{Bu_2}\}\{N(SiHMe_2)_2\}(THF)$  (**5a**) /  $^iPrSH$  (1:1) in toluene (Table 1, entry 13), with a plot of experimental  $m/z$  values vs. theoretical number of TBL repeat units. For  $n = 18$ ,  $m/z$  exp = 1859.246 vs.  $m/z$  theo = 1859.240 for  $\{[C_4H_6OS]_{18}+Na\}^+$ .

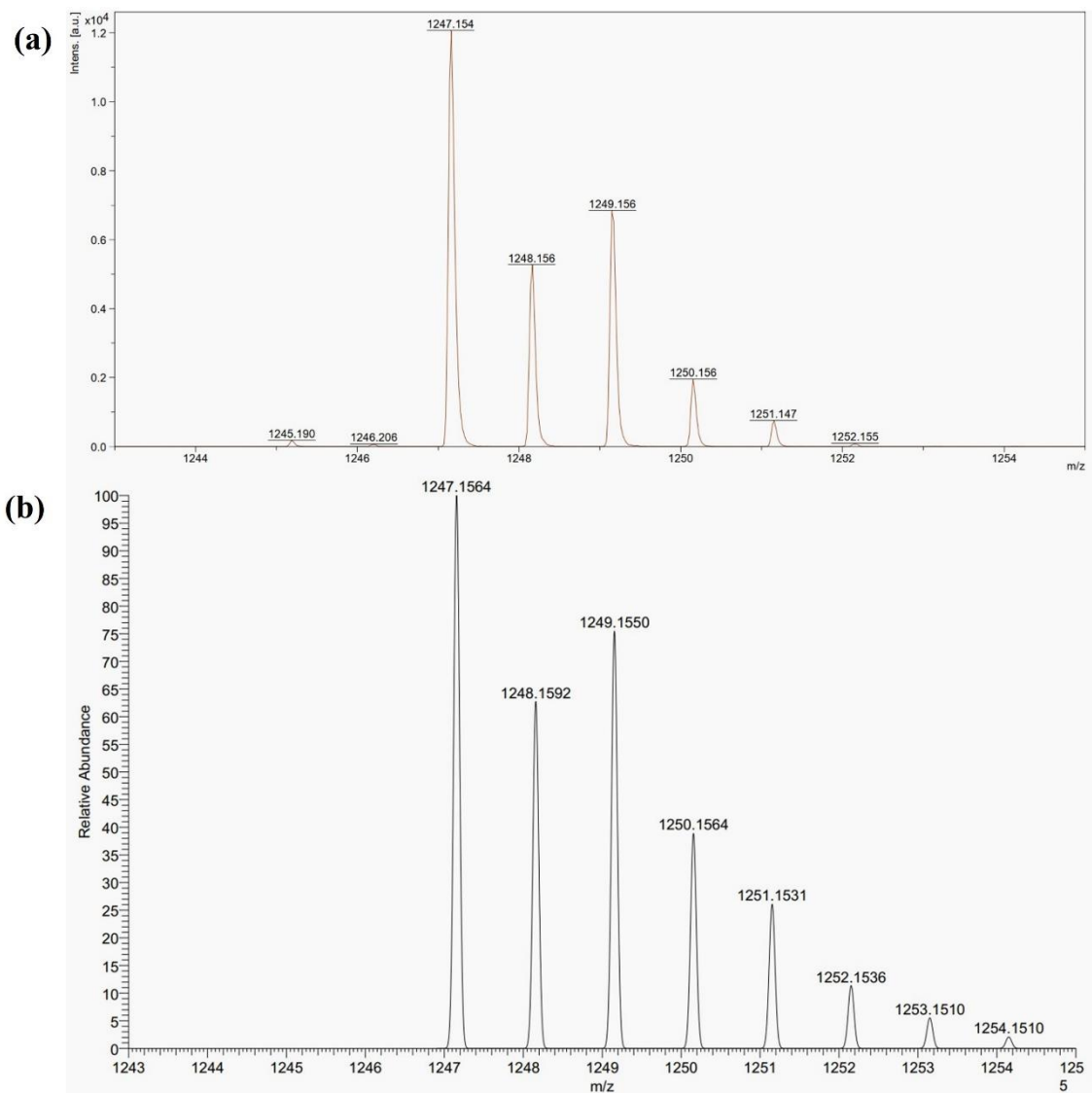


**Figure S13.** Details (isotopic distribution) of the MALDI-ToF mass spectrum of a cyclic P3TB produced by  $Y\{ONNO^{tBu2}\}N(SiHMe_2)_2(THF)$  (**5a**) in toluene in the absence of co-initiator, showing the isotopic distribution for macromolecules  $[C_4H_6SO]_{12}+Na^+$ : a) experimental spectrum (Table 1, entry 10); b) calculated spectrum.

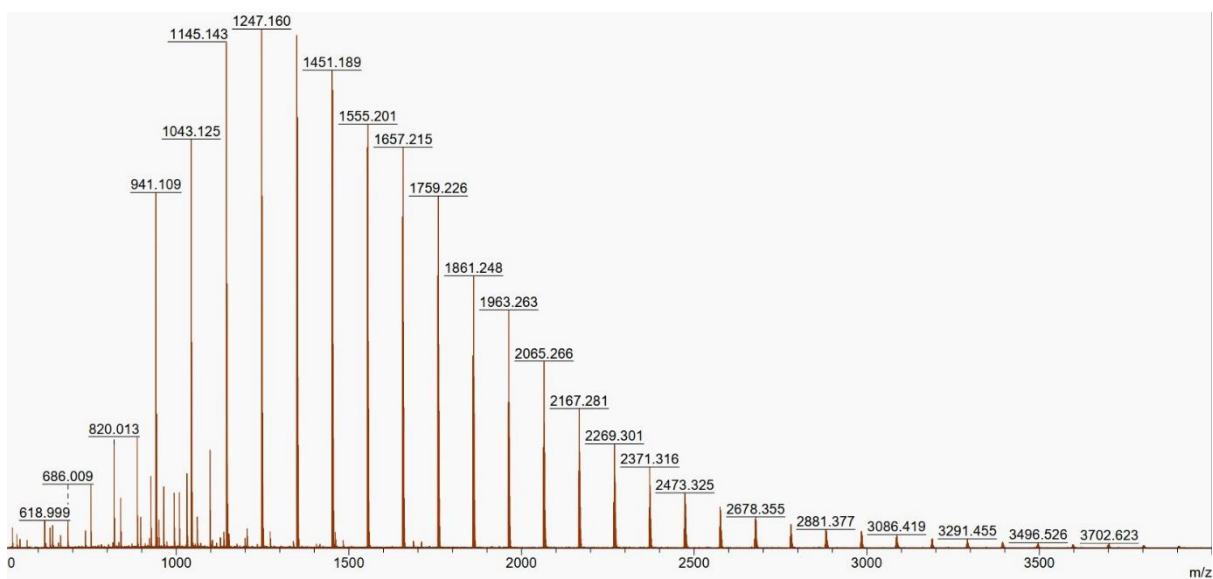


**Figure S14.** MALDI-ToF mass spectrum of a cyclic P3TB produced by  $Y\{\text{ONNO}^{\text{IBu}_2}\}\{\text{N}(\text{SiHMe}_2)_2\}(\text{THF})$  (**5a**) in THF in the absence of co-initiator (25:1:0, at r.t., in THF, 1 min, conv = 99%). For  $n = 12$ ,  $m/z$  exp = 1247.160 vs.  $m/z$  theo = 1247.156 for  $\{[\text{C}_4\text{H}_6\text{OS}]_{12}+\text{Na}\}^+$ .

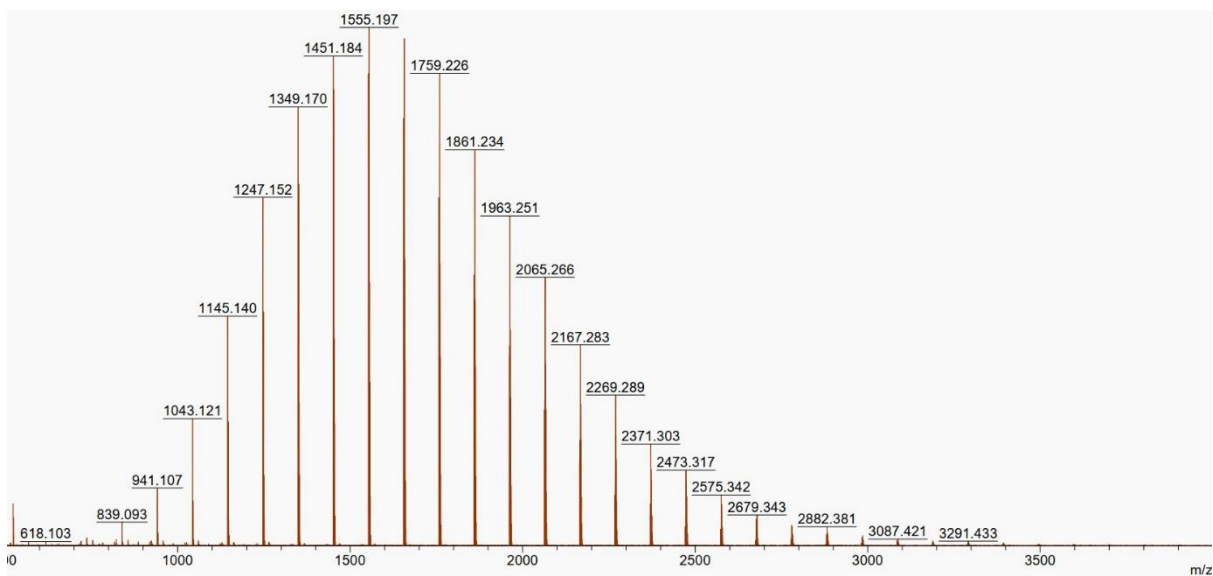


**Figure S15.** MALDI-ToF mass spectrum of a cyclic P3TB produced by  $Y\{\text{ONNO}^{\text{Cl}_2}\}\{\text{N}(\text{SiHMe}_2)_2\}(\text{THF})$  (**5k**) in THF in the absence of co-initiator (25:1:0, at r.t., 1 min, conv = 99%,  $M_{n,\text{SEC}} = 4100 \text{ g mol}^{-1}$ ,  $D_M = 1.72$ ). For  $n = 15$ ,  $m/z$  exp = 1553.194 vs.  $m/z$  theo = 1553.198 for  $\{[\text{C}_4\text{H}_6\text{OS}]_{15}+\text{Na}\}^+$ .

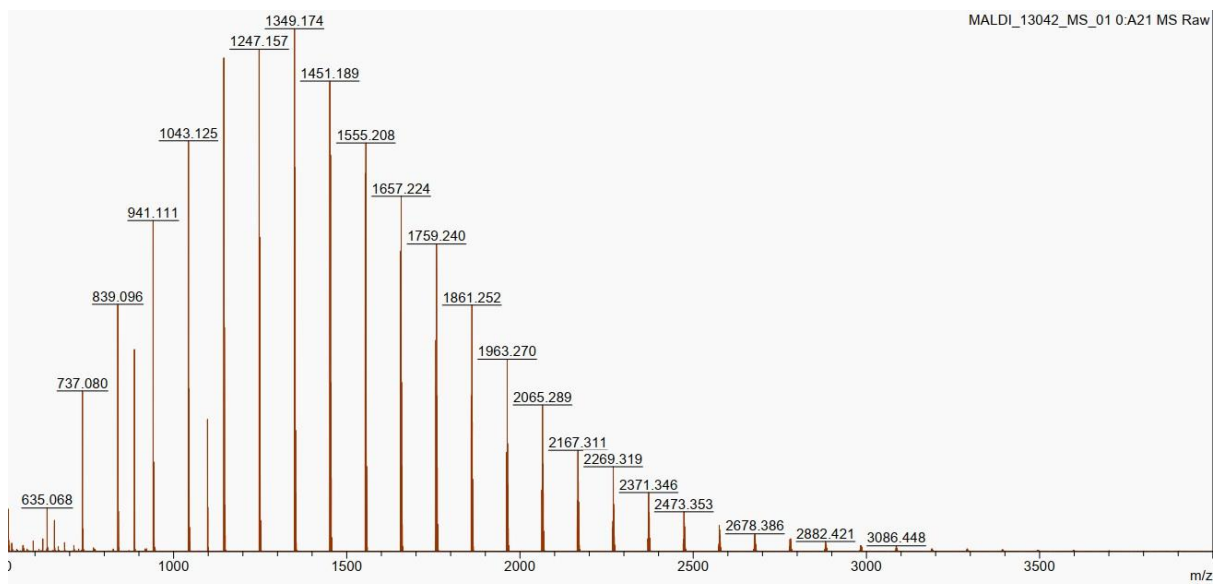


**Figure S16.** MALDI-ToF mass spectrum of a cyclic P3TB produced by  $Y\{ONNO^{Cl_2}\}_2\{N(SiHMe_2)_2\}(THF)$  (**5k**) in THF in the absence of co-initiator (25:1:0, at r.t., 1 min, conv = 99%). For  $n = 13$ ,  $m/z$  exp = 1349.174 vs.  $m/z$  theo = 1349.170 for  $\{[C_4H_6OS]_{13}+Na\}^+$ .



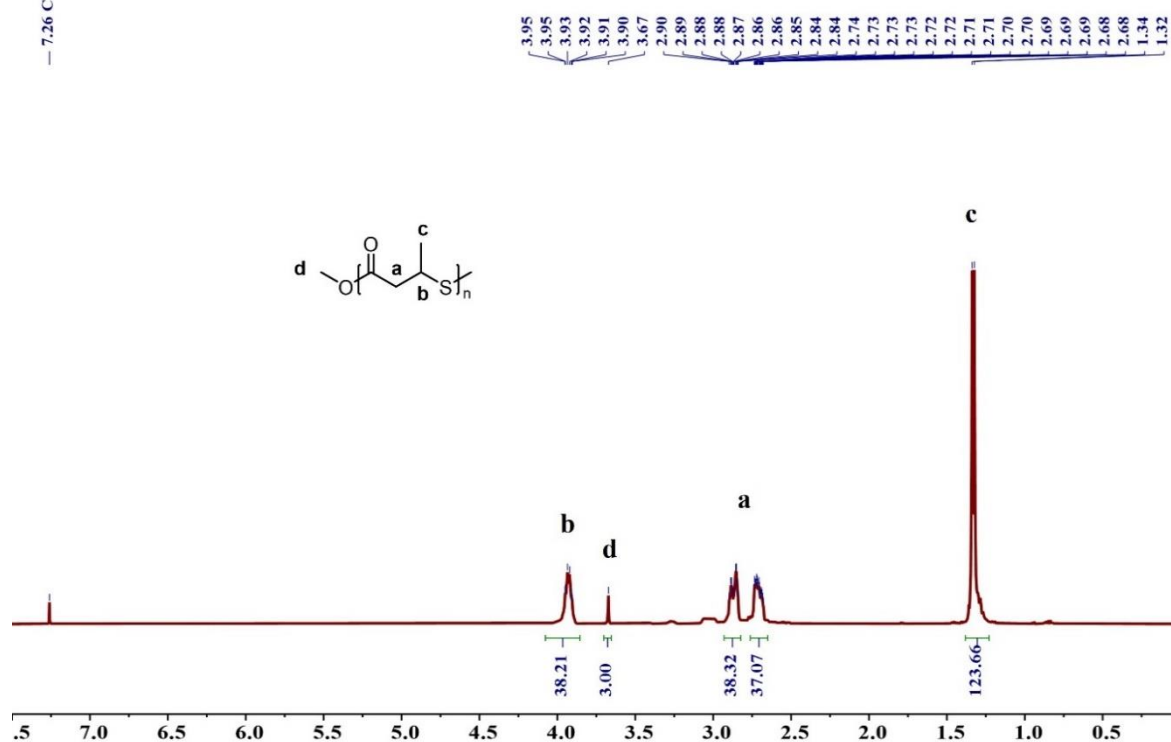


**Figure S17.** <sup>1</sup>H NMR spectrum (400 MHz, CDCl<sub>3</sub>, 25 °C) of an isolated P3TB (at least in part linear) produced by the NaOMe system (23:1, r.t., C<sub>6</sub>D<sub>6</sub>; Table 1, entry 1; *DP*<sub>n,NMR</sub> = ca. 38; *M*<sub>n,NMR</sub> = ca. 3900 g mol<sup>-1</sup>).

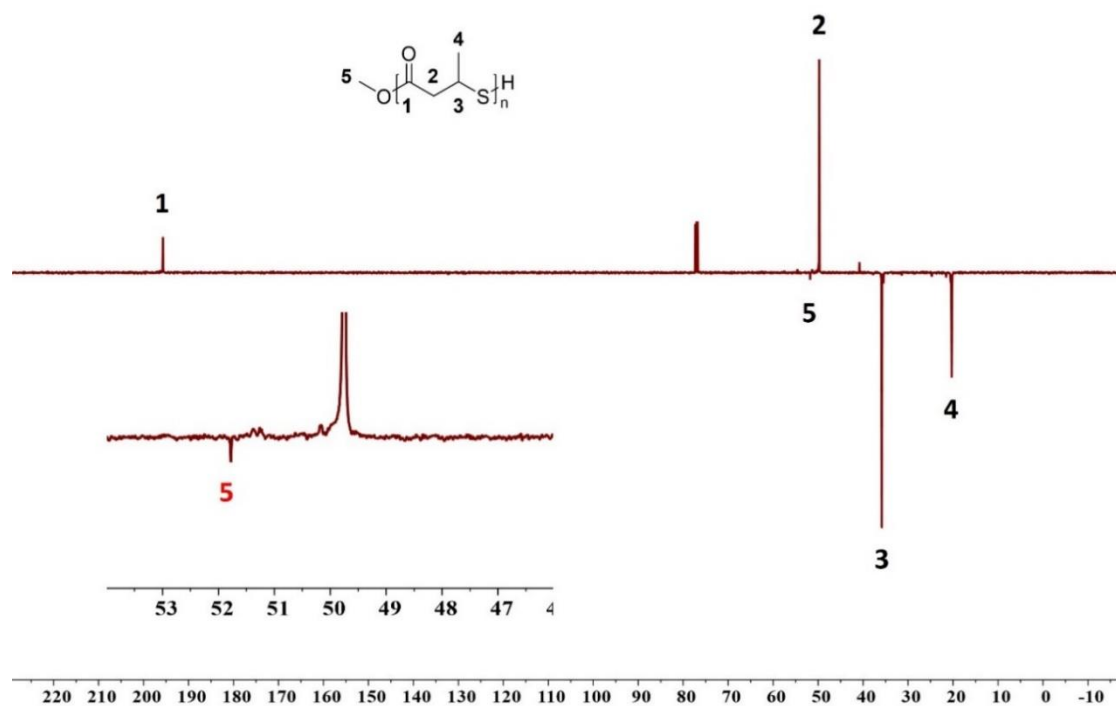


**Figure S18.** J-MOD spectrum (125 MHz, CDCl<sub>3</sub>, 25 °C) of an isolated P3TB (at least in part linear) produced by the NaOMe system (23:1, r.t., C<sub>6</sub>D<sub>6</sub>; Table 1, entry 1).

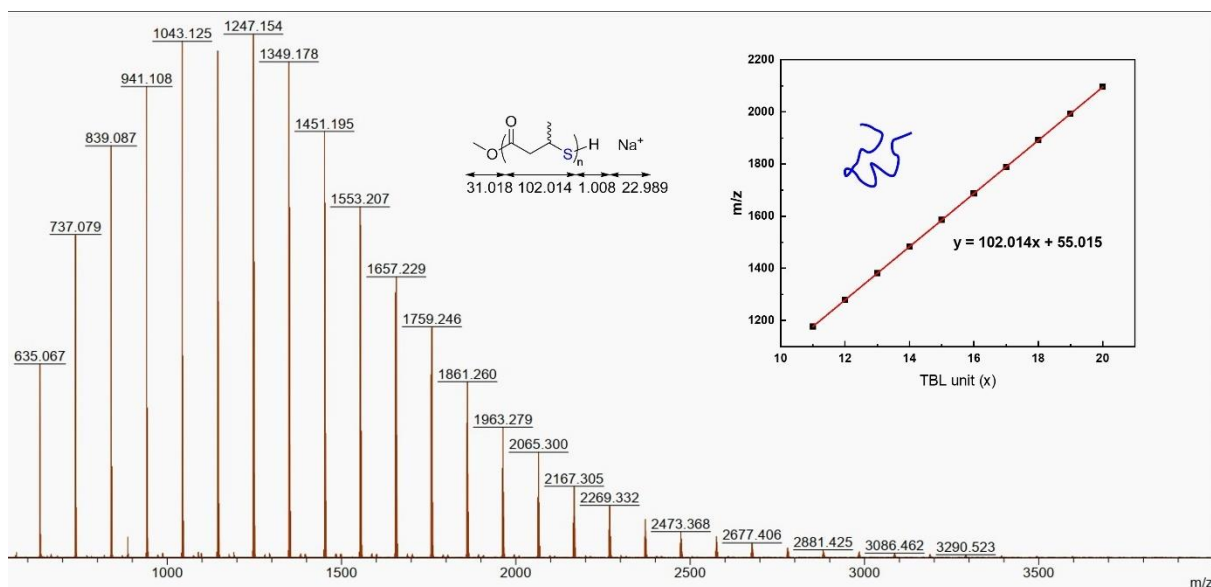


**Figure S19.** MALDI-ToF mass spectrum of an essentially linear P3TB produced by the system NaOMe in  $C_6D_6$ , (Table 1, entry 1), with a plot of experimental m/z values vs. theoretical number of TBL repeat units; the minor population corresponds to cyclic P3TB. For  $n = 20$ ,  $m/z$  exp = 2095.306 vs.  $m/z$  theo = 2095.294 for  $\{MeO-[C_4H_6OS]_{20}-H+Na\}^+$  (see details in Figure S20).

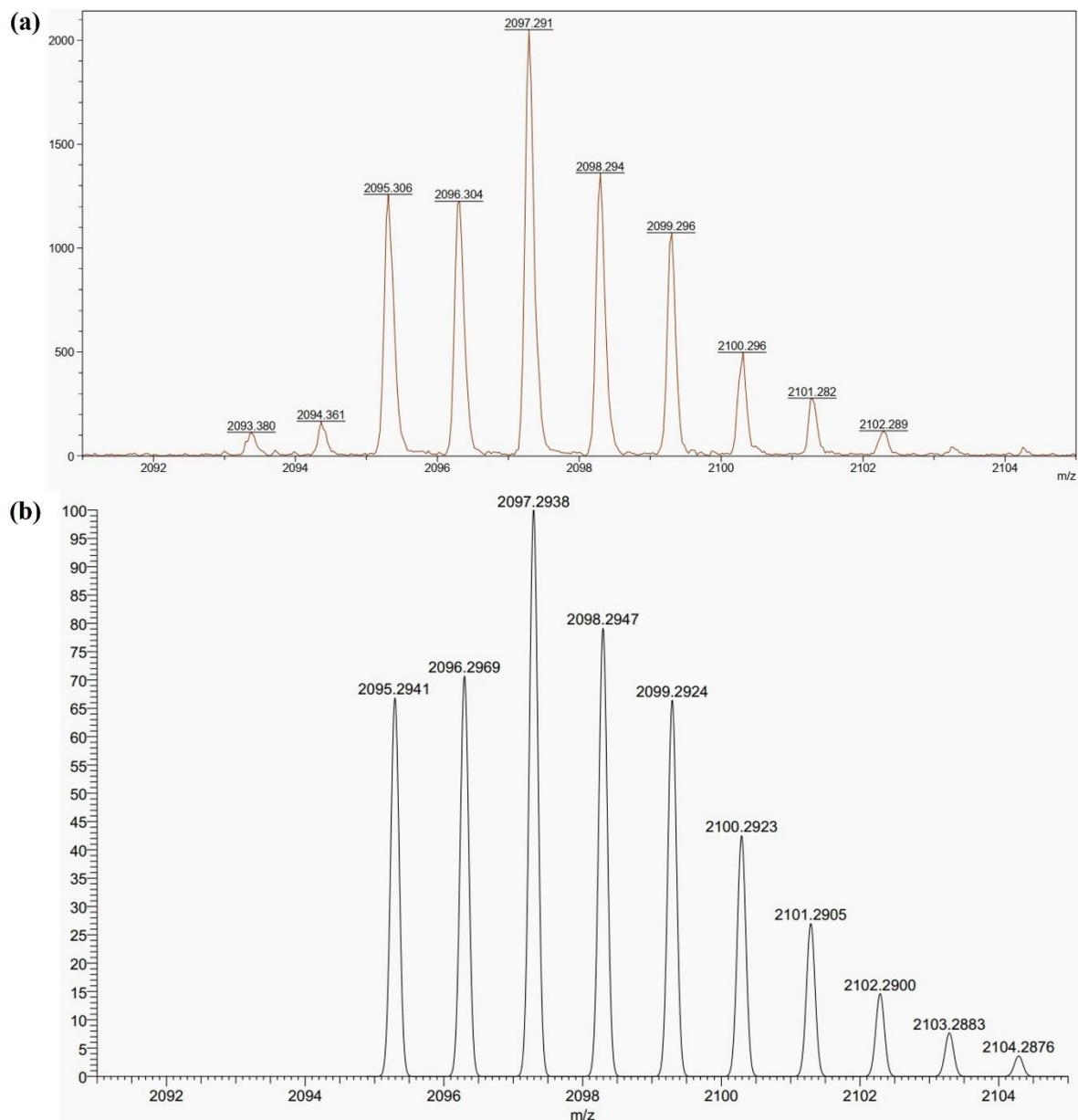


**Figure S20.** Details (isotopic distribution) of the MALDI-ToF mass spectrum of a linear P3TB produced by NaOMe in  $C_6D_6$ , showing the isotopic distribution for macromolecules  $\{MeO-[C_4H_6SO]_{20}-H+Na\}^+$ : a) experimental spectrum (Table 1, entry 1); b) calculated spectrum.

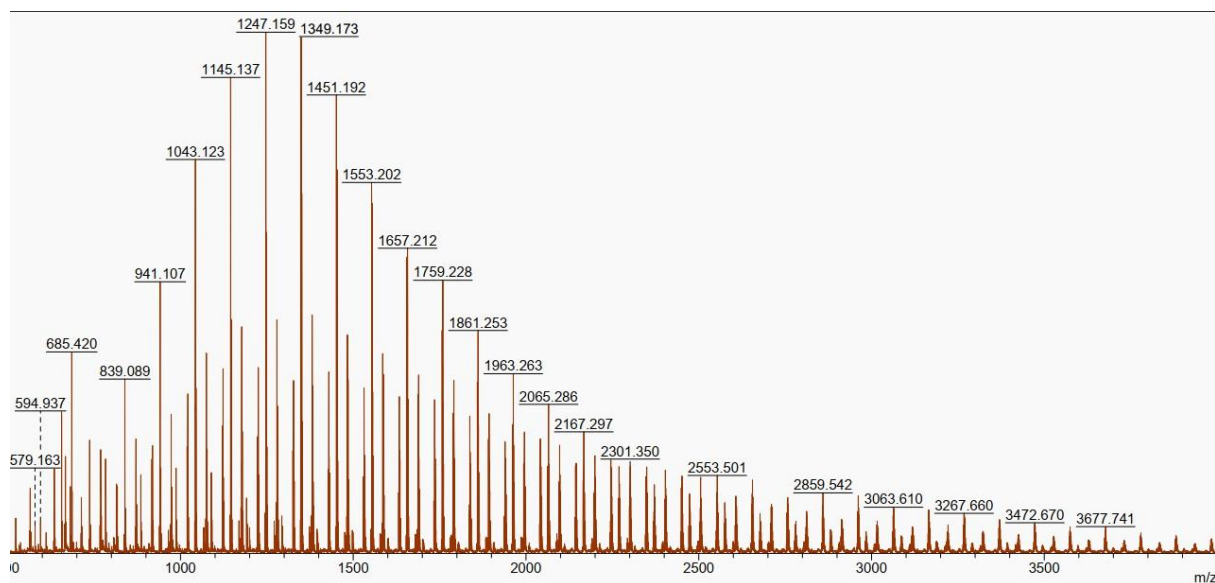


**Figure S21a.** MALDI-ToF mass spectrum of a mixture of several populations of P3TB, including cyclic (major) and linear (less intense) P3TB, produced by the ROP of *rac*-TBL with NaOMe in toluene (40:1, toluene, 35 °C, 1 h, conv = 52 %). One of the two less intense populations corresponds to linear  $\{\text{MeO}-[\text{TBL}_n]\text{-H}+\text{Na}\}^+$  macromolecules; for instance, for  $n = 12$ ,  $m/z$  exp = 1279.185 vs.  $m/z$  theo = 1279.183 for  $\{\text{MeO}-[\text{C}_4\text{H}_6\text{SO}]_n\text{-H}+\text{Na}\}^+$ ; the second less intense population ( $m/z$  obs. = 1225.265) and other minor ones could not be unambiguously identified (see details in Fig. S21b).

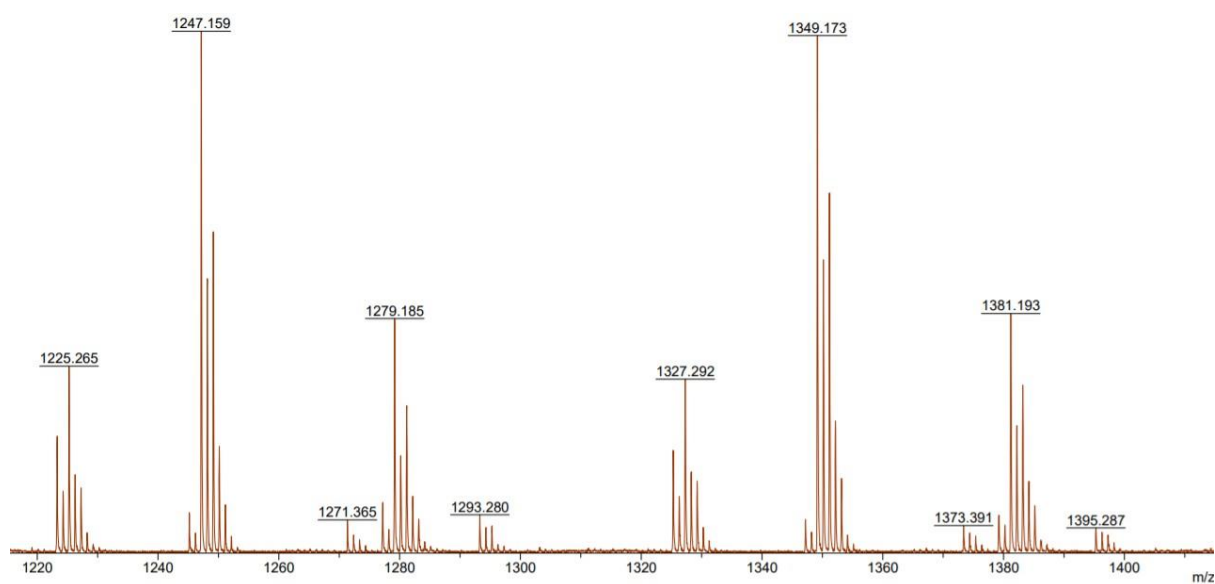


**Figure S21b.** Details of the MALDI-ToF mass spectrum of a mixture of several populations of P3TB, including a cyclic (major) and a linear (less intense) P3TB, produced by the ROP of *rac*-TBL with NaOMe in toluene (40:1, toluene, 35 °C, 1 h, conv = 52 %). One of the two less intense populations corresponds to linear  $\{\text{MeO}-[\text{TBL}_n]\text{-H}+\text{Na}\}^+$  macromolecules; for instance, for  $n = 12$ ,  $m/z$  exp = 1279.185 vs.  $m/z$  theo = 1279.183 for  $\{\text{MeO}-[\text{C}_4\text{H}_6\text{SO}]_n\text{-H}+\text{Na}\}^+$ ; the second less intense population and other minor ones could not be unambiguously identified.

## Representative SEC traces of P3TBs

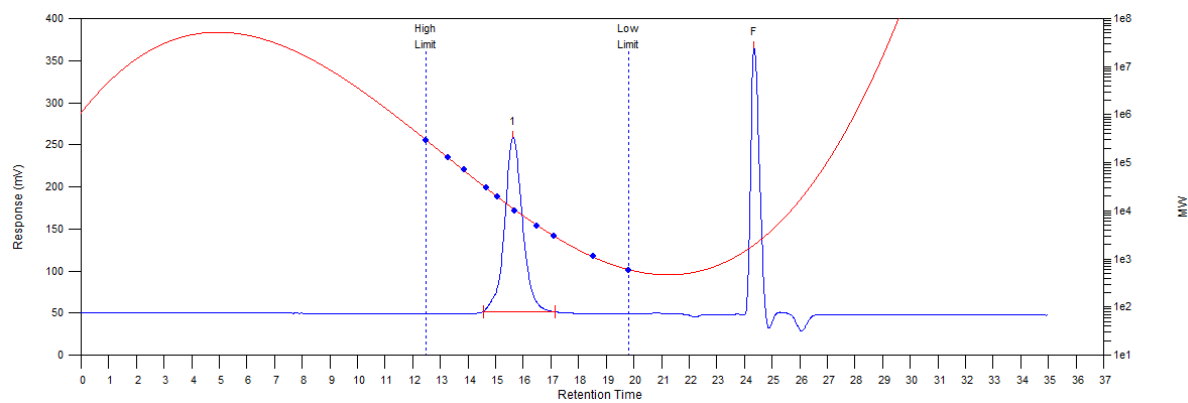


Figure S22. SEC trace of an isolated P3TB (Table S2, entry 11)

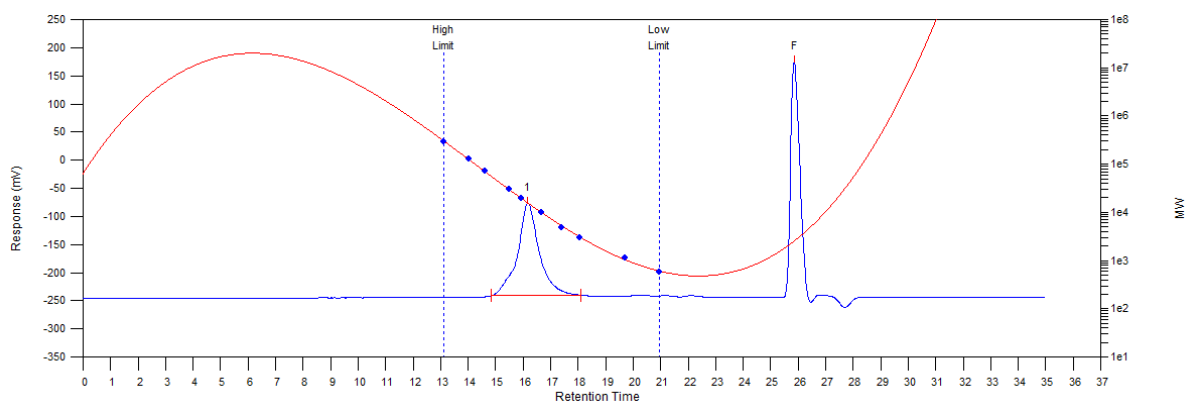


Figure S23. SEC trace of an isolated P3TB (Table S2, entry 10)

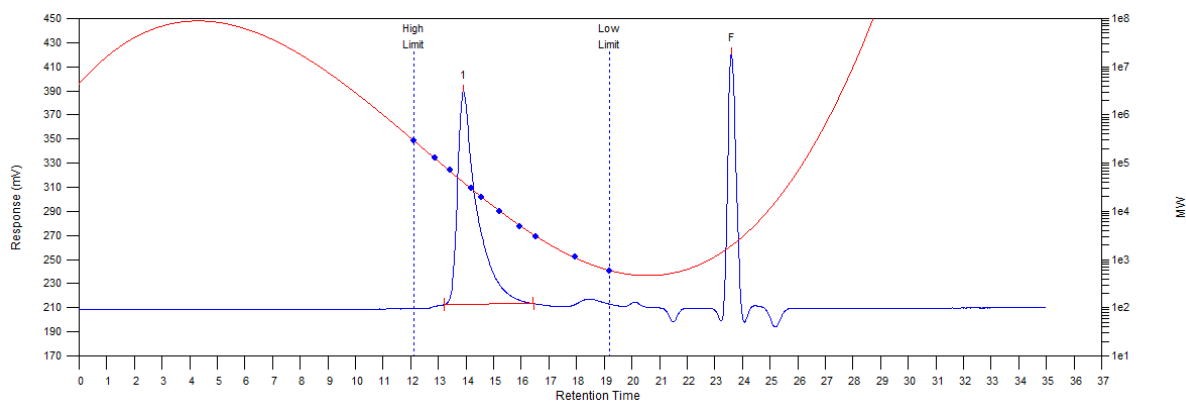
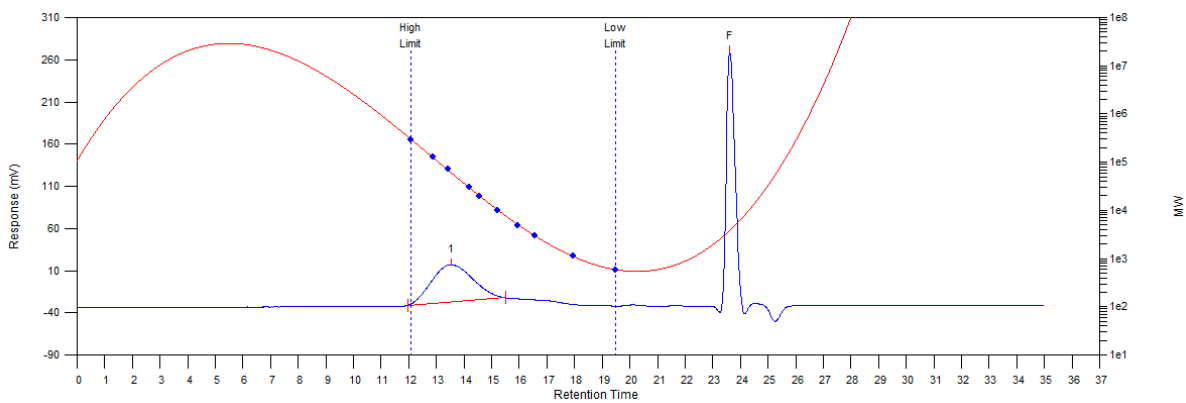
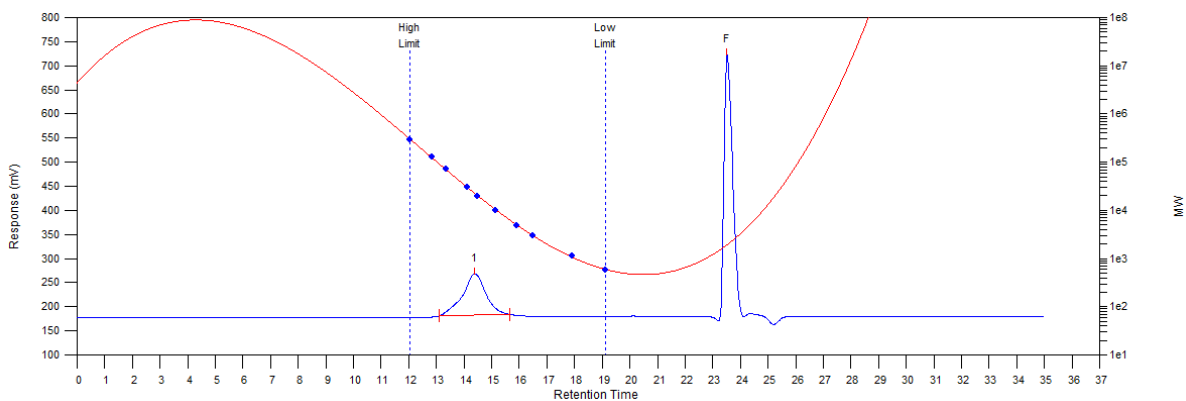


Figure S24. SEC trace of an isolated P3TB (Table 2, entry 48)



**Figure S25.** SEC trace of an isolated P3TB (Table 2, entry 32)



**Figure S26.** SEC trace of an isolated P3TB (Table 2, entry 34)

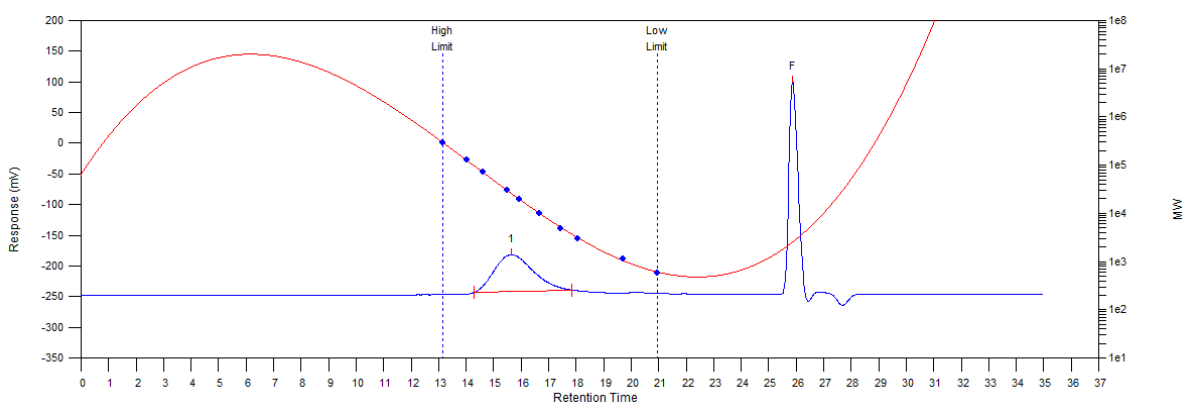


**Figure S27.** SEC trace of an isolated P3TB (Table 2, entry 17)

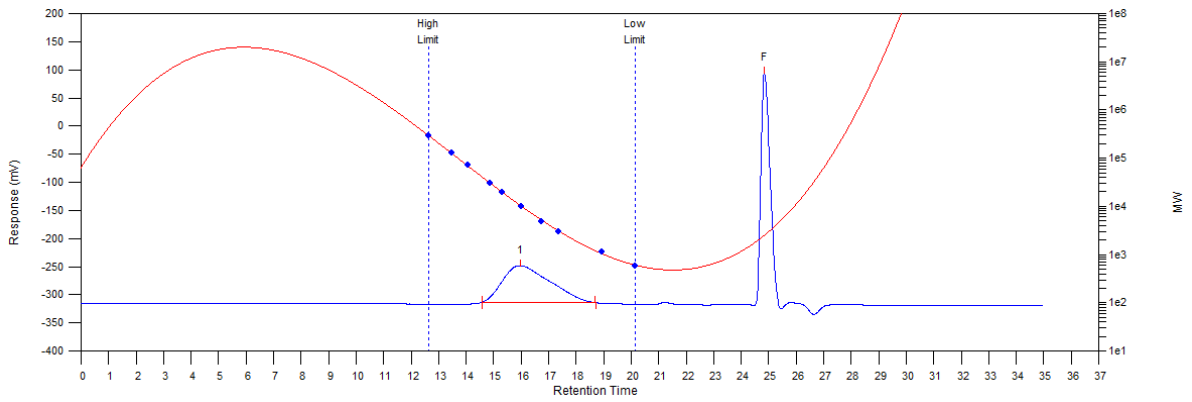


Figure S28. SEC trace of an isolated P3TB (Table 1, entry 15)

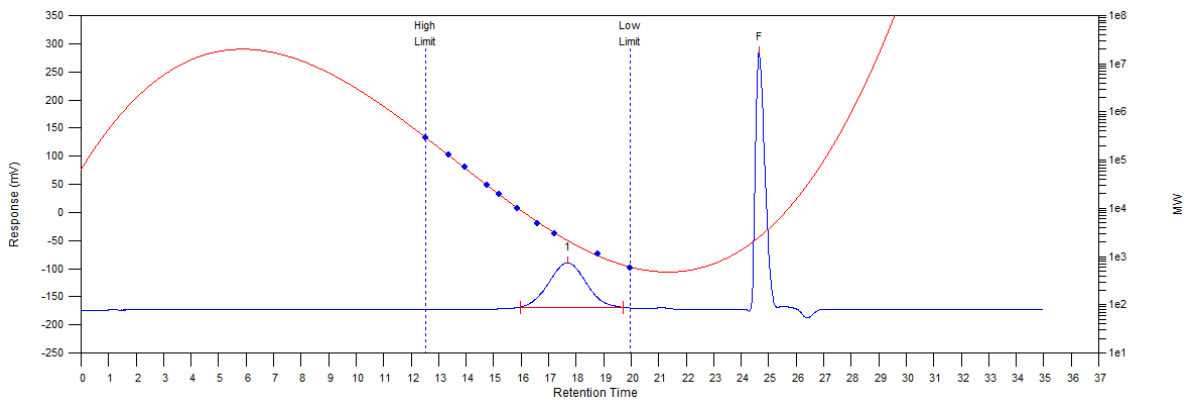


Figure S29. SEC trace of an isolated P3TB (Table 2, entry 35)

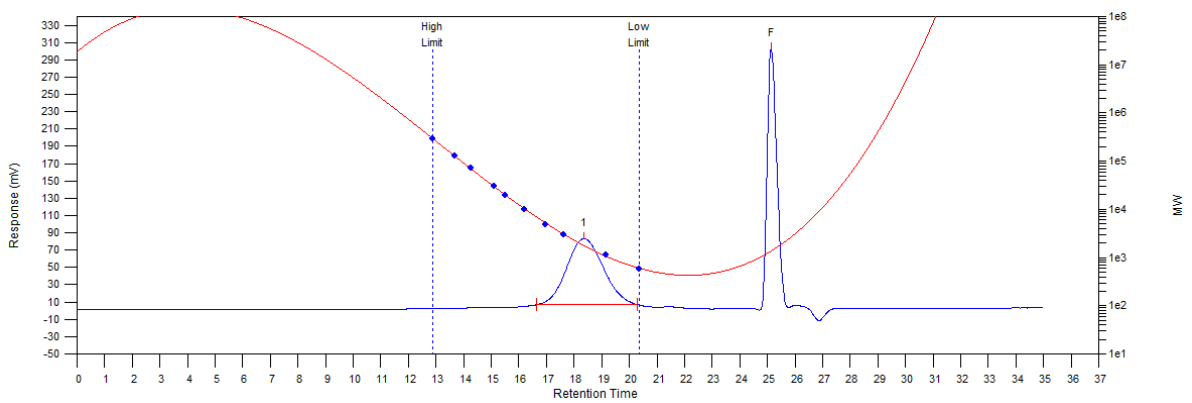
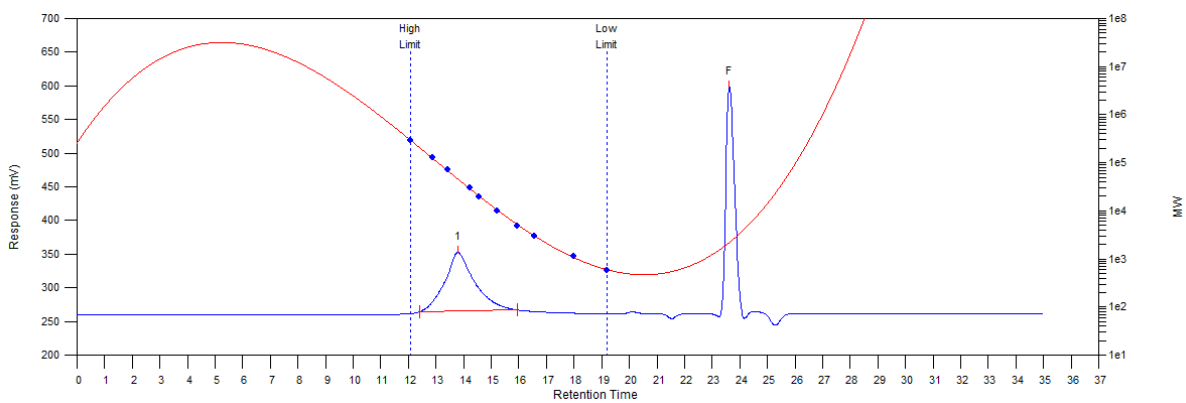
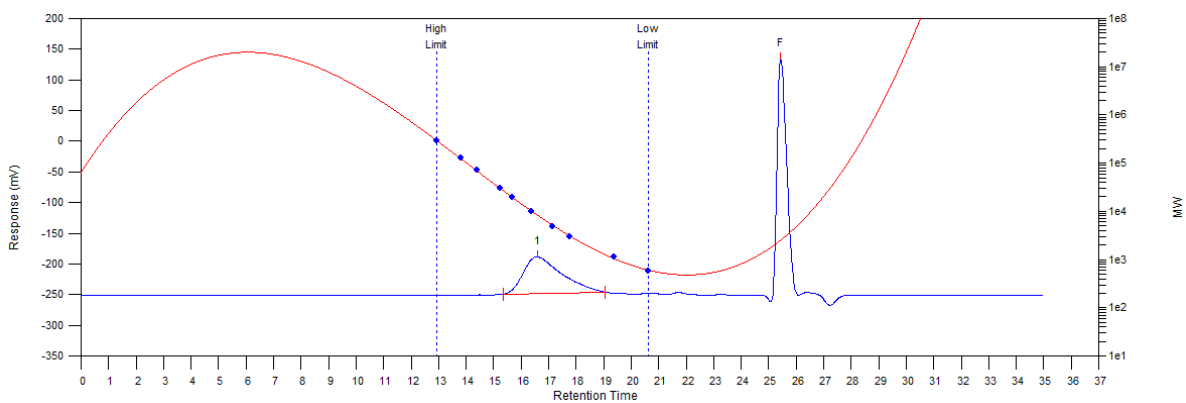


Figure S30. SEC trace of an isolated P3TB (Table 1, entry 7)



**Figure S31.** SEC trace of an isolated P3TB (Table 2, entry 21)



**Figure S32.** SEC trace of an isolated P3TB (Table 2, entry 26)



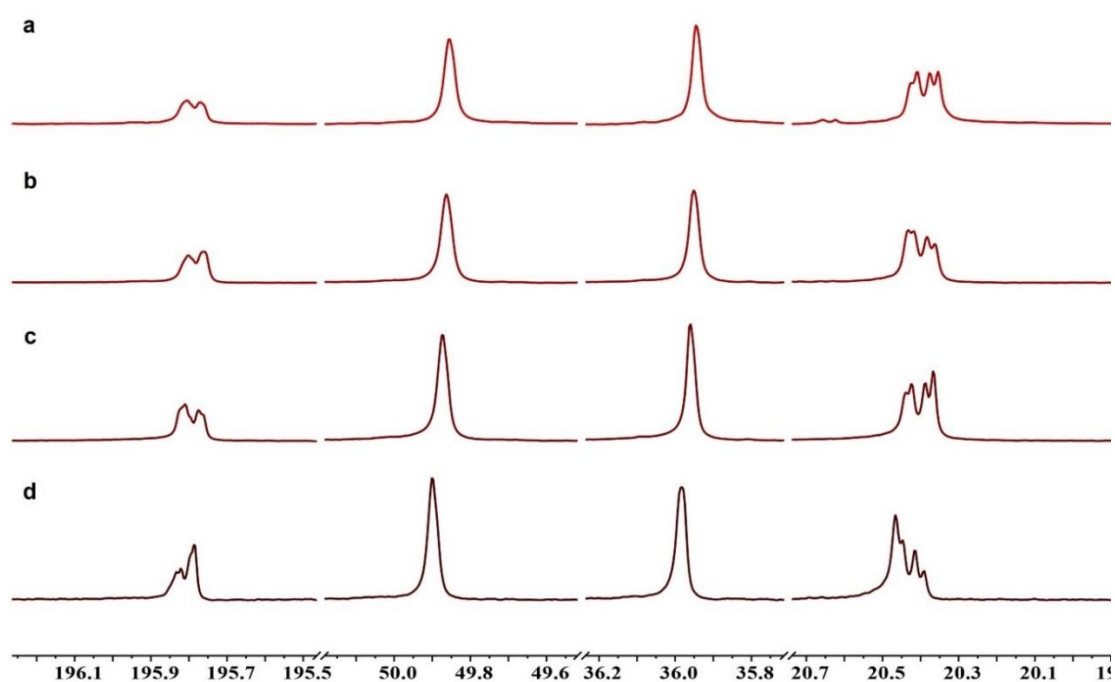


**Figure S33.** Carbonyl, methine, methylene and methyl regions of the  $^{13}\text{C}\{^1\text{H}\}$  NMR spectra (125 MHz,  $\text{CDCl}_3$ , 20 °C) of isolated P3TBs. a) atactic, essentially linear P3TB produced by NaOMe in  $\text{C}_6\text{D}_6$  at room temperature (Table 1, entry 1,  $P_m = 0.51$ ). b) atactic cyclic P3TB produced by complex **1** in toluene at room temperature (Table 1, entry 2,  $P_m = 0.48$ ). c) atactic cyclic P3TB produced by the system **4**/PrOH (1:1) in toluene at room temperature (Table 1, entry 9,  $P_m = 0.52$ ). d) syndiotactic-biased cyclic P3TB produced by complex **5a** in the absence of co-initiator in toluene at room temperature (Table 1, entry 11,  $P_m = 0.32$ ).

**Table S1.** Influence of the solvent on the stereoselective ROP of *rac*-TBL promoted by complex **5k** without a co-initiator.<sup>a</sup>

Entry	[TBL] <sub>0</sub> /[Cat.]	Solvent	Dielectric constant	[TBL] <sub>0</sub> (mol/L)	Reaction time (min) <sup>b</sup>	TBL Conv. (%) <sup>c</sup>	<i>M</i> <sub>n,theo</sub> (kg/mol) <sup>d</sup>	<i>M</i> <sub>n,SEC</sub> (kg/mol) <sup>d</sup>	<i>D</i> <sub>M</sub> <sup>e</sup>	<i>P</i> <sub>m</sub> <sup>f</sup>
1	100:1	<i>n</i> -Hexane	1.89	0.2	1	67	10.2	5.5	1.46	0.53
2	100:1	1,4-Dioxane	2.21	0.5	1	>99	10.2	5.3	1.61	0.50
3	100:1	Toluene	2.38	0.5	1	93	9.4	4.3	1.41	0.55
4	100:1	2-MeTHF	6.75	0.5	1	>99	10.2	4.9	1.55	0.53
5	100:1	THF	7.52	0.5	1	68	7.0	4.4	1.42	0.57
6	100:1	DCM	9.0	0.5	1	>99	10.2	4.4	1.34	0.53
7	100:1	Acetonitrile	36.64	0.5	1	21	2.1	n.d.	n.d.	n.d.

<sup>a</sup> Polymerizations performed at ambient temperature (15–20 °C). <sup>b</sup> The reaction times were not necessarily optimized. <sup>c</sup> Conversion of *rac*-TBL as determined by <sup>1</sup>H NMR analysis of the crude polymerization mixture. <sup>d</sup> Molar mass calculated according to  $M_{n,theo} = [TBL]_0/[Cat.] \times Conv_{TBL} \times M_{TBL}$ . <sup>e</sup> Number-average molar mass (*M*<sub>n,SEC</sub>) and dispersity (*D*<sub>M</sub>) of isolated P3TBs as determined by SEC analysis in THF at 30 °C vs. polystyrene standards (uncorrected values). <sup>f</sup> *P*<sub>m</sub> is the probability of *meso* enchainment between TBL units as determined by <sup>13</sup>C{<sup>1</sup>H} NMR analysis of isolated P3TBs.

**Table S2.** Influence of the solvent on the stereoselective ROP of *rac*-TBL promoted by the system **5c**/PrOH (1:1).<sup>a</sup>

Ref.	[M] <sub>0</sub> /[Cat.] /[Init.]	Solvent	Dielectric constant	[M] <sub>0</sub> (mol/L)	Reaction time (min) <sup>b</sup>	TBL Conv. (%) <sup>c</sup>	M <sub>n,theo</sub> <sup>d</sup> (kg/mol)	M <sub>n,SEC</sub> <sup>e</sup> (kg/mol)	Đ <sub>M</sub> <sup>e</sup>	P <sub>m</sub> <sup>f</sup>
8	100:1:1	<i>n</i> -Hexane	1.89	0.2	1	>99	10.2	21.9	1.37	0.37
9	100:1:1	1,4-Dioxane	2.21	1.0	1	>99	10.2	19.0	1.16	0.39
10	100:1:1	Toluene	2.38	1.0	1	>99	10.2	13.8	1.19	0.38
11	100:1:1	2-MeTHF	6.75	1.0	1	>99	10.2	10.3	1.10	0.35
12	100:1:1	THF	7.52	1.0	2	>99	10.2	6.7	1.26	0.58
13	100:1:1	DCM	9.0	1.0	1	>99	10.2	35.0	1.48	0.35
14	100:1:1	Acetonitrile	36.64	1.0	2	>99	10.2	28.9	1.52	0.34

<sup>a</sup> Polymerizations performed at ambient temperature (15-20 °C), co-initiator ([Init.]) is PrOH. <sup>b</sup> The reaction times were not necessarily optimized. <sup>c</sup> Conversion of *rac*-TBL as determined by <sup>1</sup>H NMR analysis of the crude polymerization mixture. <sup>d</sup> Molar mass calculated according to  $M_{n,theo} = [TBL]_0/[Cat.] \times Conv_{TBL} \times M_{w,TBL}$ . <sup>e</sup> Number-average molar mass ( $M_{n,SEC}$ ) and dispersity ( $\Delta_M$ ) of isolated P3TBs as determined by SEC analysis in THF at 30 °C vs. polystyrene standards (uncorrected values). <sup>f</sup>  $P_m$  is the probability of *meso* enchainment between TBL units as determined by <sup>13</sup>C{<sup>1</sup>H} NMR analysis of isolated P3TBs.

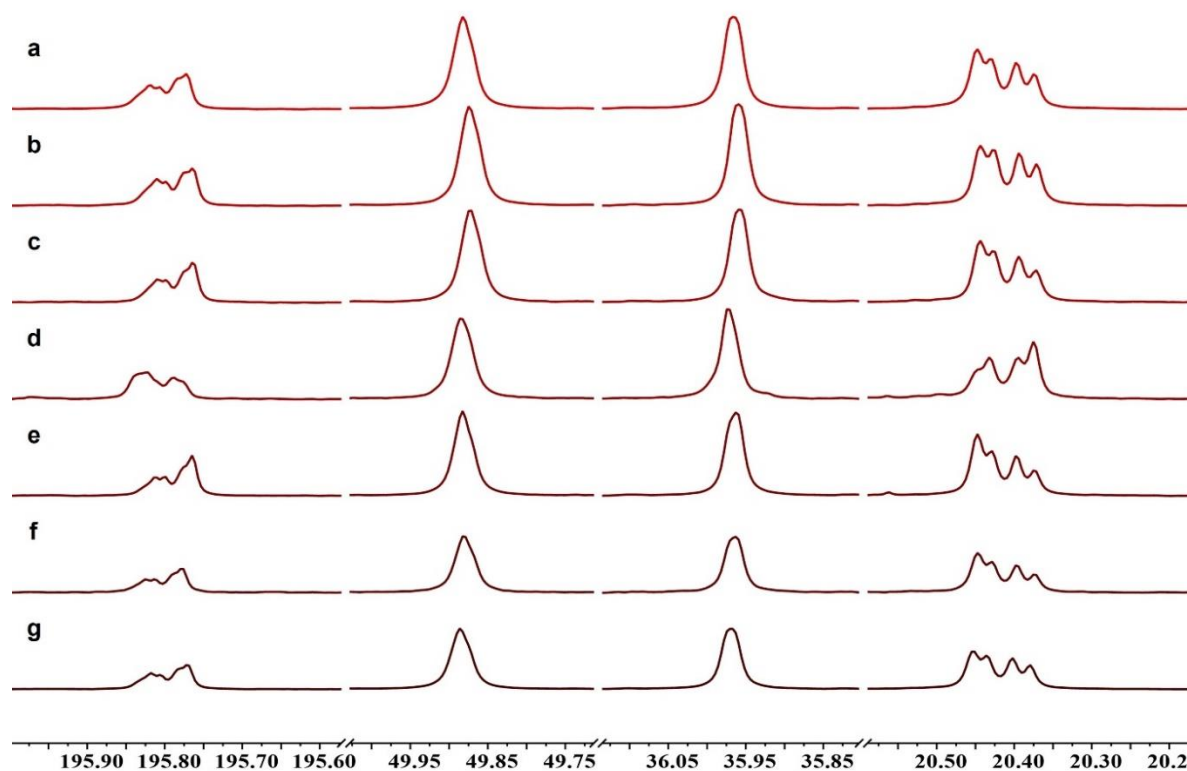


**Figure S34.** Carbonyl, methine, methylene and methyl regions of the <sup>13</sup>C{<sup>1</sup>H} NMR spectra (125 MHz, CDCl<sub>3</sub>, 20 °C) of isolated cyclic P3TBs produced in different solvents by the system **5c**/PrOH (1:1) (Table S2): a) acetonitrile,  $P_m = 0.34$ ; b) 1,4-dioxane,  $P_m = 0.39$ ; c) Me-THF,  $P_m = 0.35$ ; d) THF,  $P_m = 0.58$ ; e) dichloromethane,  $P_m = 0.35$ ; f) toluene,  $P_m = 0.38$ ; g) *n*-hexane,  $P_m = 0.37$ .

## Determination of tacticity of P3TB by $^{13}\text{C}$ NMR spectroscopy

Deconvolutions-calculations performed on the two series of methyl and carbonyl  $^{13}\text{C}$  NMR resonances returned consistent  $P_m/P_r$  values. For instance, for entry 48 (Table 2; see spectra below), the normalized intensity of the  $m$  dyad accounts for 0.897, i.e.  $P_m = \text{ca. } 0.90$ . From this experimental value, one can calculate the theoretical value of the triad distribution, and then compare it to the experimental ones (Table S3). The  $P_m$  values reported in Tables 1, 2, S1 and S2 correspond to the square root of the relative normalized intensity of the  $mm$  triad.

**Table S3.** Statistical analysis of the carbonyl and methyl resonances of isotactic cyclic P3TB (entry 48) made from integration determined by regular  $^{13}\text{C}\{^1\text{H}\}$  NMR.

Theoretical values	Experimental values
$(mm) = (m) \times (m) = 0.805$	$(mm) = (m) \times (m) = 0.828$
$(rr) = (r) \times (r) = 0.011$	$(rr) = (r) \times (r) = 0.003$
$(rm) = (mr) = (m) \times (r) = 0.092$	$(rm) = (mr) = (m) \times (r) = 0.084^*$

\* average experimental value =  $[0.085 + 0.082]/2$ ; the Bernoulli model triad test was not calculated due to large error on the  $rr$  value.

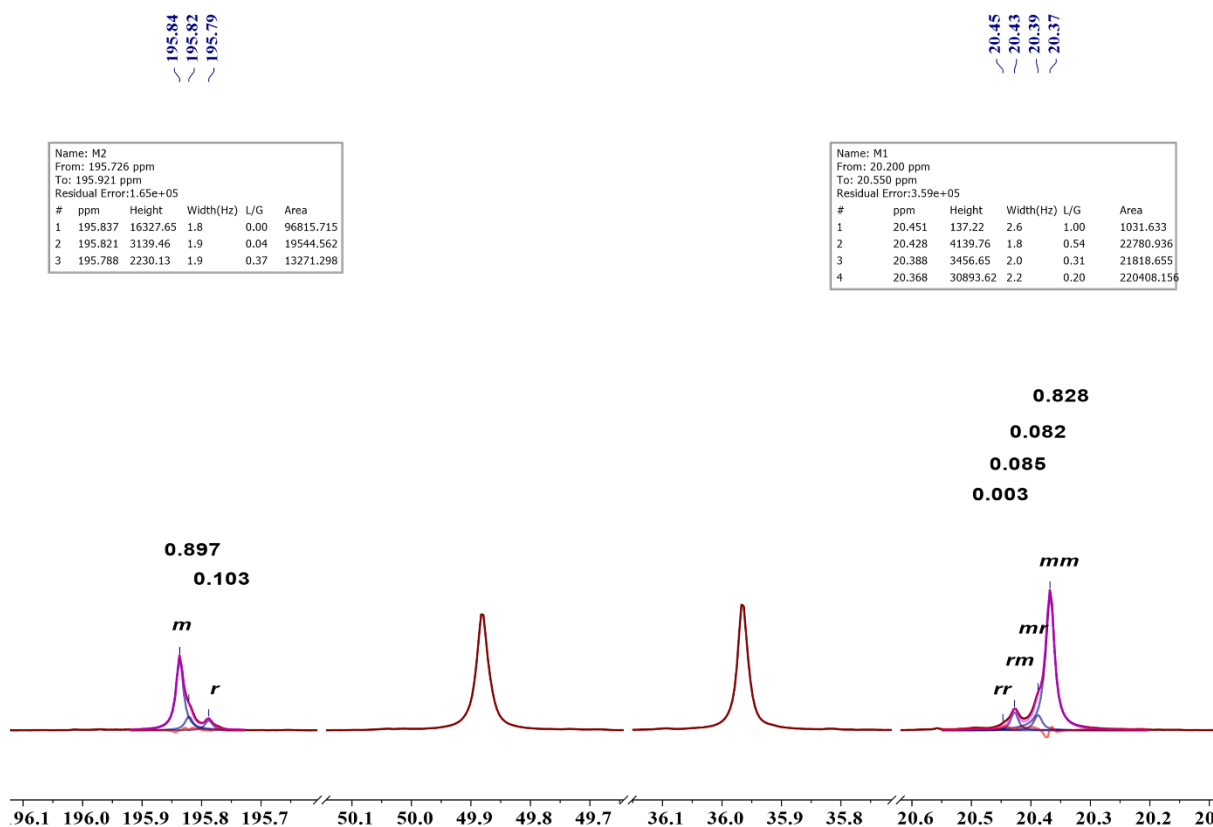


**Figure S35.** Carbonyl, methine, methylene and methyl regions of the  $^{13}\text{C}\{^1\text{H}\}$  NMR spectrum (125 MHz,  $\text{CDCl}_3$ , 25 °C) of an isotactic-enriched cyclic P3TB (Table 2, entry 48).

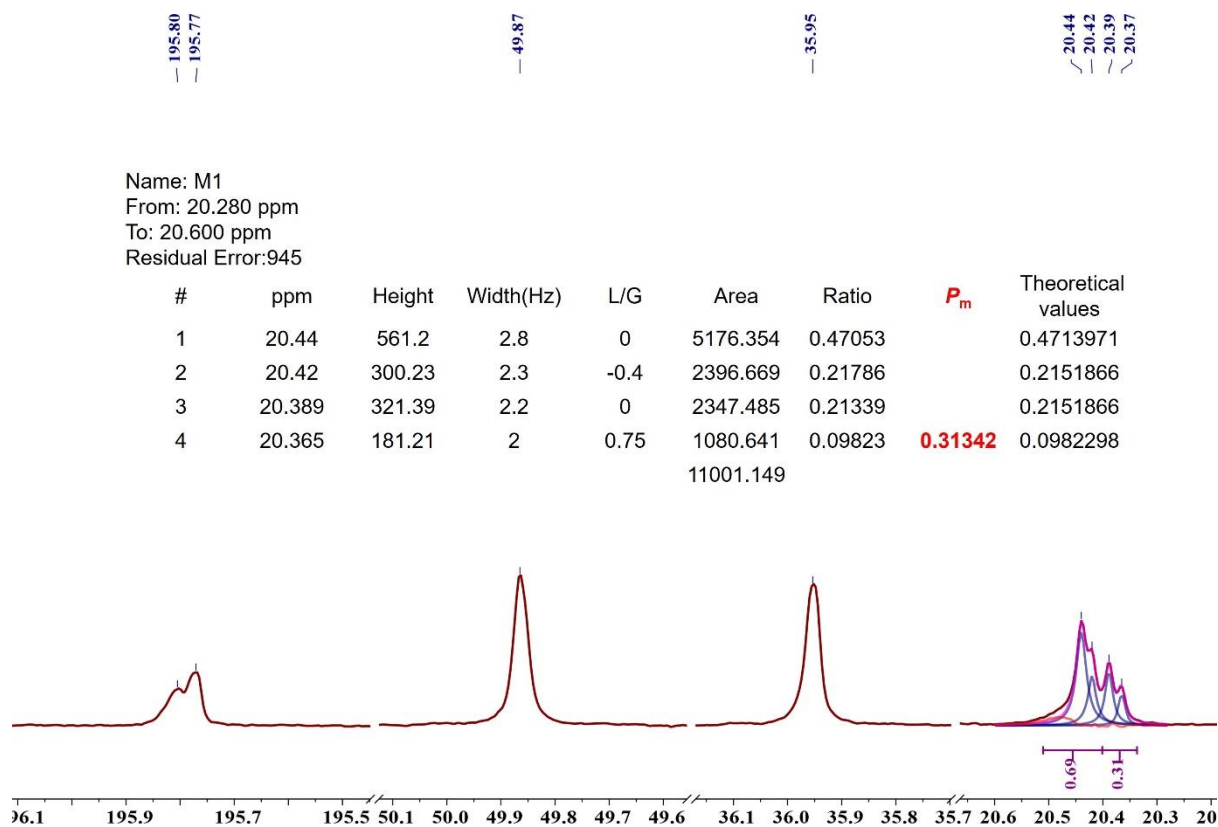


**Figure S36.** Carbonyl, methine, methylene and methyl regions of the “regular”  $^{13}\text{C}\{^1\text{H}\}$  NMR spectrum (125 MHz,  $\text{CDCl}_3$ , 25 °C) of a syndiotactic cyclic P3TB (Table 1, entry 14).

Some deconvolutions-calculations were also performed on the carbonyl  $^{13}\text{C}$  projection extracted from the band-selective HMBC spectrum. For instance, for entry 14 (Table 1; see spectra below), the normalized intensity of the *rr* triad accounts for 0.463, i.e.,  $P_r = \text{ca. } 0.68$  ( $P_m = 1 - P_r = 0.32$ ). From this experimental value, one can calculate the theoretical value of the triad distribution, and then compare it to the experimental ones (Table S4).

**Table S4.** Statistical analysis of the carbonyl resonances of a syndiotactic P3TB (Table 1, entry 14) made from integration determined by  $^{13}\text{C}$  projection extracted from band-selective HMBC spectrum.

Theoretical values	Experimental values
$(mm) = (m) \times (m) = 0.102$	$(mm) = (m) \times (m) = 0.104$
$(rr) = (r) \times (r) = 0.463$	$(rr) = (r) \times (r) = 0.463$
$(rm) = (mr) = (m) \times (r) = 0.217$	$(rm) = (mr) = (m) \times (r) = 0.216^*$

\* average experimental value =  $[0.247 + 0.185]/2$ . Bernoulli model triad test,  $B = \frac{[(mm) \times (rr)]}{[(rm) \times (mr)]} = 1.03$

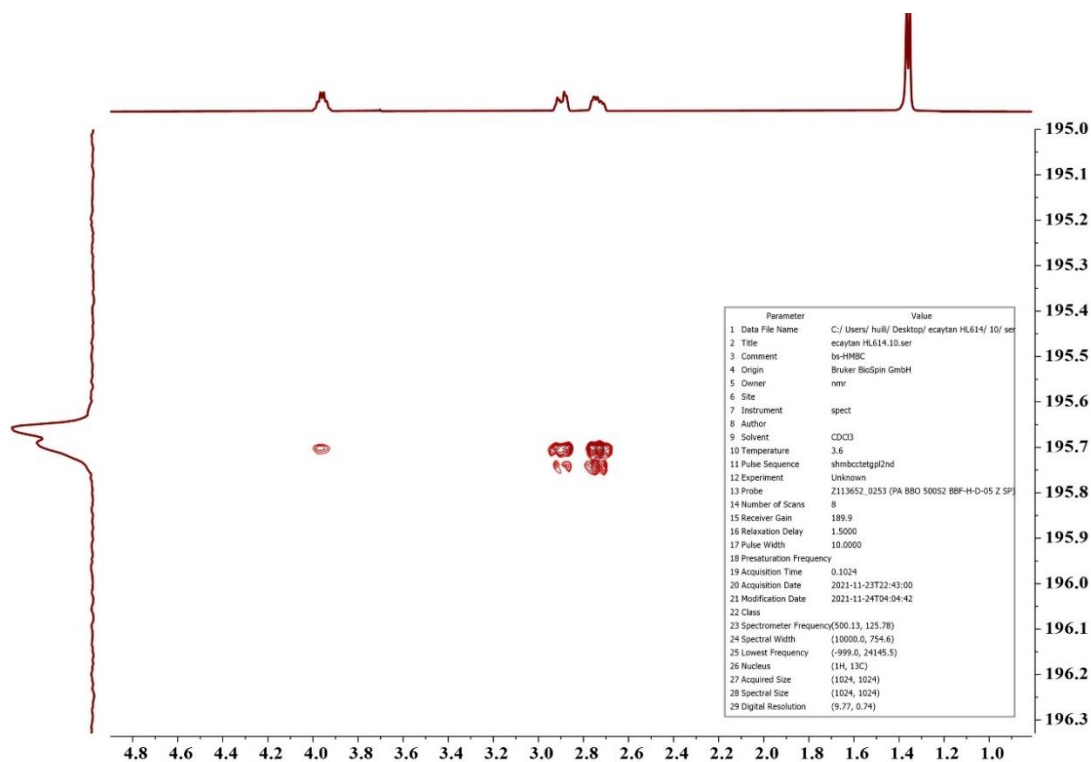


**Figure S37.** Band-selective HMBC spectrum of a syndiotactic cyclic P3TB (Table 1, entry 14). The  $^1\text{H}$  NMR (500 MHz) spectrum is plotted on the F2 axis and the  $^{13}\text{C}$  NMR (125 MHz) spectrum is plotted on the F1 axis.

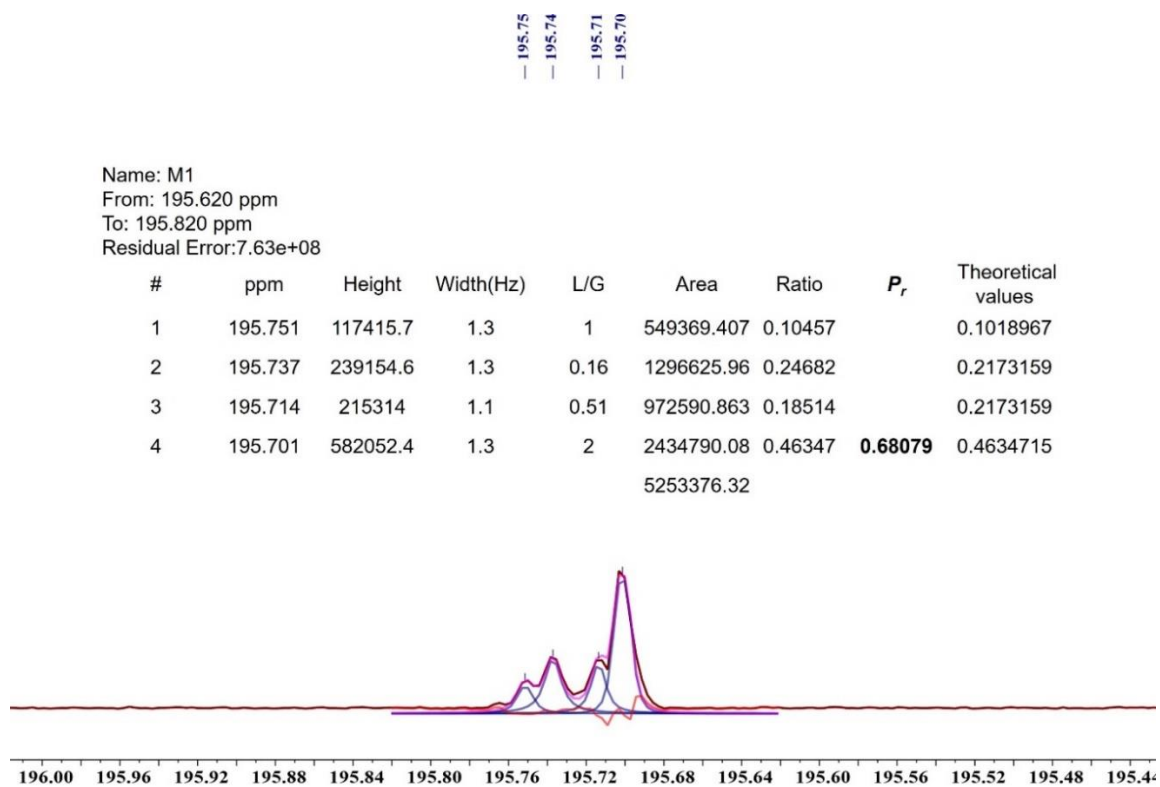


**Figure S38.**  $^{13}\text{C}$  projection extracted from the band-selective HMBC of a syndiotactic cyclic P3TB (Table 1, entry 14) by summing columns between  $\delta^1\text{H}$  2.60 and 3.00 ppm.

The same deconvolutions-calculations can be performed on the methyl  $^{13}\text{C}$  projection extracted from the band-selective HSQC spectrum. For instance, for entry 14 (Table 1, see spectra below), the normalized intensity of the *mm* triad accounts for 0.100, i.e.,  $P_m = \text{ca. } 0.32$  ( $P_r = 1 - P_m = 0.68$ ). From this experimental value, one can calculate the theoretical value of the triad distribution, and then compare it to the experimental ones (Table S5).

**Table S5.** Statistical analysis of the methyl resonances of a syndiotactic-enriched P3TB (Table 1, entry 14) made from integration determined by  $^{13}\text{C}$  projection extracted from band-selective HSQC spectrum.

Theoretical values	Experimental values
$(mm) = (m) \times (m) = 0.100$	$(mm) = (m) \times (m) = 0.100$
$(rr) = (r) \times (r) = 0.467$	$(rr) = (r) \times (r) = 0.454$
$(rm) = (mr) = (m) \times (r) = 0.216$	$(rm) = (mr) = (m) \times (r) = 0.216$

Bernoulli model triad test,  $B = [(mm) \times (rr)] / [(rm) \times (mr)] = 0.97$ .

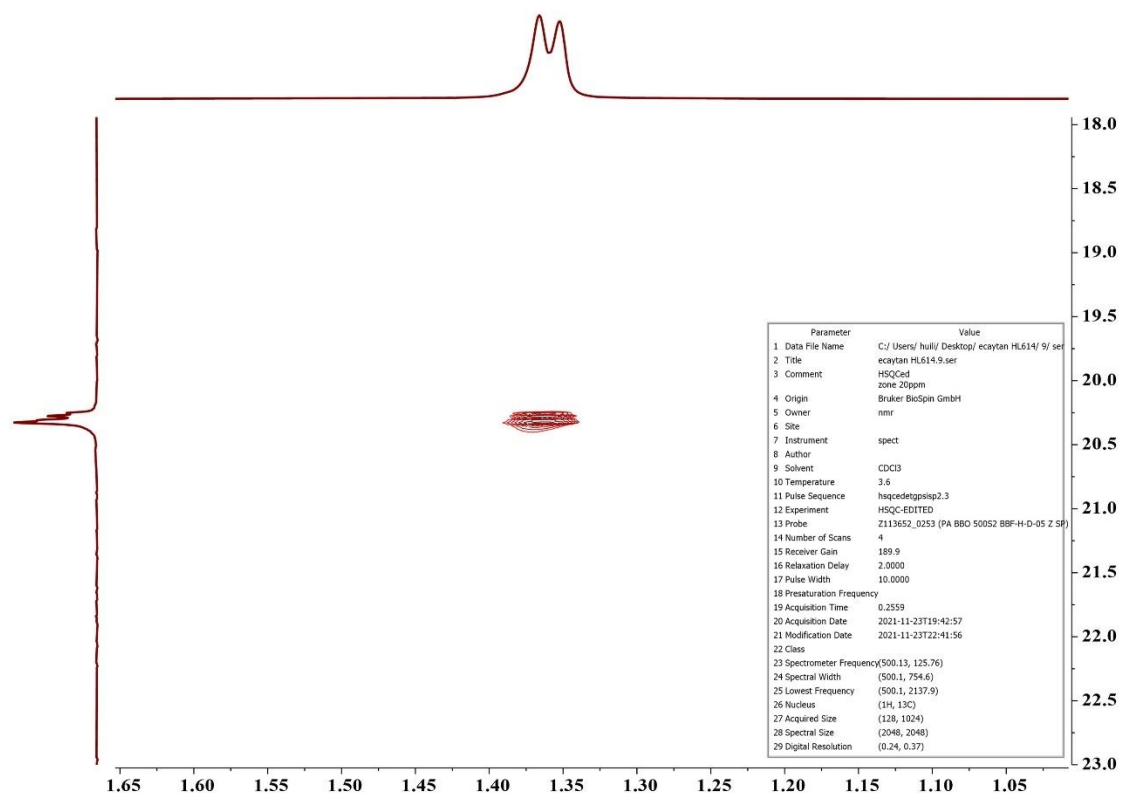


**Figure S39.** Band-selective HSQC spectrum of a syndiotactic-enriched cyclic P3TB (Table 1, entry 14). The  $^1\text{H}$  NMR (500 MHz) spectrum is plotted on the F2 axis and the  $^{13}\text{C}$  NMR (125 MHz) spectrum is plotted on the F1 axis.



20.44  
20.42  
20.39  
20.37

Name: M1

From: 20.086 ppm

To: 20.497 ppm

Residual Error: 4.61e+05

#	ppm	Height	Width(Hz)	L/G	Area	Ratio	$P_m$	Theoretical values
1	20.326	17735.37	2.5	0.45	177637.425	0.45378		0.4671904
2	20.306	10601.27	1.8	-0.4	85216.435	0.21769		0.2163229
3	20.276	10294.9	2.1	0.13	89396.77	0.22837		0.2163229
4	20.252	5546.13	1.8	0.59	39210.227	0.10016	<b>0.31649</b>	0.1001639
					391460.857			

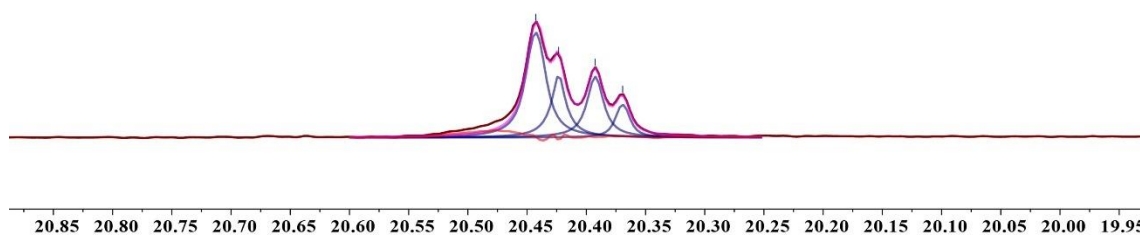


**Figure S40.**  $^{13}\text{C}$  projection extracted from the band-selective HSQC of a syndiotactic-enriched cyclic P3TB (Table 1, entry 14) by summing columns between  $\delta$   $^1\text{H}$  1.30 and 1.45 ppm.

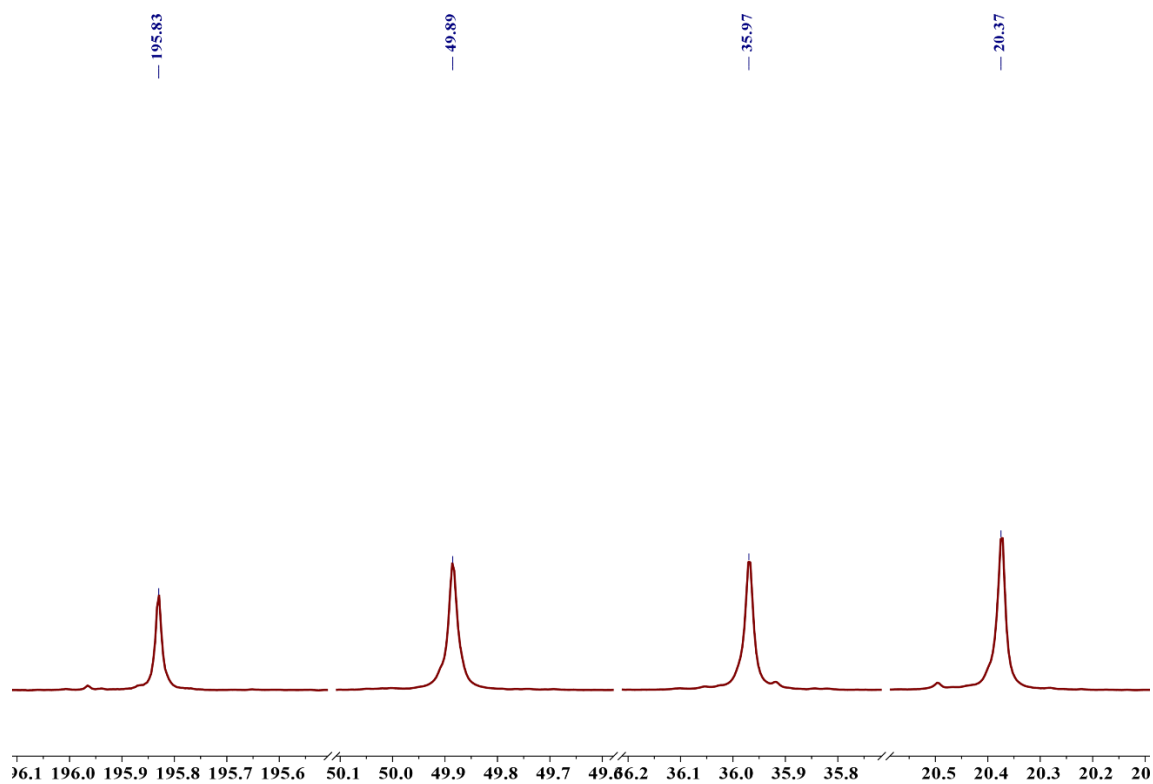


**Figure S41.** Carbonyl, methine, methylene and methyl regions of the  $^{13}\text{C}\{^1\text{H}\}$  NMR spectrum (125 MHz,  $\text{CDCl}_3$ , 25 °C) of a highly isotactic cyclic P3TB ( $P_m > 0.95$ ) prepared from the ROP of (S)-TBL.

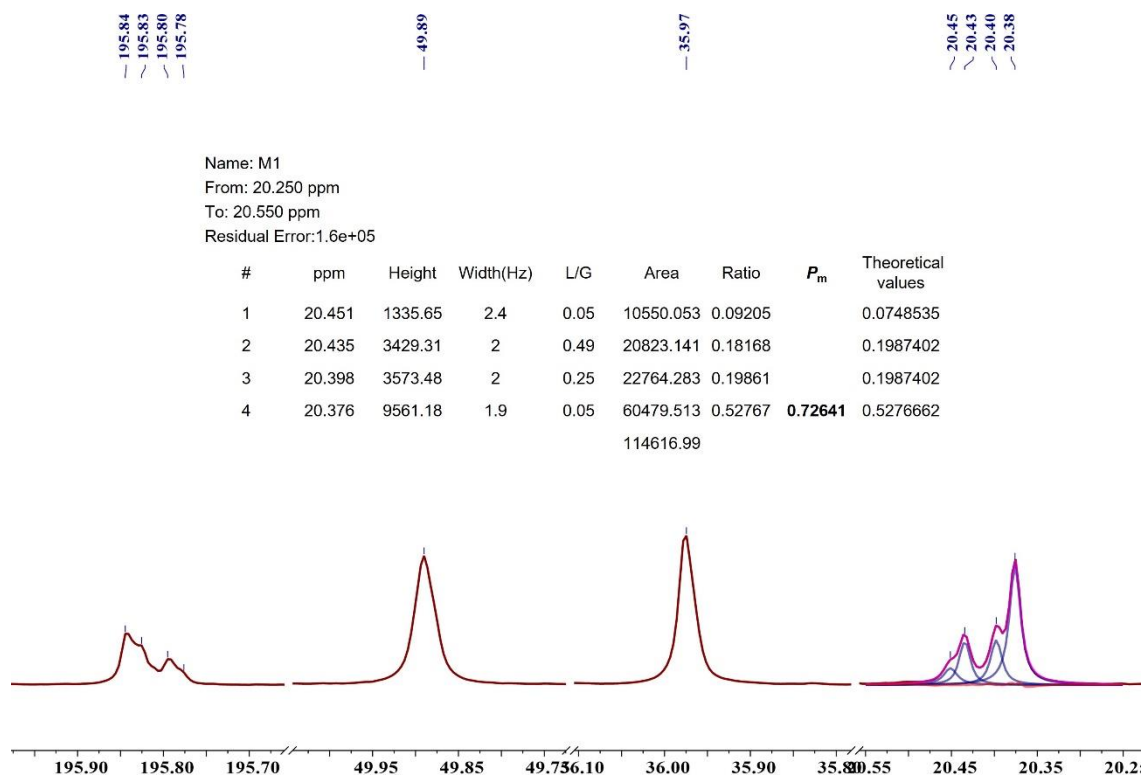


**Figure S42.** Carbonyl, methine, methylene and methyl regions of the  $^{13}\text{C}\{^1\text{H}\}$  NMR spectrum (125 MHz,  $\text{CDCl}_3$ , 25 °C) of an isotactic-enriched cyclic P3TB (Table 2, entry 30).

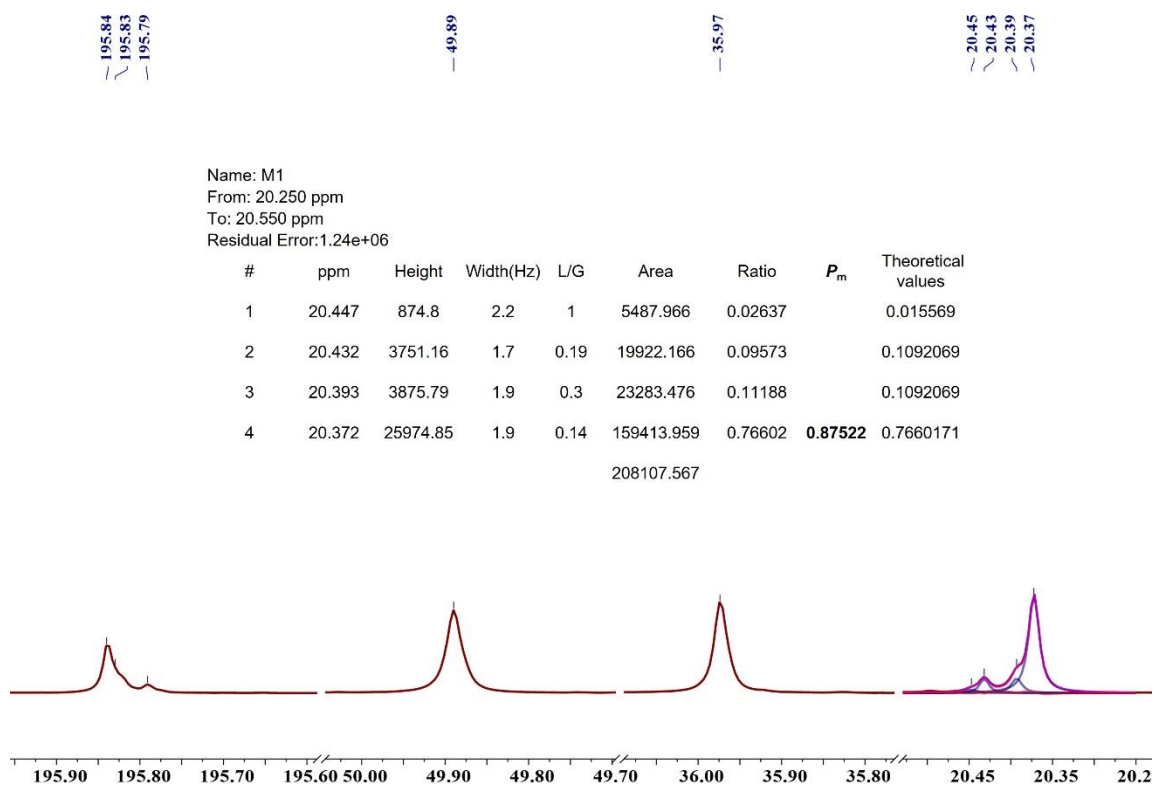


**Figure S43.** Carbonyl, methine, methylene and methyl regions of the  $^{13}\text{C}\{^1\text{H}\}$  NMR spectrum (125 MHz,  $\text{CDCl}_3$ , 25 °C) of an isotactic-enriched cyclic P3TB (Table 2, entry 33).

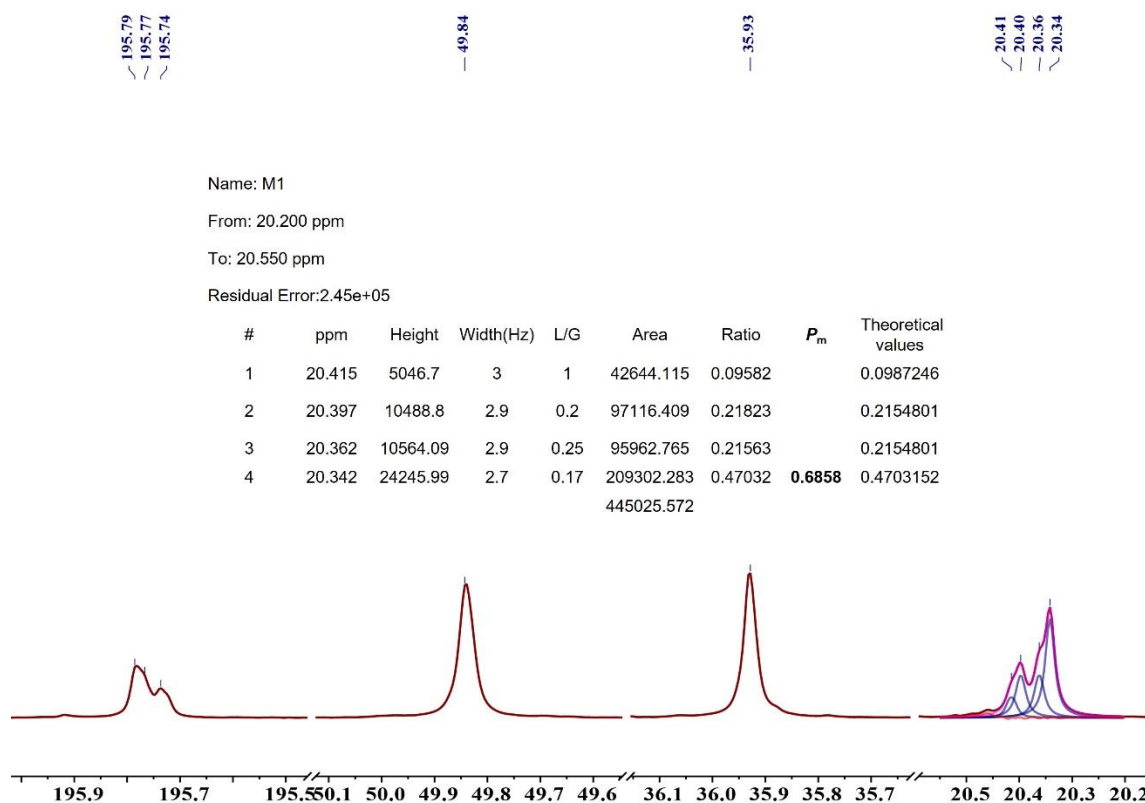


**Figure S44.** Carbonyl, methine, methylene and methyl regions of the  $^{13}\text{C}\{^1\text{H}\}$  NMR spectrum (125 MHz,  $\text{CDCl}_3$ , 25 °C) of an isotactic-enriched cyclic P3TB (Table 2, entry 42).

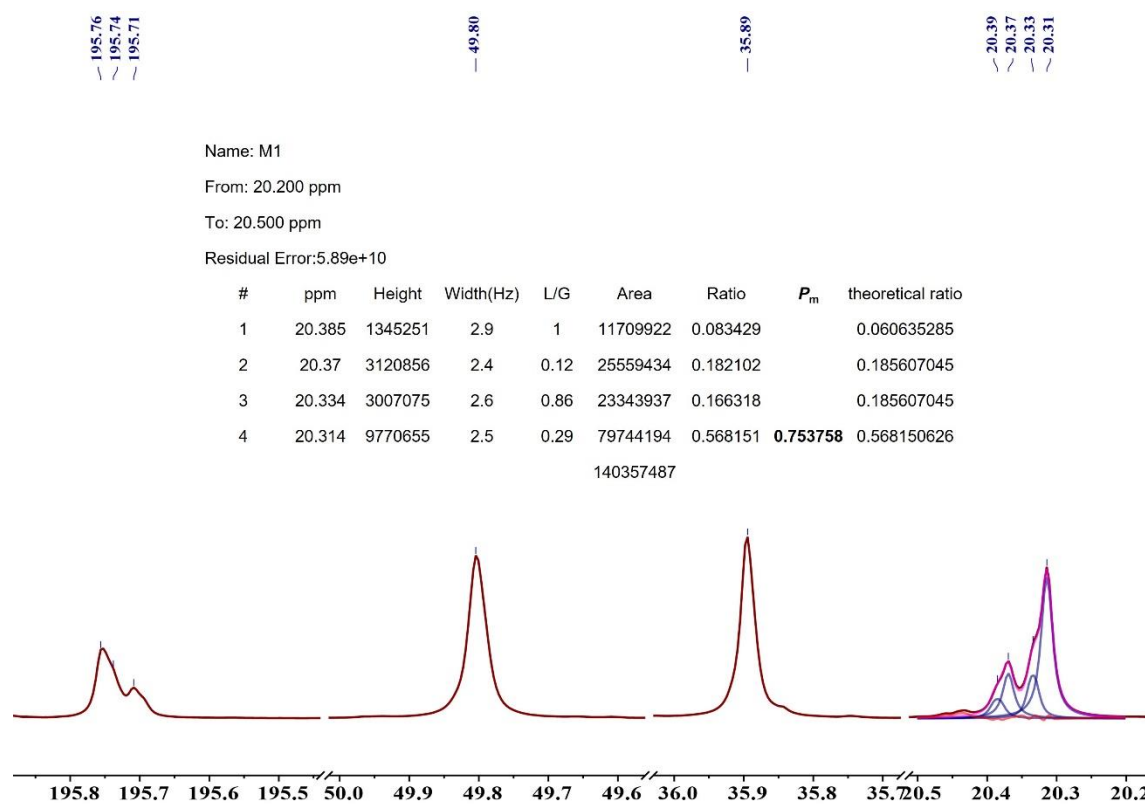


**Figure S45.** Carbonyl, methine, methylene and methyl regions of the  $^{13}\text{C}\{^1\text{H}\}$  NMR spectrum (125 MHz,  $\text{CDCl}_3$ , 25 °C) of an isotactic-enriched cyclic P3TB (Table 2, entry 44).

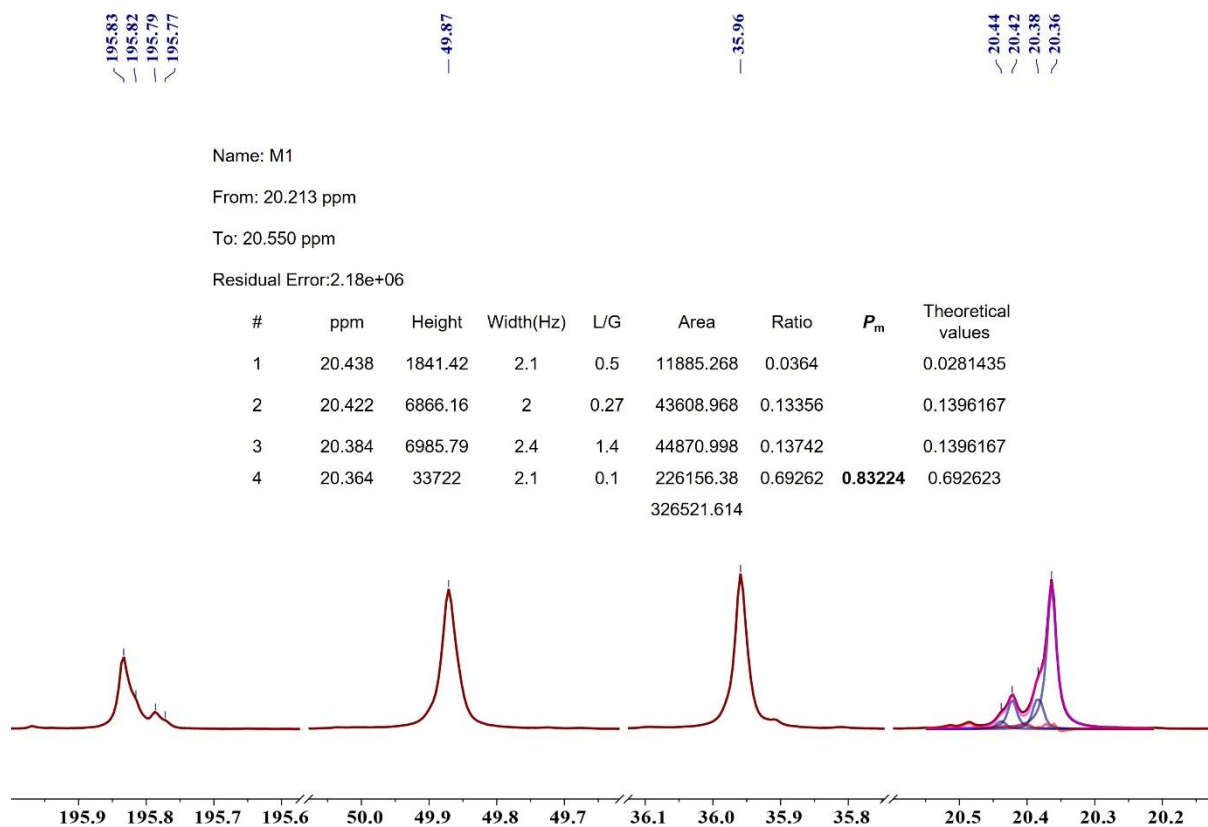


**Figure S46.** Carbonyl, methine, methylene and methyl regions of the  $^{13}\text{C}\{^1\text{H}\}$  NMR spectrum (125 MHz,  $\text{CDCl}_3$ , 25 °C) of an isotactic-enriched cyclic P3TB (Table 2, entry 50).

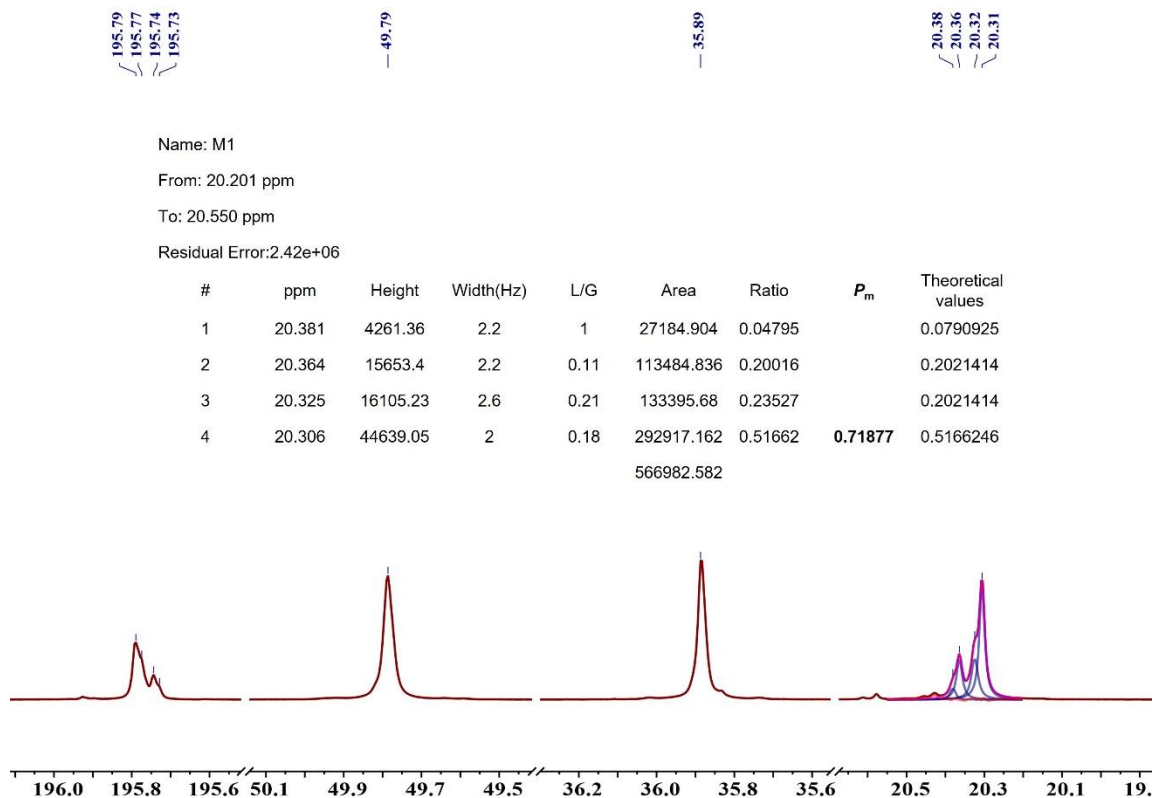


**Figure S47.** Carbonyl, methine, methylene and methyl regions of the  $^{13}\text{C}\{^1\text{H}\}$  NMR spectrum (125 MHz,  $\text{CDCl}_3$ , 25 °C) of an isotactic-enriched cyclic P3TB (Table 2, entry 47).

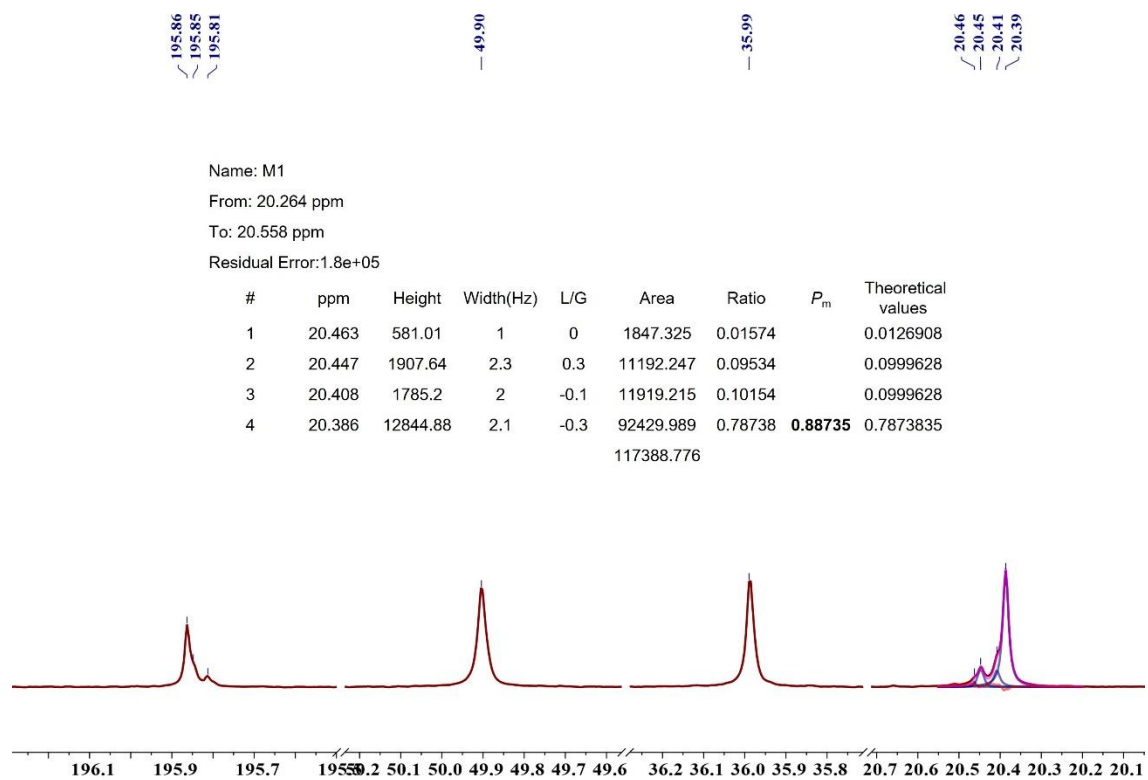


**Figure S48.** Carbonyl, methine, methylene and methyl regions of the  $^{13}\text{C}\{^1\text{H}\}$  NMR spectrum (125 MHz,  $\text{CDCl}_3$ , 25 °C) of an isotactic-enriched cyclic P3TB (Table 2, entry 34).

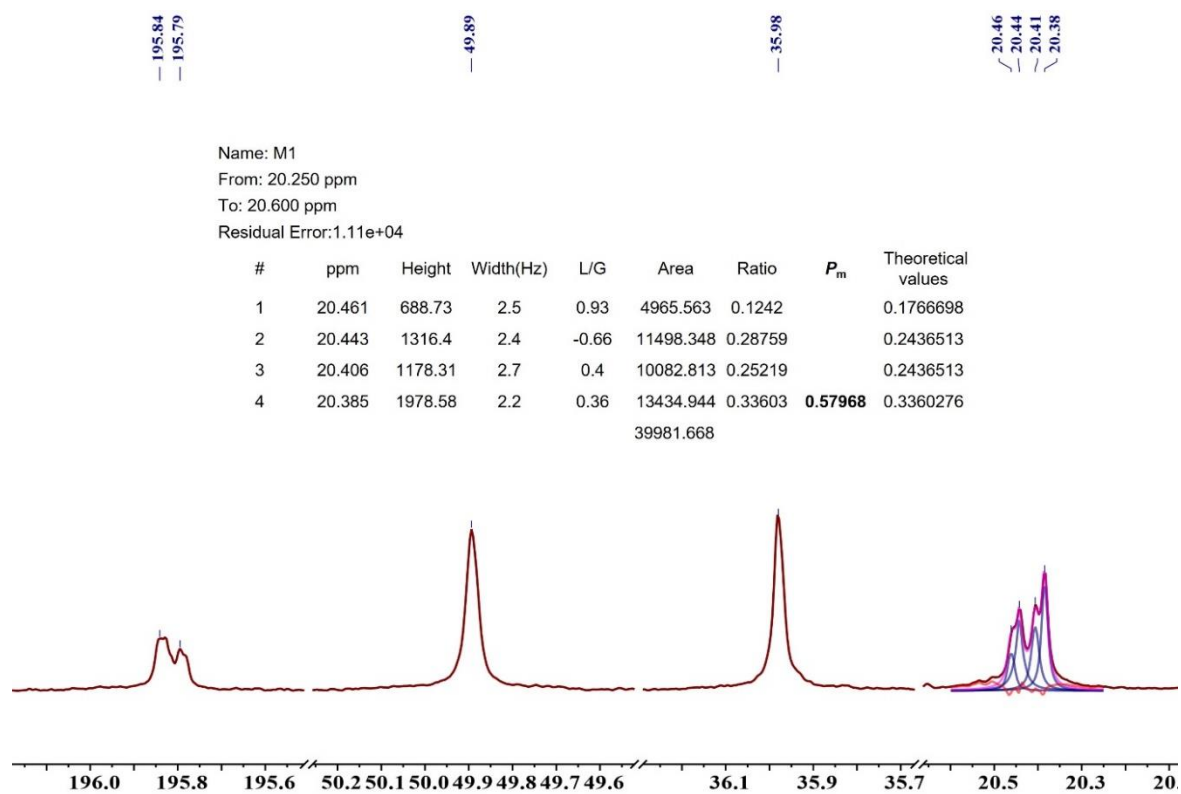


**Figure S49.** Carbonyl, methine, methylene and methyl regions of the  $^{13}\text{C}\{^1\text{H}\}$  NMR spectrum (125 MHz,  $\text{CDCl}_3$ , 25 °C) of an atactic cyclic P3TB (Table 2, entry 29).

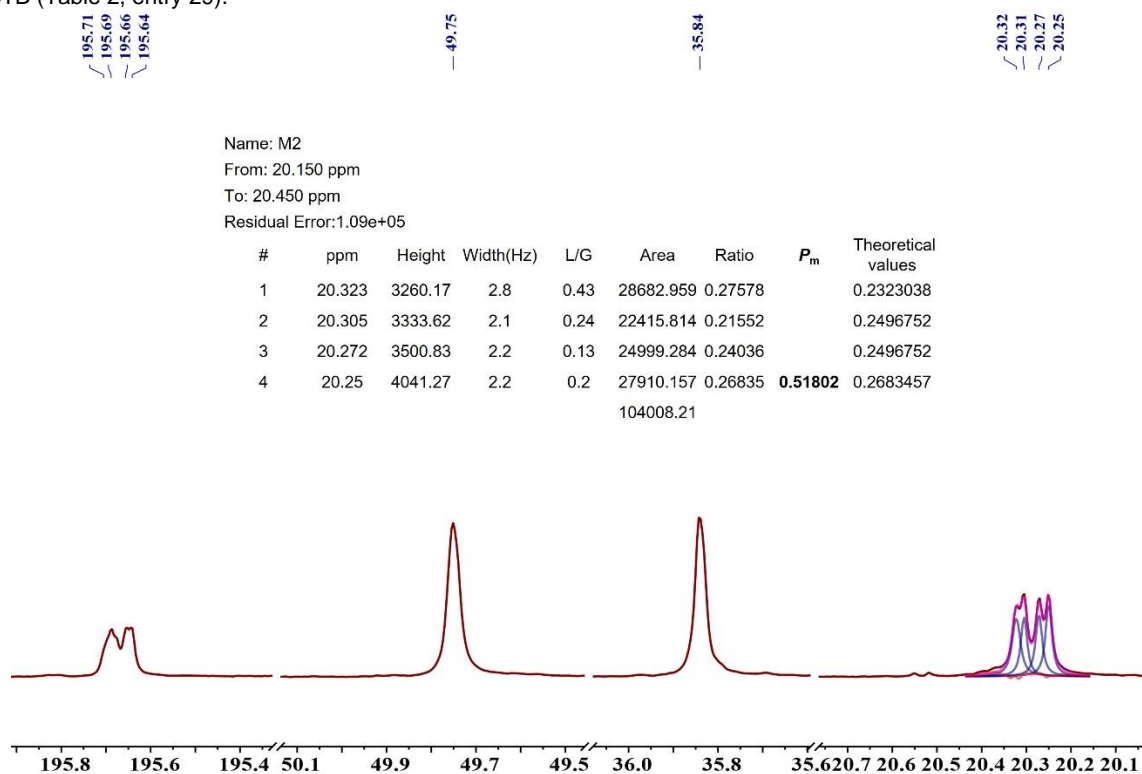


**Figure S50.** Carbonyl, methine, methylene and methyl regions of the  $^{13}\text{C}\{^1\text{H}\}$  NMR spectrum (125 MHz,  $\text{CDCl}_3$ , 25 °C) of an atactic cyclic P3TB (Table 2, entry 26).

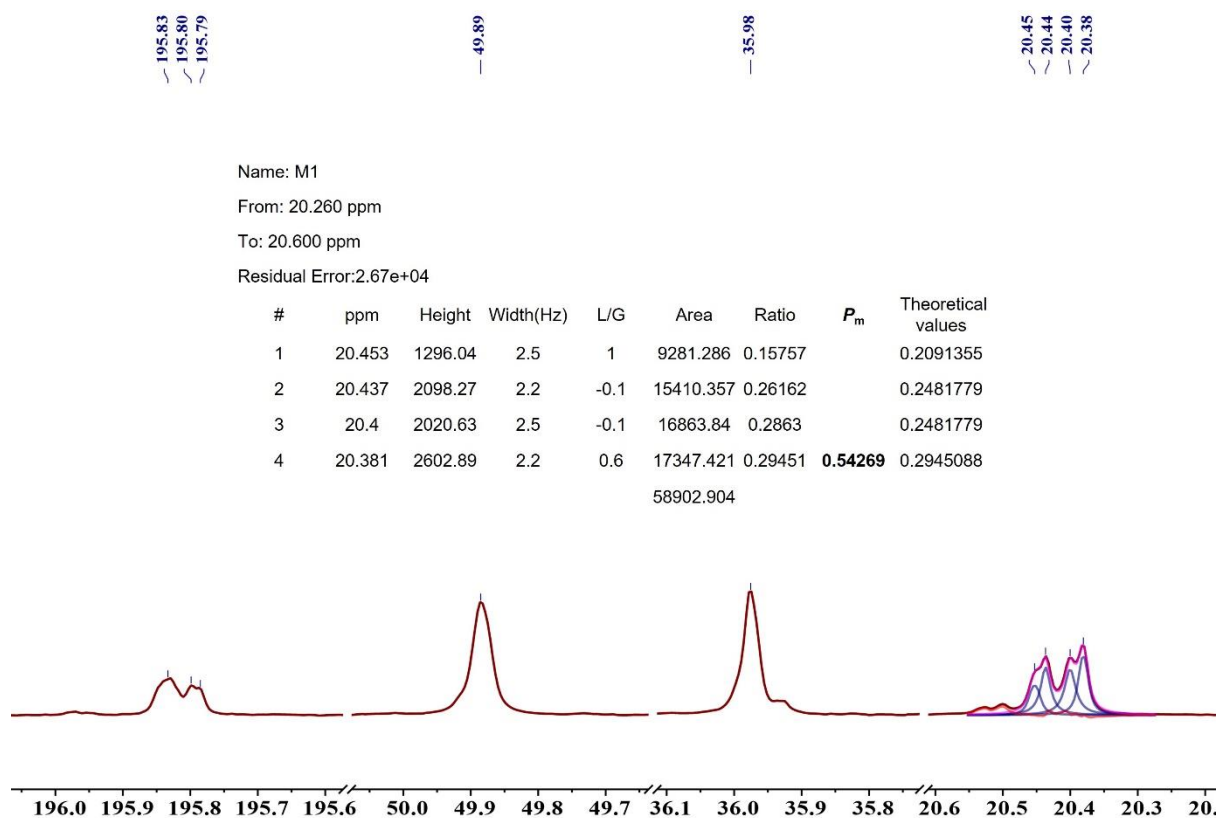


**Figure S51.** Carbonyl, methine, methylene and methyl regions of the  $^{13}\text{C}\{^1\text{H}\}$  NMR spectrum (125 MHz,  $\text{CDCl}_3$ , 25 °C) of an atactic cyclic P3TB (Table 2, entry 35).

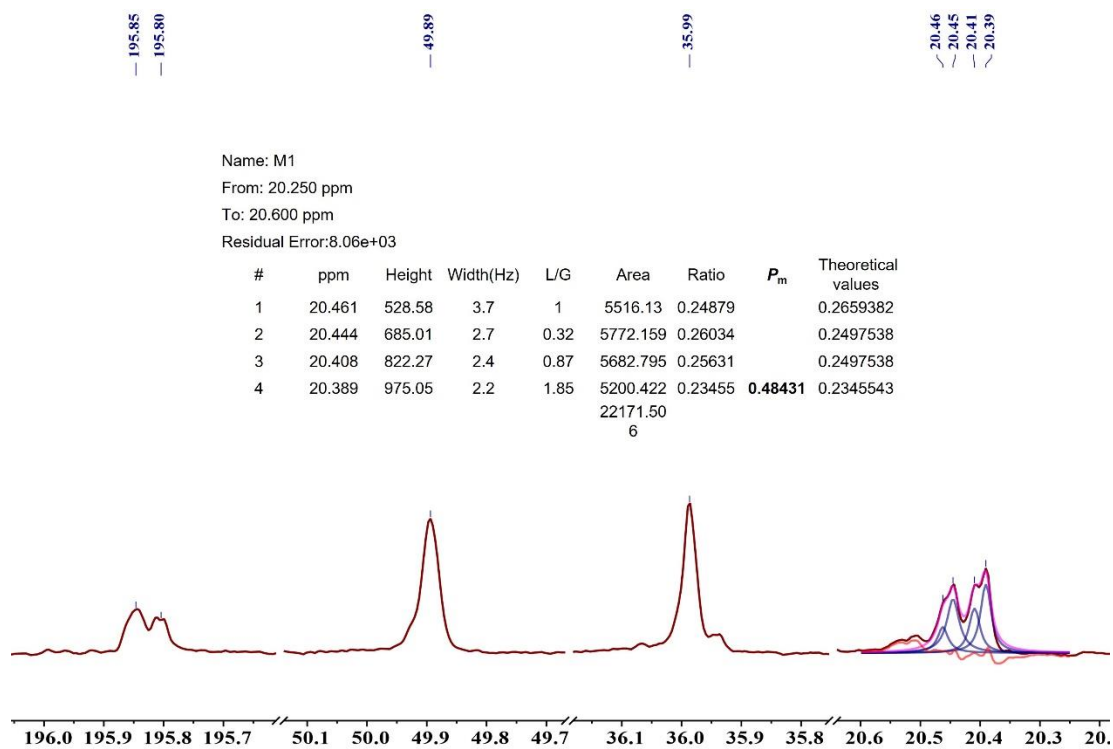


**Figure S52.** Carbonyl, methine, methylene and methyl regions of the  $^{13}\text{C}\{^1\text{H}\}$  NMR spectrum (125 MHz,  $\text{CDCl}_3$ , 25 °C) of an atactic cyclic P3TB (Table 1, entry 7).



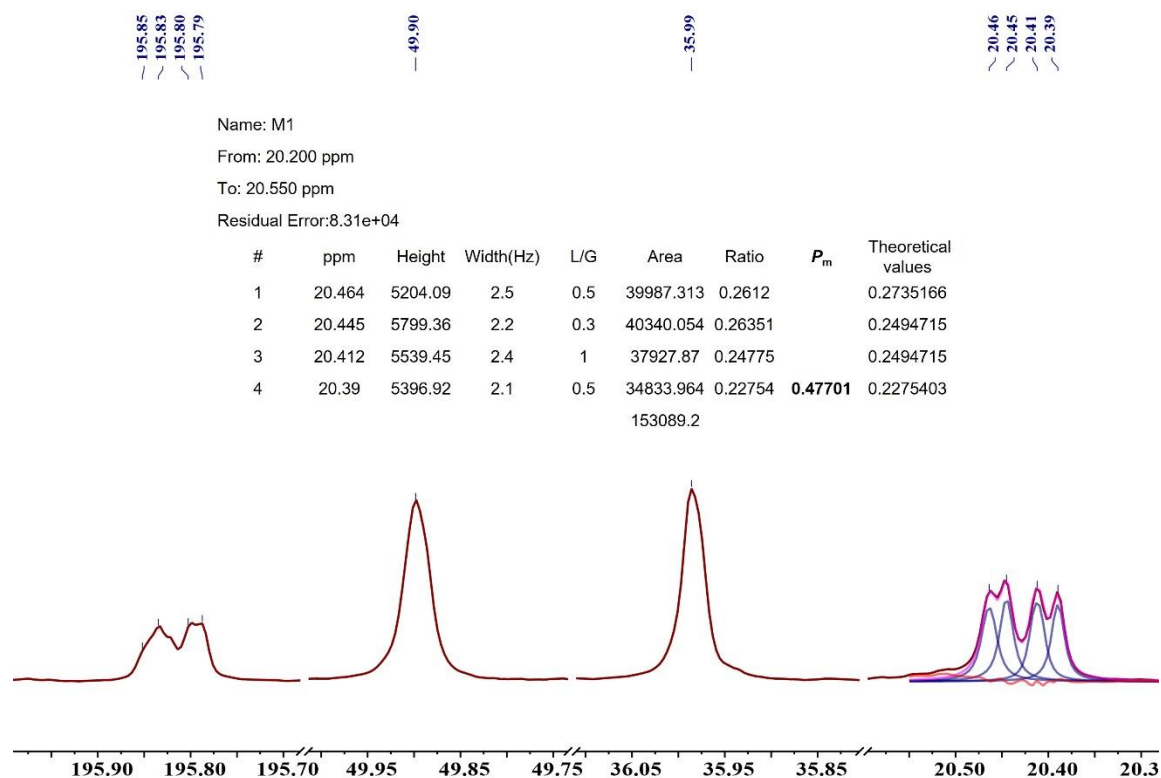


**Figure S53.** Carbonyl, methine, methylene and methyl regions of the  $^{13}\text{C}\{^1\text{H}\}$  NMR spectrum (125 MHz,  $\text{CDCl}_3$ , 25 °C) of an atactic cyclic P3TB (Table 2, entry 19).

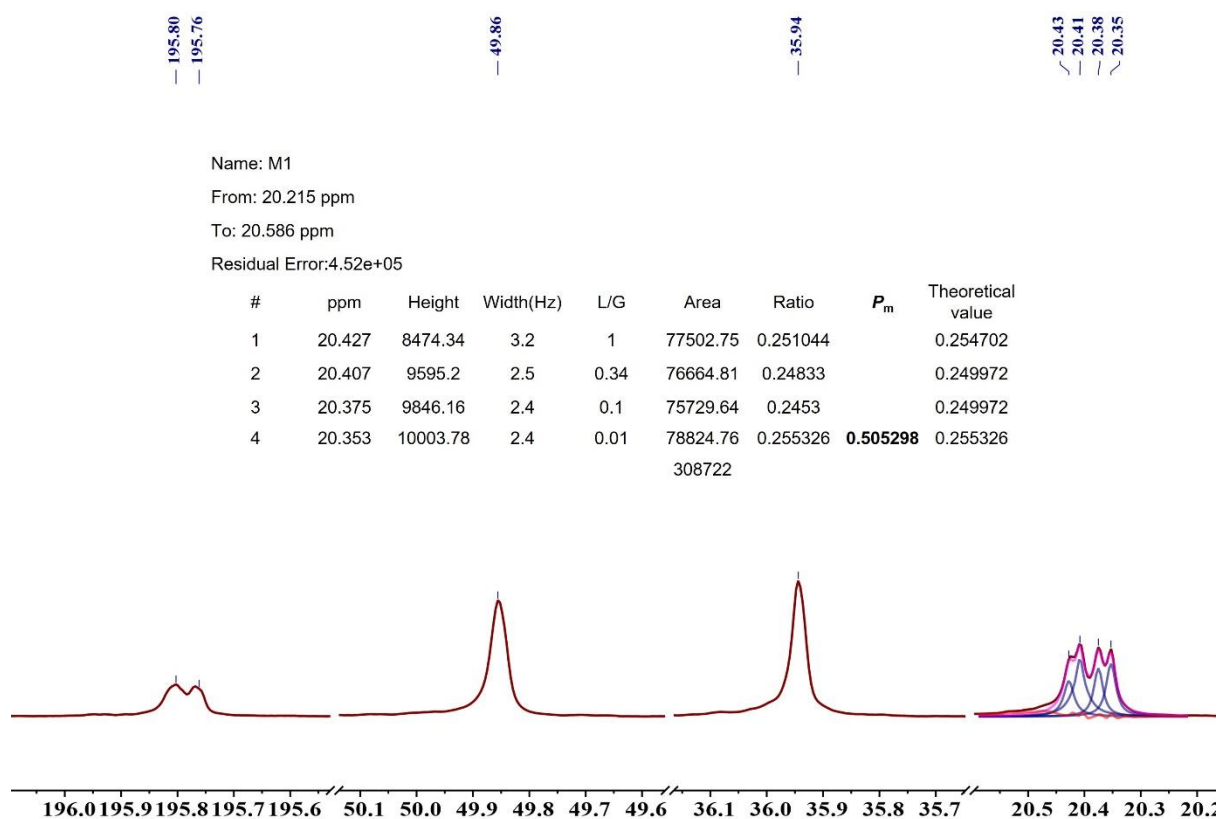


**Figure S54.** Carbonyl, methine, methylene and methyl regions of the  $^{13}\text{C}\{^1\text{H}\}$  NMR spectrum (125 MHz,  $\text{CDCl}_3$ , 25 °C) of an atactic cyclic P3TB (Table 1, entry 1).

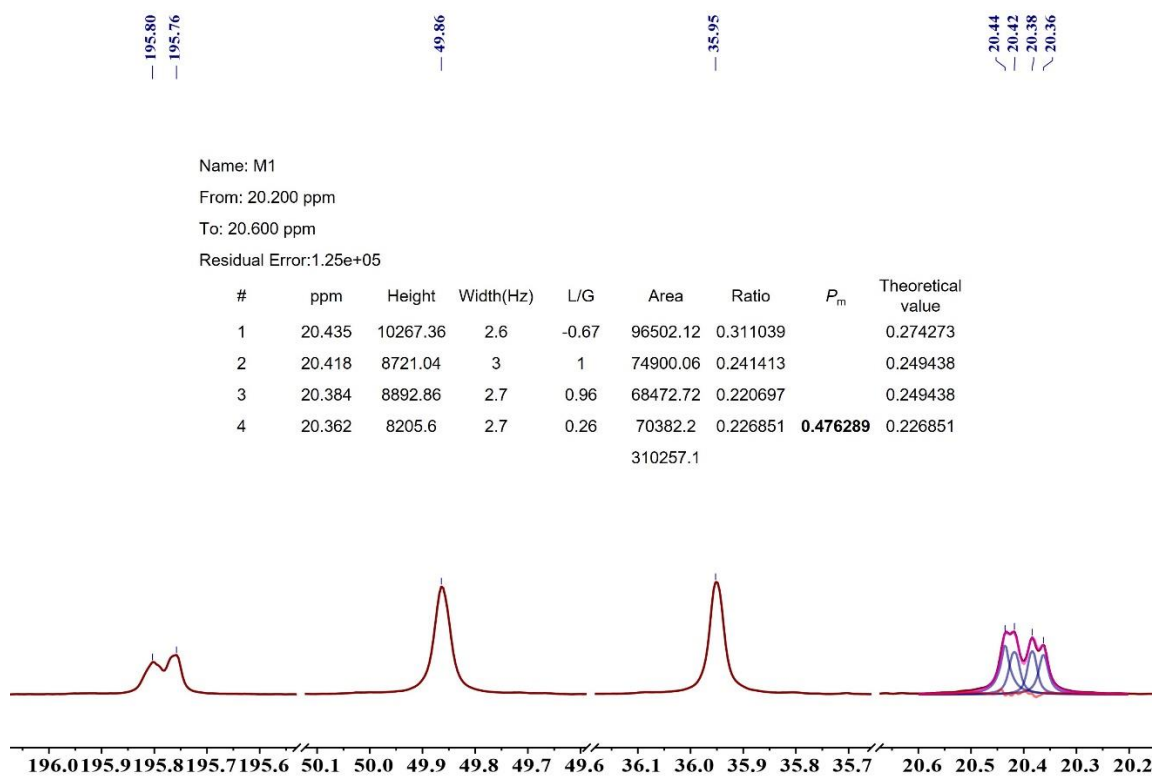


**Figure S55.** Carbonyl, methine, methylene and methyl regions of the  $^{13}\text{C}\{^1\text{H}\}$  NMR spectrum (125 MHz,  $\text{CDCl}_3$ , 25 °C) of an atactic cyclic P3TB (Table 1, entry 2).

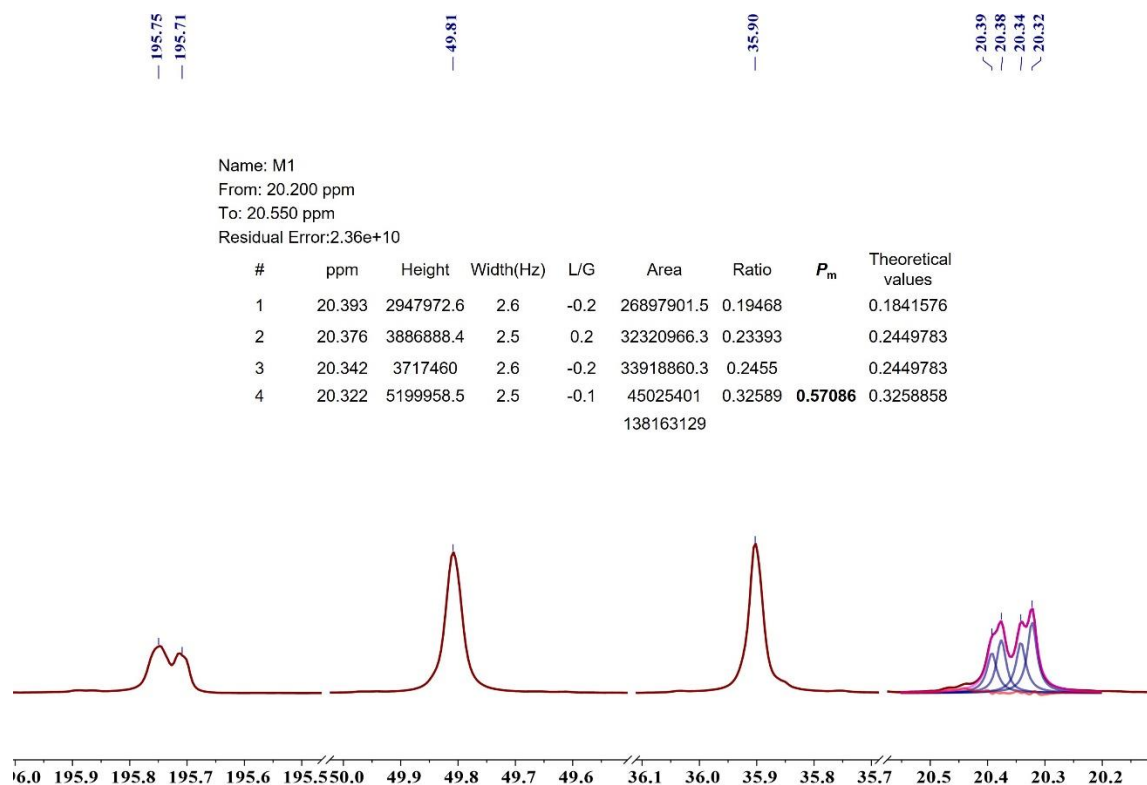


**Figure S56.** Carbonyl, methine, methylene and methyl regions of the  $^{13}\text{C}\{^1\text{H}\}$  NMR spectrum (125 MHz,  $\text{CDCl}_3$ , 25 °C) of an atactic cyclic P3TB (Table 2, entry 46).

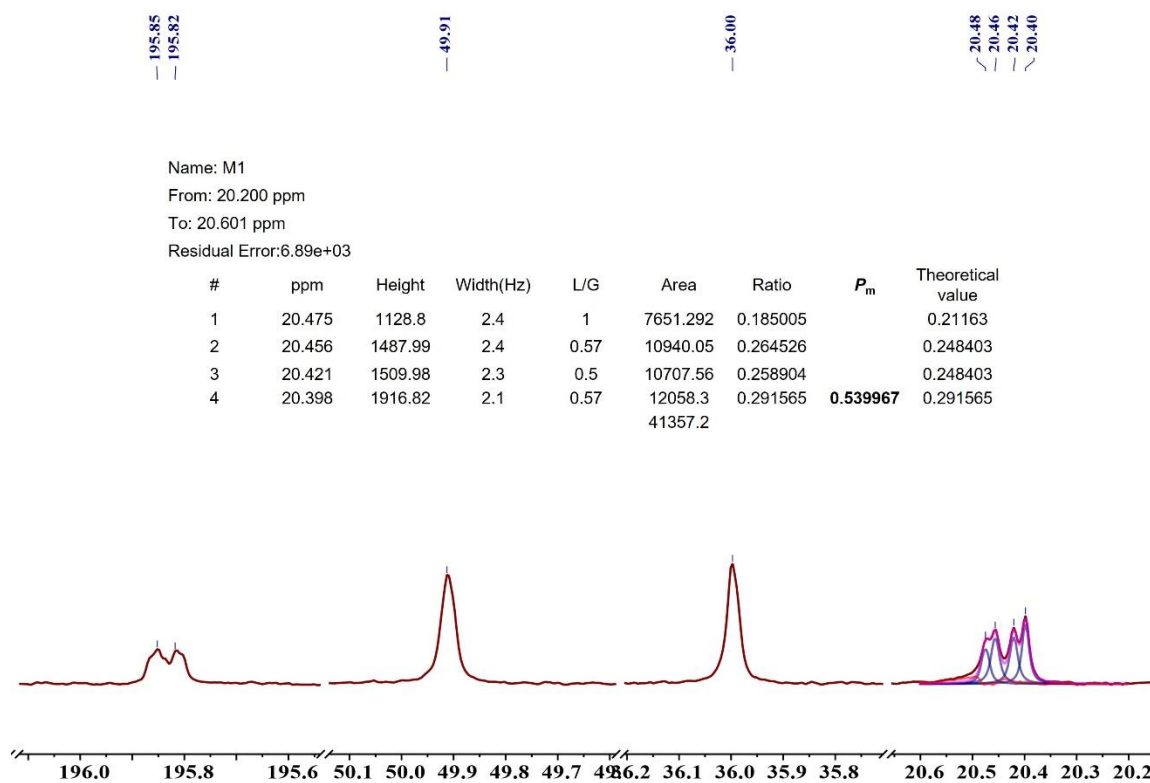


**Figure S57.** Carbonyl, methine, methylene and methyl regions of the  $^{13}\text{C}\{^1\text{H}\}$  NMR spectrum (125 MHz,  $\text{CDCl}_3$ , 25 °C) of an atactic cyclic P3TB (Table 1, entry 8).

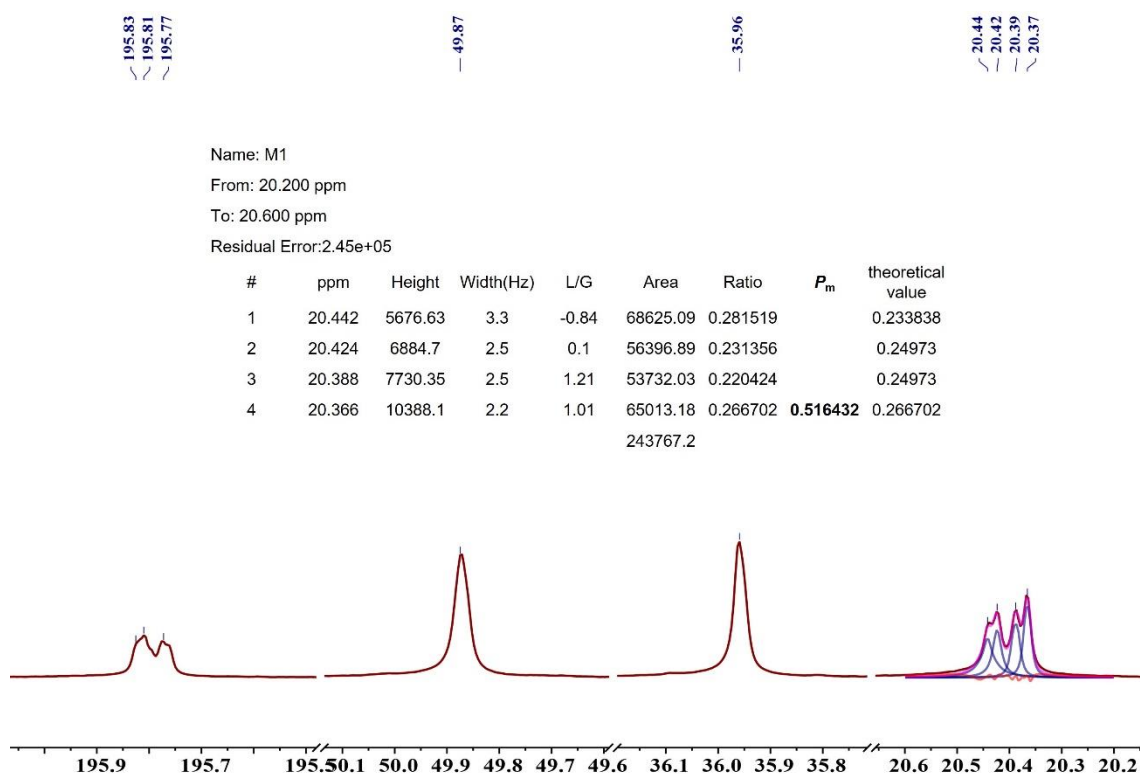


**Figure S58.** Carbonyl, methine, methylene and methyl regions of the  $^{13}\text{C}\{^1\text{H}\}$  NMR spectrum (125 MHz,  $\text{CDCl}_3$ , 25 °C) of an atactic cyclic P3TB (Table 1, entry 9).

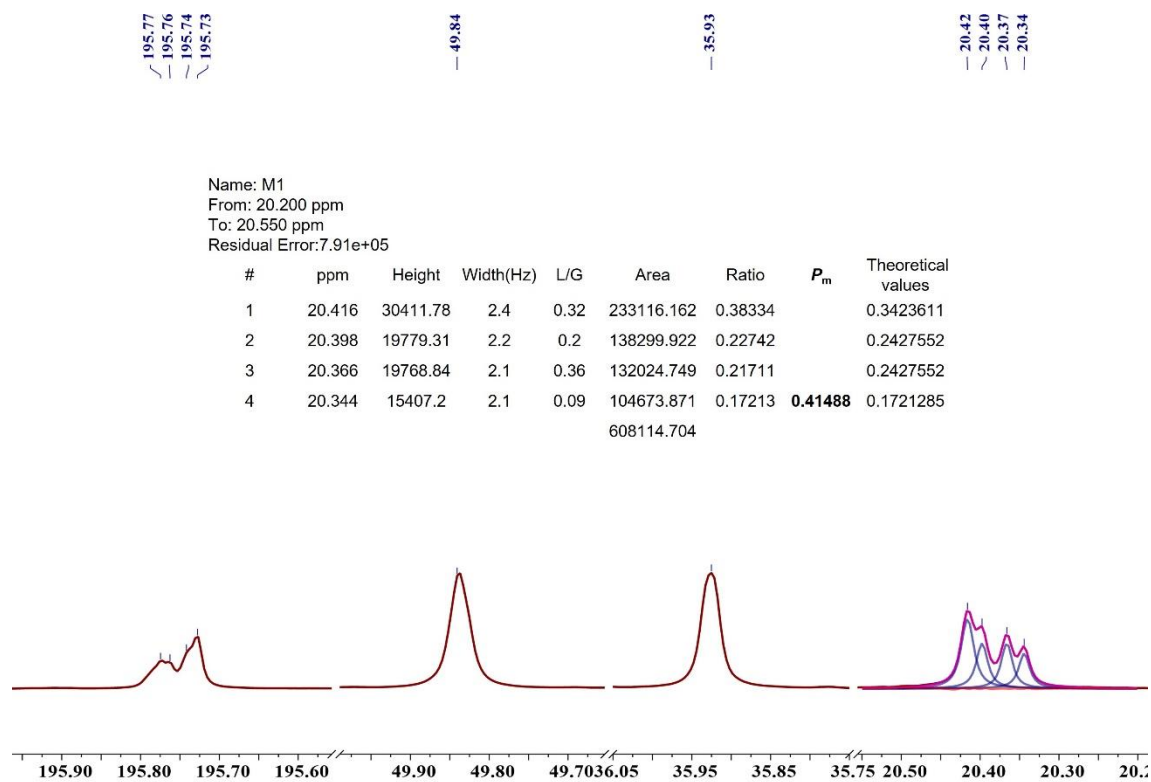


**Figure S59.** Carbonyl, methine, methylene and methyl regions of the  $^{13}\text{C}\{^1\text{H}\}$  NMR spectrum (125 MHz,  $\text{CDCl}_3$ , 25 °C) of an atactic cyclic P3TB (Table 2, entry 27).

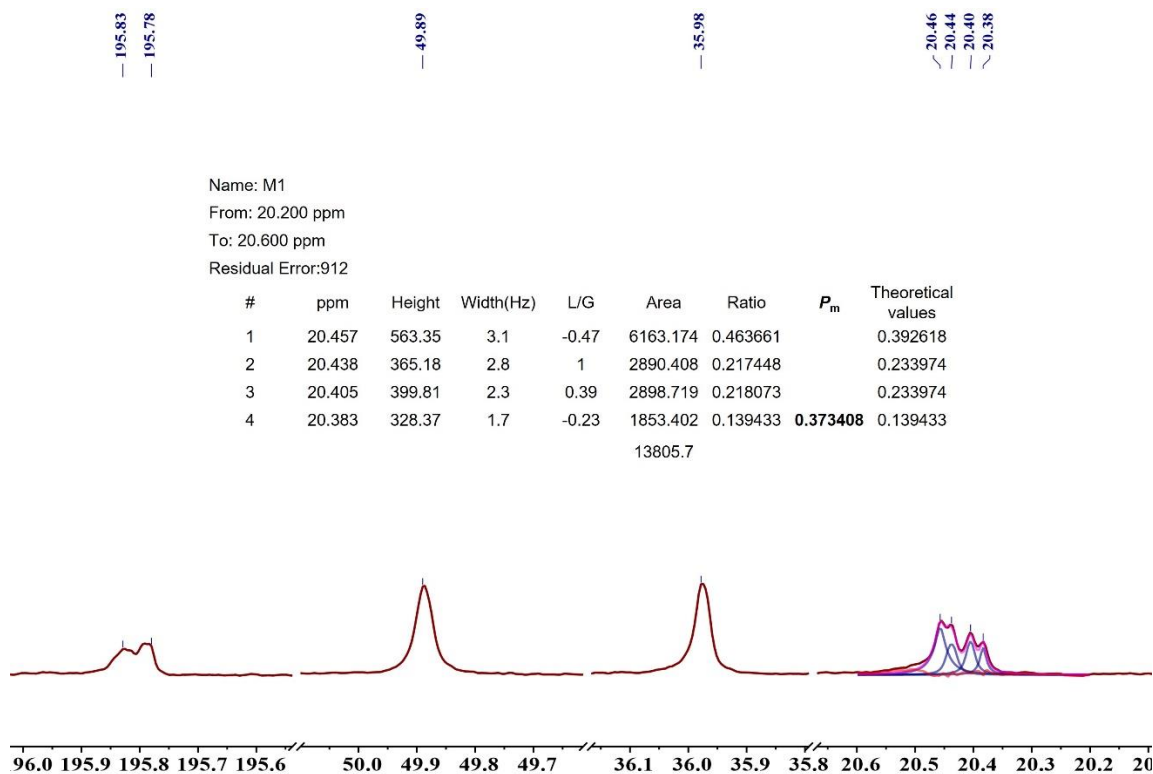


**Figure S60.** Carbonyl, methine, methylene and methyl regions of the  $^{13}\text{C}\{^1\text{H}\}$  NMR spectrum (125 MHz,  $\text{CDCl}_3$ , 25 °C) of a syndiotactic-biased cyclic P3TB (Table 1, entry 10).

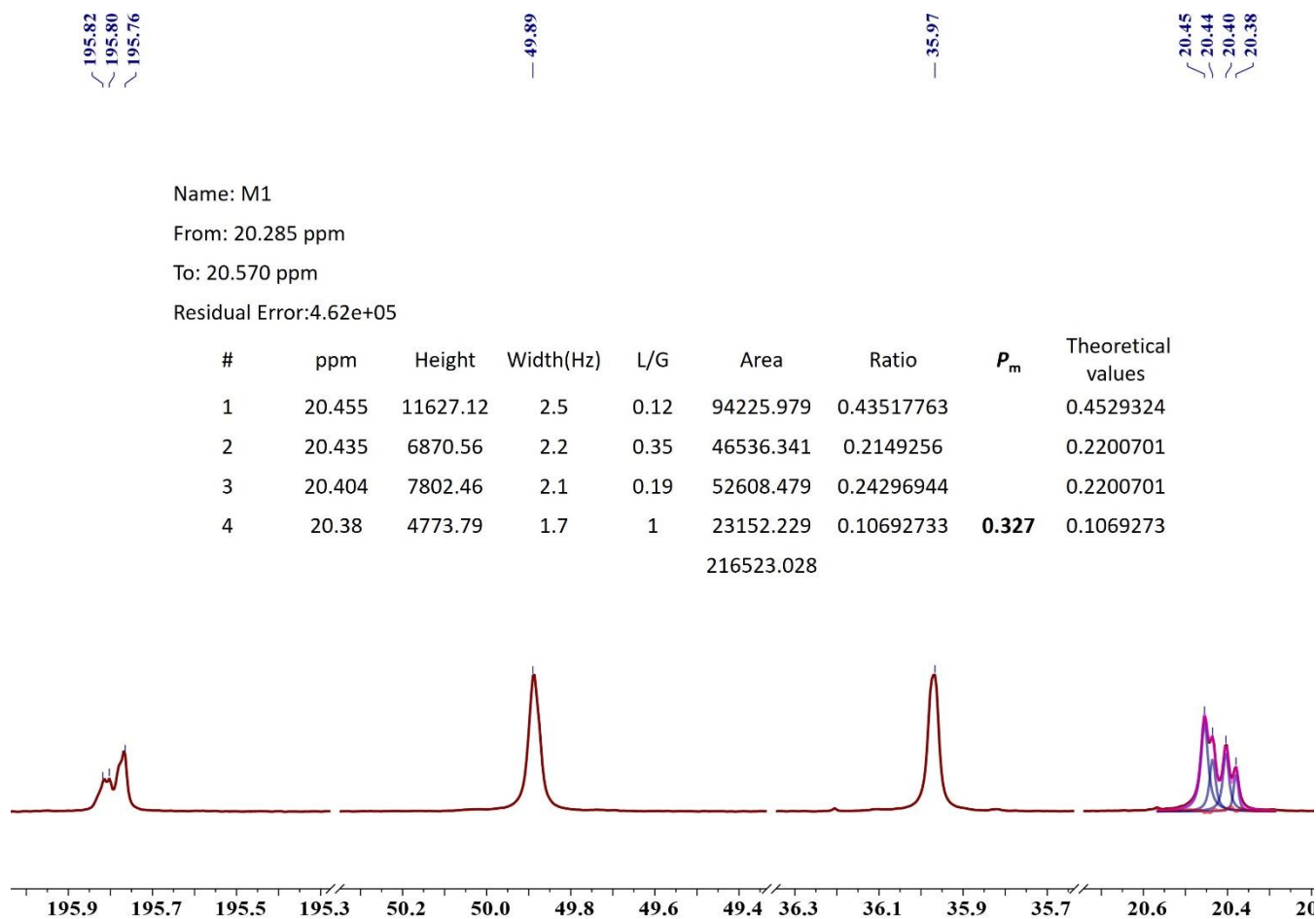


**Figure S61.** Carbonyl, methine, methylene and methyl regions of the  $^{13}\text{C}\{^1\text{H}\}$  NMR spectrum (125 MHz,  $\text{CDCl}_3$ , 25 °C) of a syndiotactic-biased cyclic P3TB (Table 2, entry 20).

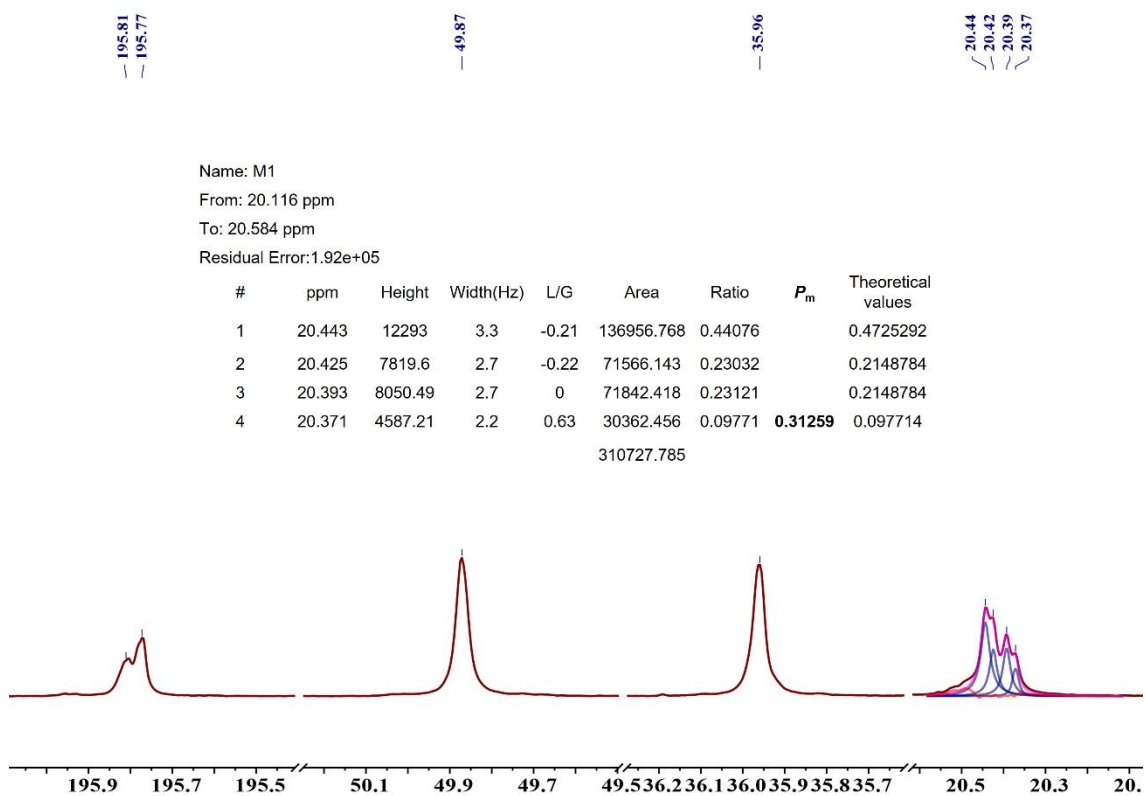


**Figure S62.** Carbonyl, methine, methylene and methyl regions of the  $^{13}\text{C}\{^1\text{H}\}$  NMR spectrum (125 MHz,  $\text{CDCl}_3$ , 25 °C) of a syndiotactic-enriched cyclic P3TB (Table 1, entry 11).

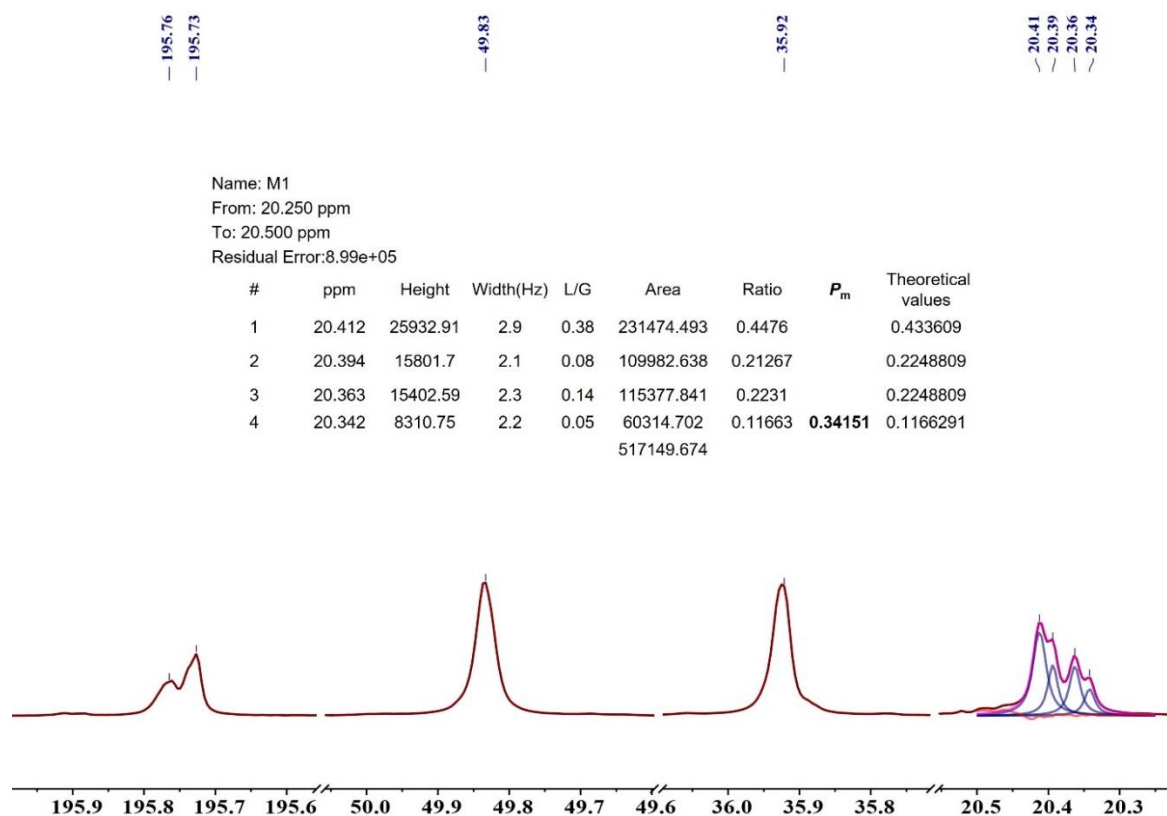


**Figure S63.** Carbonyl, methine, methylene and methyl regions of the  $^{13}\text{C}\{^1\text{H}\}$  NMR spectrum (125 MHz,  $\text{CDCl}_3$ , 25 °C) of a syndiotactic-enriched cyclic P3TB (Table 1, entry 12).

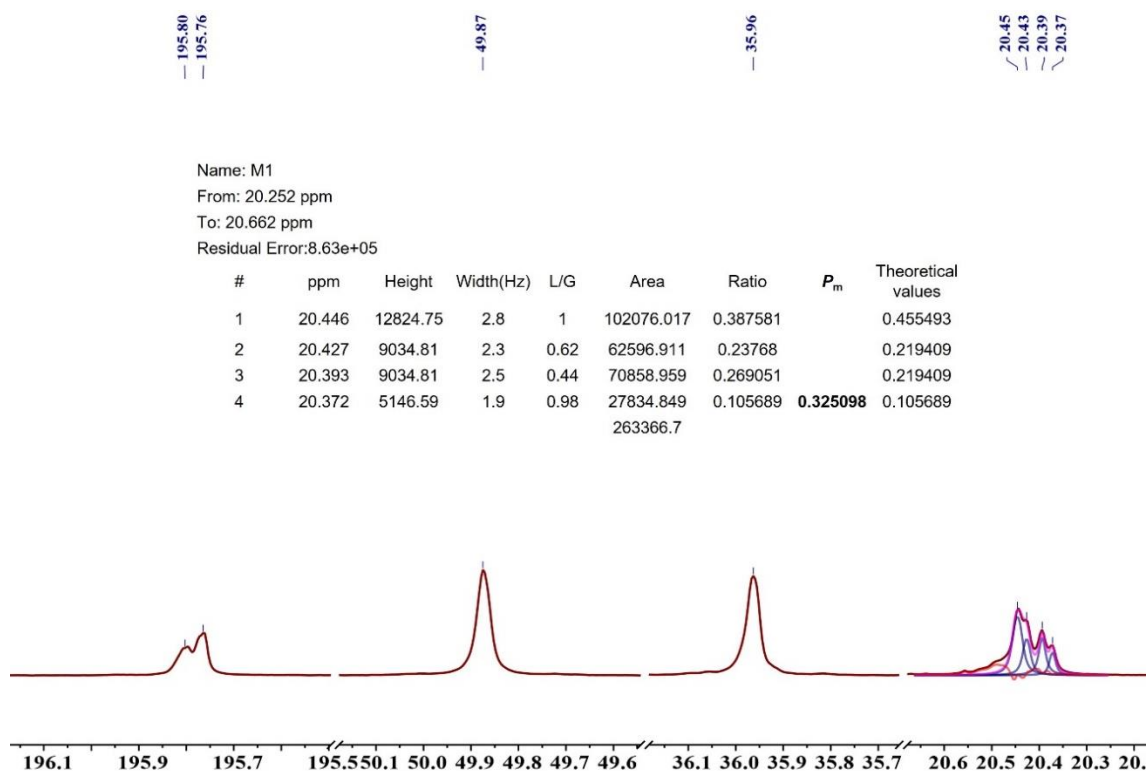


**Figure S64.** Carbonyl, methine, methylene and methyl regions of the  $^{13}\text{C}\{^1\text{H}\}$  NMR spectrum (125 MHz,  $\text{CDCl}_3$ , 25 °C) of a syndiotactic-enriched cyclic P3TB (Table 1, entry 13).

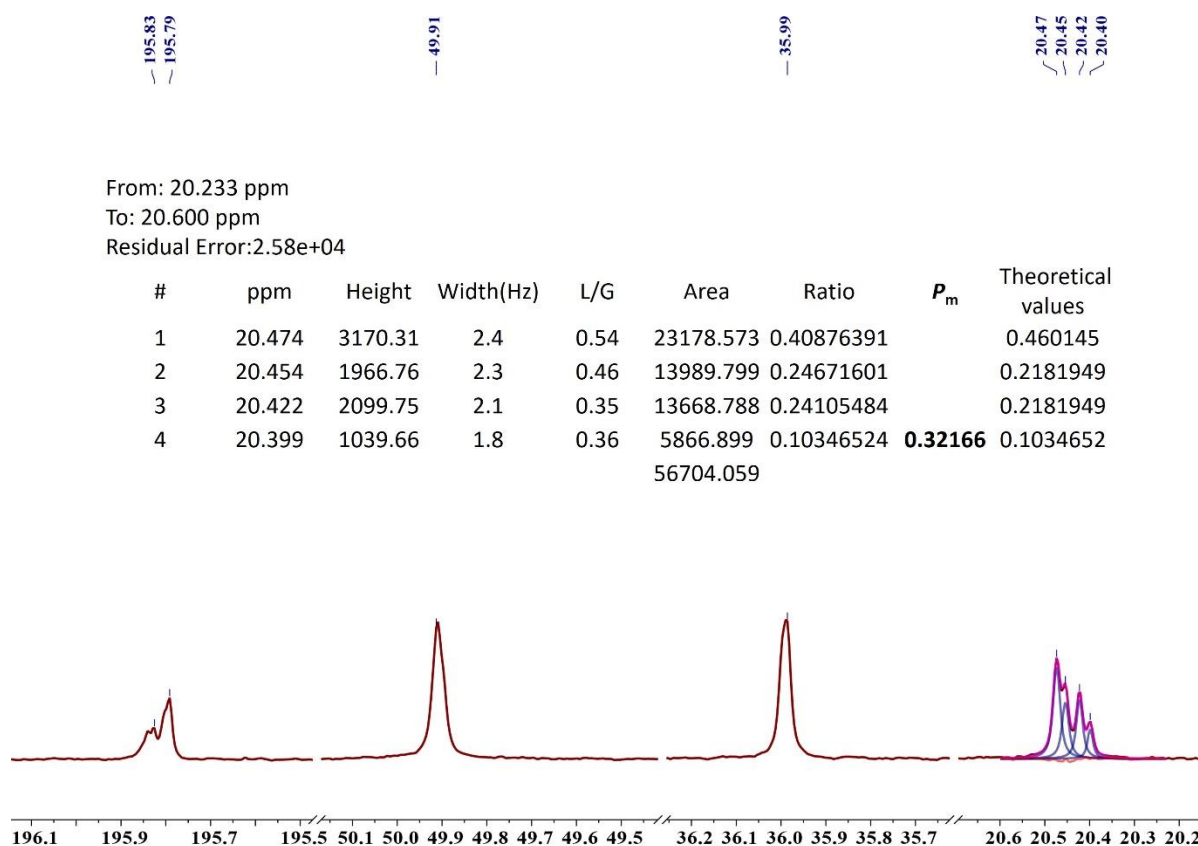


**Figure S65.** Carbonyl, methine, methylene and methyl regions of the  $^{13}\text{C}\{^1\text{H}\}$  NMR spectrum (125 MHz,  $\text{CDCl}_3$ , 25 °C) of a syndiotactic-enriched cyclic P3TB (Table 2, entry 25).



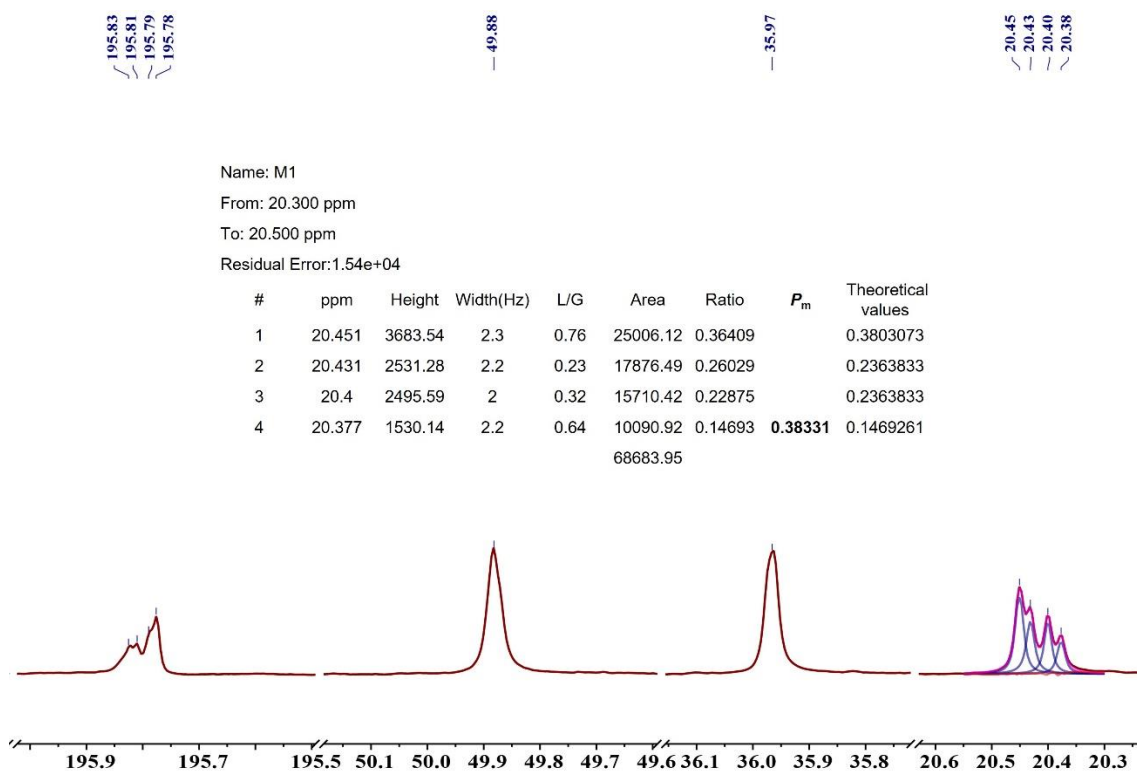


**Figure S66.** Carbonyl, methine, methylene and methyl regions of the  $^{13}\text{C}\{^1\text{H}\}$  NMR spectrum (125 MHz,  $\text{CDCl}_3$ , 25 °C) of a syndiotactic-enriched cyclic P3TB (Table 2, entry 17).

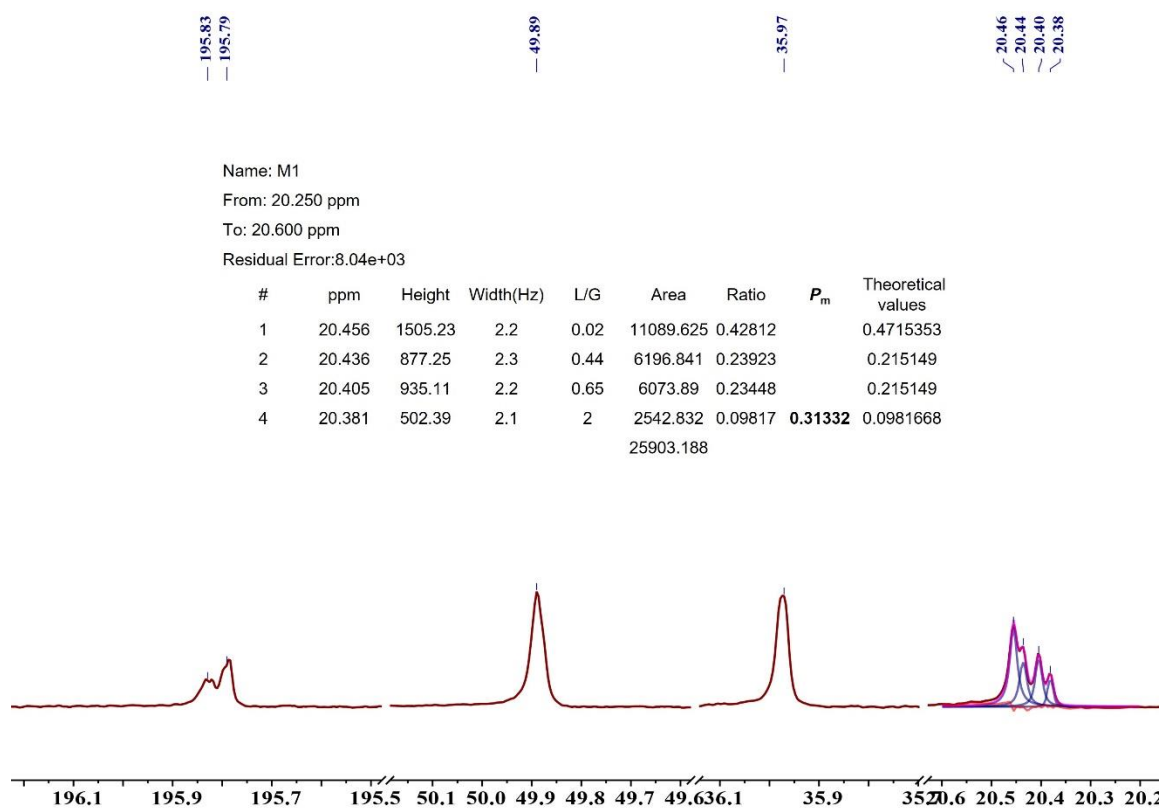


**Figure S67.** Carbonyl, methine, methylene and methyl regions of the  $^{13}\text{C}\{^1\text{H}\}$  NMR spectrum (125 MHz,  $\text{CDCl}_3$ , 25 °C) of a syndiotactic-enriched cyclic P3TB (Table S2, entry 10).



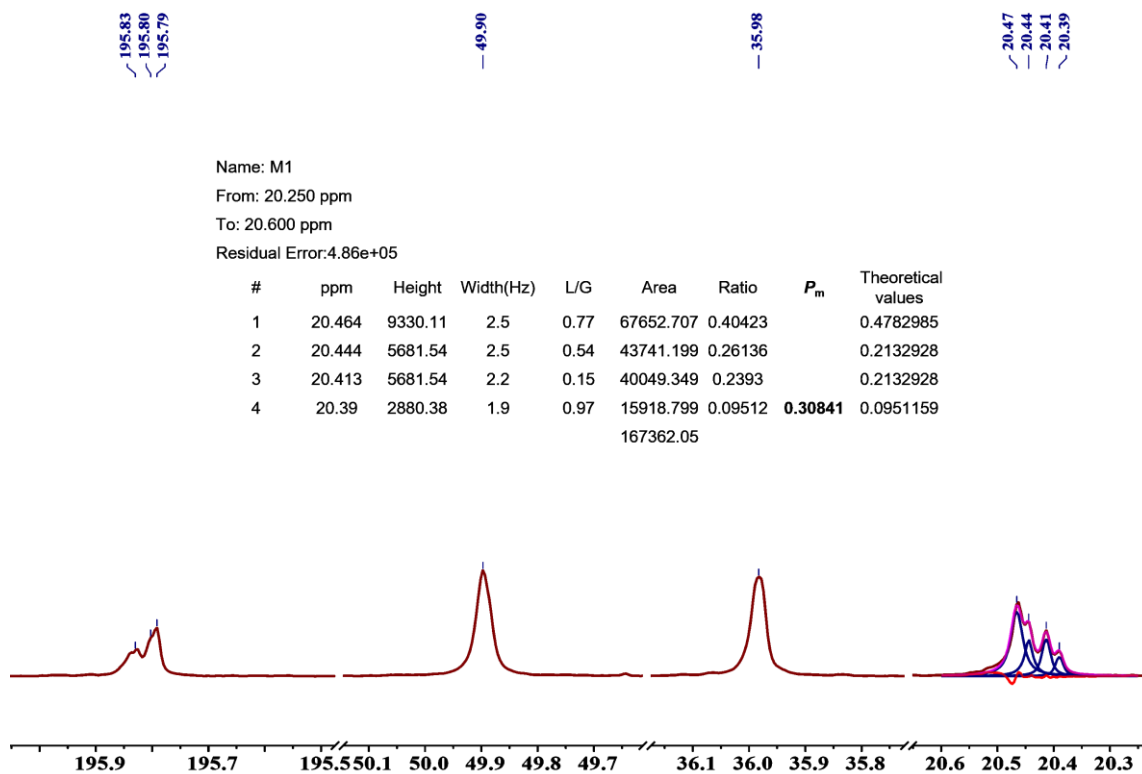


**Figure S68.** Carbonyl, methine, methylene and methyl regions of the  $^{13}\text{C}\{^1\text{H}\}$  NMR spectrum (125 MHz,  $\text{CDCl}_3$ , 25 °C) of a syndiotactic-enriched cyclic P3TB (Table 1, entry 15).

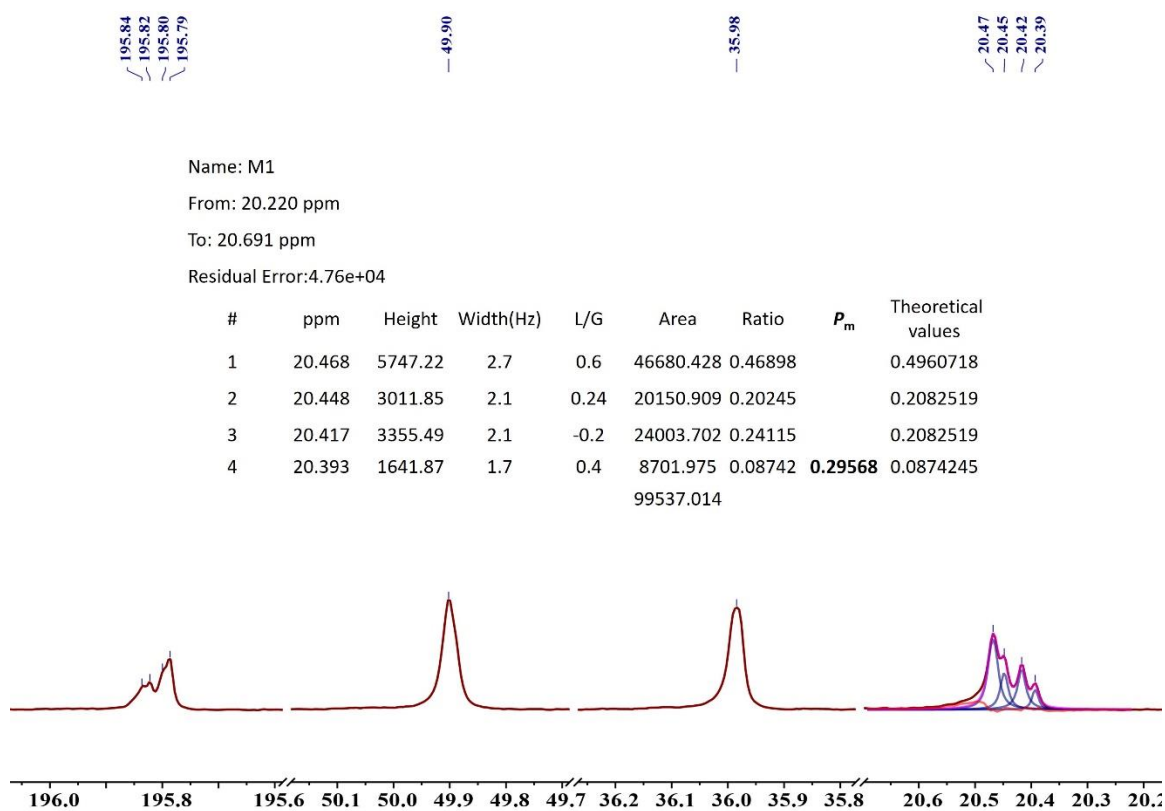


**Figure S69.** Carbonyl, methine, methylene and methyl regions of the  $^{13}\text{C}\{^1\text{H}\}$  NMR spectrum (125 MHz,  $\text{CDCl}_3$ , 25 °C) of a syndiotactic-enriched cyclic P3TB (Table 2, entry 24).

## Propagation Statistics

**Table S6.** Bernoulli model triad test  $B = [(mm) \times (rr)] / [(rm) \times (mr)]$

Entry	B
Table 2, entry 34 ( $P_m = 0.89$ ), <b>cat. 5g</b>	1.28
Table 2, entry 33 ( $P_m = 0.87$ ), <b>cat. 5g</b>	1.77
Table 2, entry 50 ( $P_m = 0.83$ ), <b>cat. 5l</b>	1.37
Table 2, entry 30 ( $P_m = 0.73$ ), <b>cat. 5g</b>	1.35
Table 2, entry 47 ( $P_m = 0.72$ ), <b>cat. 5k</b>	0.53
Table 1, entry 14 ( $P_m = 0.32$ ), <b>cat. 5a</b>	1.03
Table 1, entry 11 ( $P_m = 0.32$ ), <b>cat. 5a</b>	0.81
Table 2, entry 24 ( $P_m = 0.30$ ), <b>cat. 5c</b>	0.84

## Thermal studies

### TGA thermograms

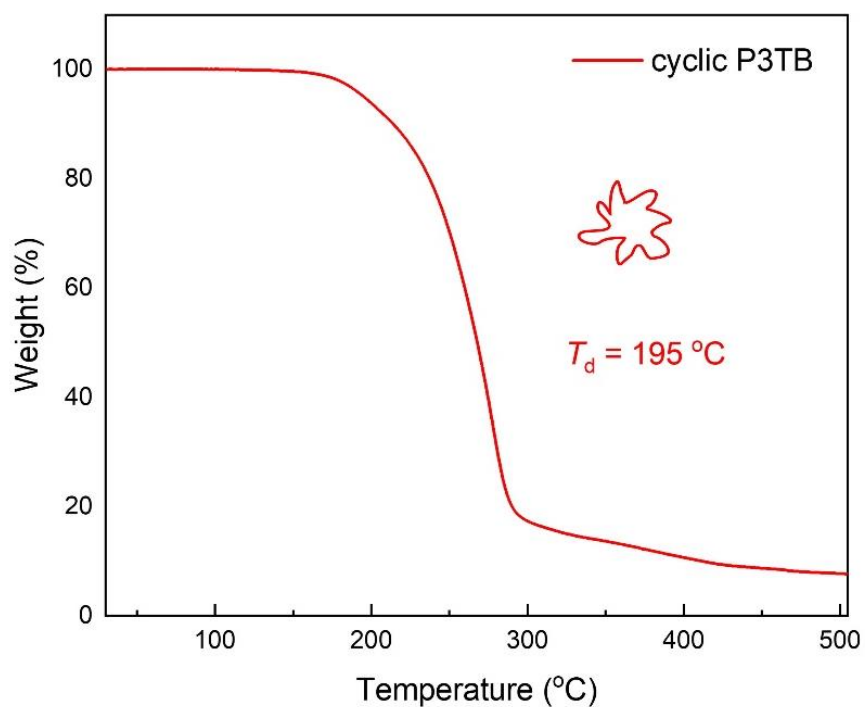


**Figure S70.** TGA thermogram of a cyclic P3TB sample prepared from complex **5a** in the presence of <sup>i</sup>PrOH in toluene at r.t. (50:1:1,  $M_{n,SEC} = 6.1\text{ kg mol}^{-1}$ ,  $P_m = 0.32$ ; entry 12).

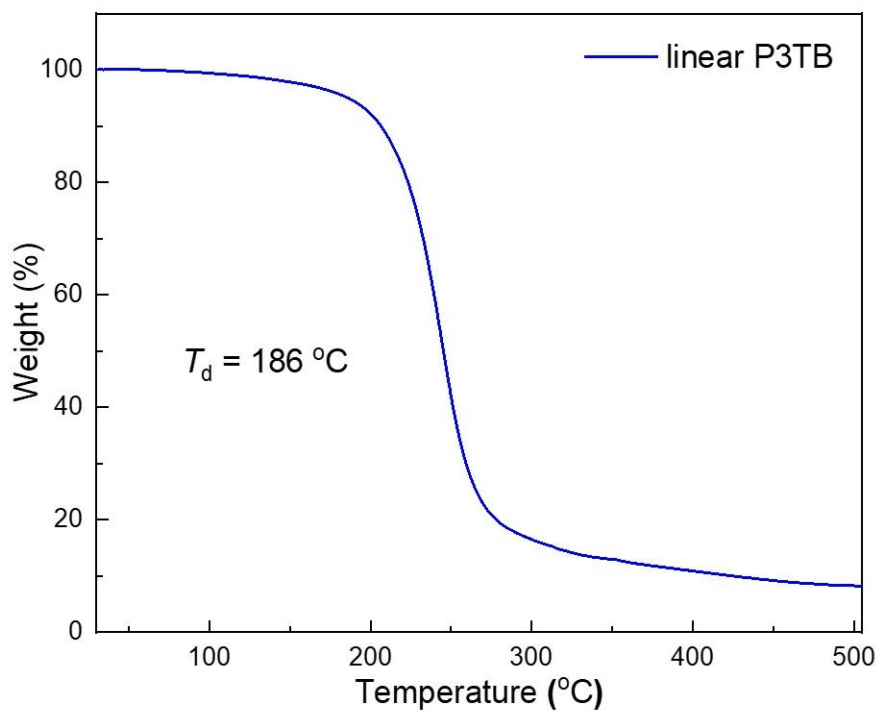


**Figure S71.** TGA thermogram of a linear P3TB sample prepared from NaOMe in the C6D6 at r.t. (23:1,  $M_{n,SEC} = 4.0\text{ kg mol}^{-1}$ ,  $P_m = 0.50$ ; entry 1).

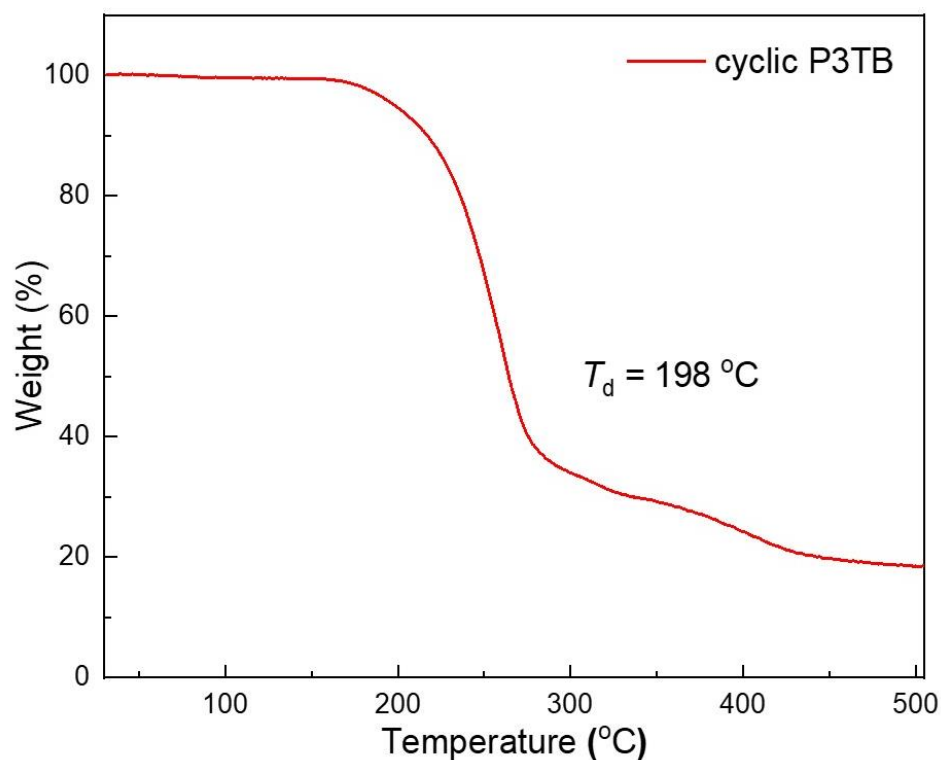


**Figure 72.** TGA thermogram of a cyclic P3TB sample prepared from complex **5a** in the absence of *i*PrOH in toluene at r.t. (25:1:0,  $M_{n,SEC} = 4.9\text{ kg mol}^{-1}$ ,  $P_m = 0.37$ ; entry 10).

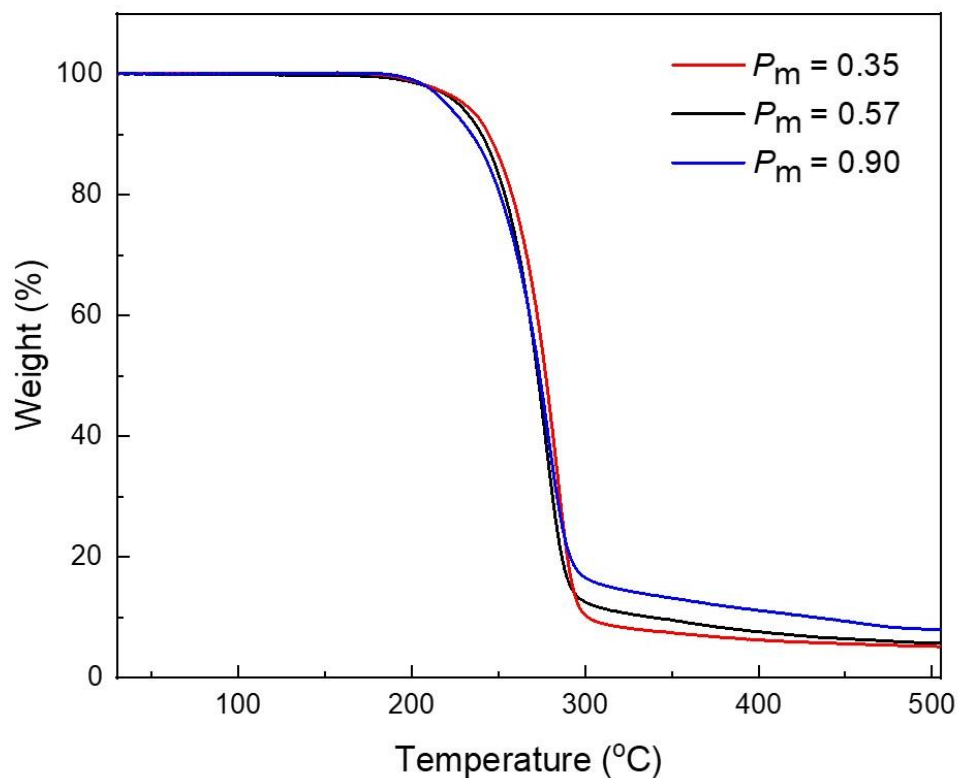


**Figure 73.** TGA thermogram of syndiotactic, atactic, isotactic cyclic P3TB samples with different stereoregularity but comparable molar mass (Table 2, entries 21, 36 and 48).

## DSC curves

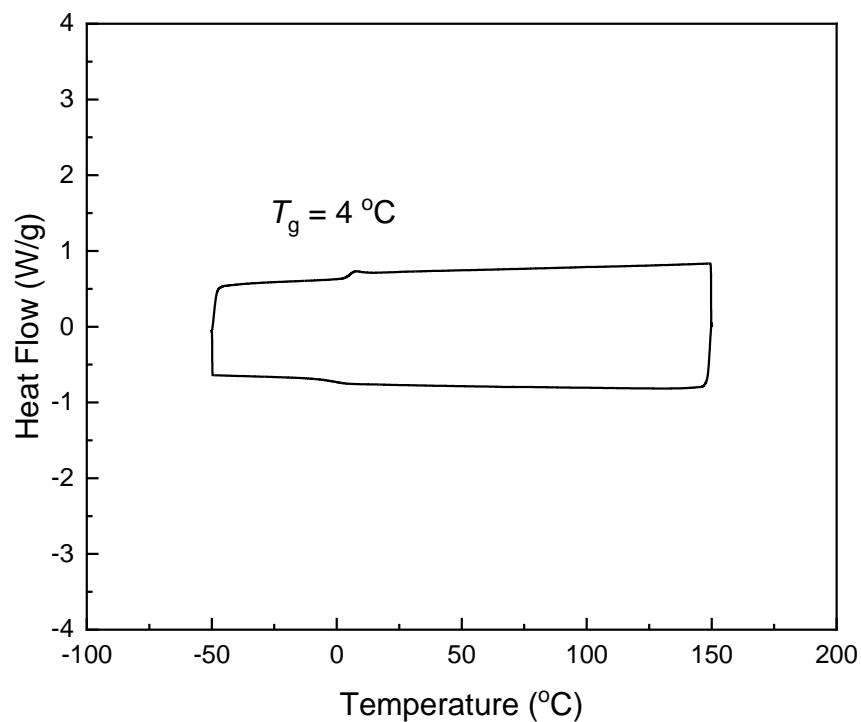


**Figure 74.** DSC curve of an isolated syndiotactic-enriched cyclic P3TB (Table 2, entry 24,  $P_m = 0.30$ ) (heating rate =  $10\text{ °C min}^{-1}$ , cooling rate =  $10\text{ °C min}^{-1}$ ).

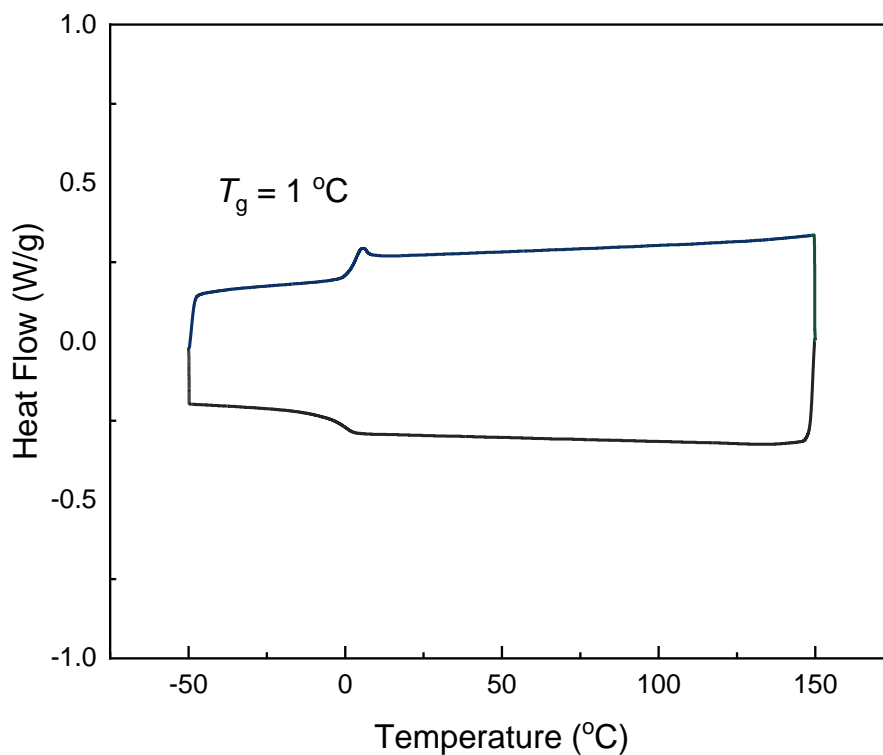


**Figure 75.** DSC curve of an isolated isotactic-enriched cyclic P3TB (Table 2, entry 30,  $P_m = 0.73$ ) (heating rate =  $10\text{ °C min}^{-1}$ , cooling rate =  $10\text{ °C min}^{-1}$ ).

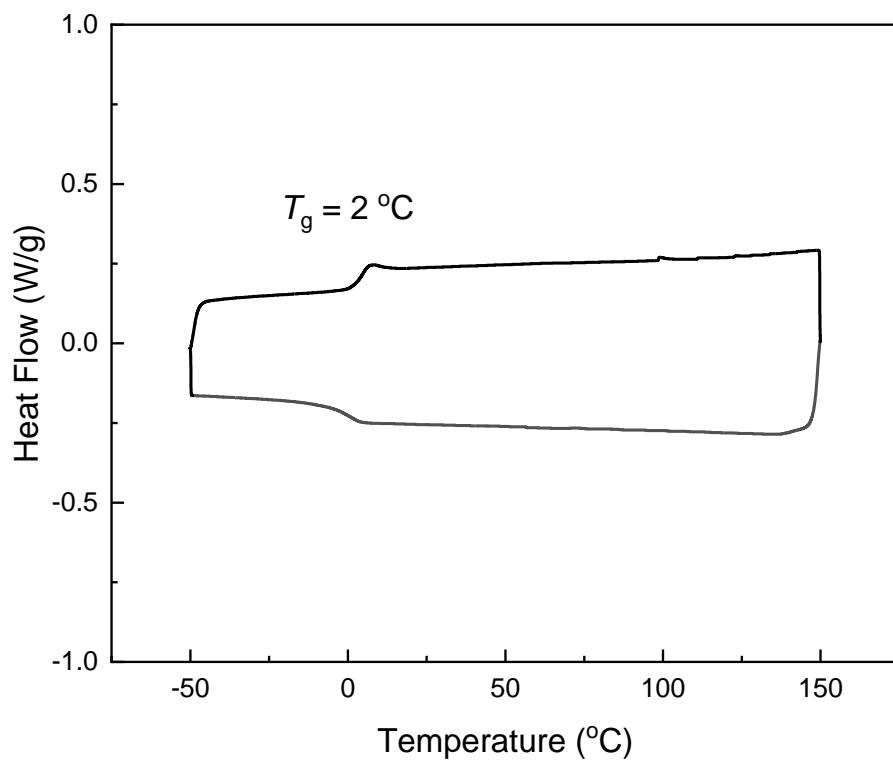


**Figure 76.** DSC curve of an isolated atactic cyclic P3TB (Table 2 entry 28,  $P_m = 0.52$ ) (heating rate =  $10\text{ °C min}^{-1}$ , cooling rate =  $10\text{ °C min}^{-1}$ ).

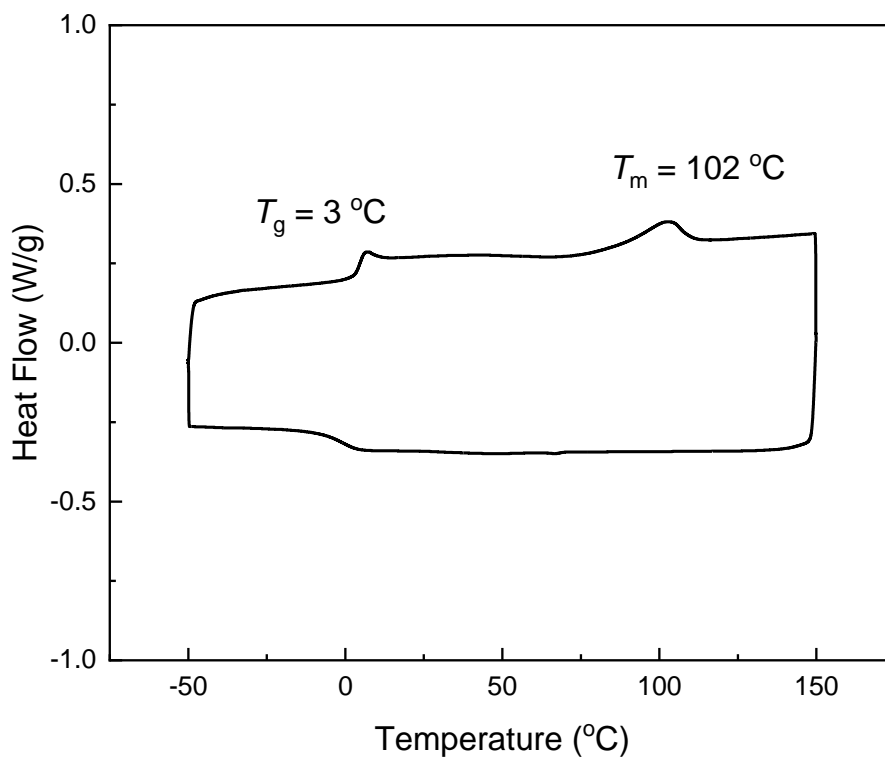


**Figure 77.** DSC curve of an isolated isotactic-enriched cyclic P3TB (Table 2, entry 33,  $P_m = 0.87$ ) (heating rate =  $10\text{ °C min}^{-1}$ , cooling rate =  $10\text{ °C min}^{-1}$ ).

## Structural parameters of $\beta$ -thiobutyrolactone vs. $\beta$ -butyrolactone

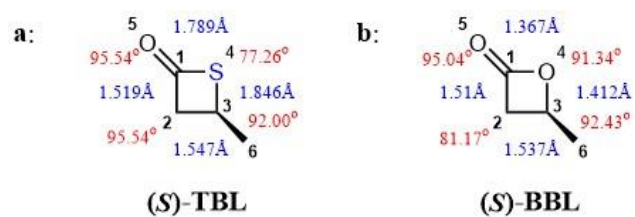


**Figure 78.** Structural parameters of (a) (S)-TBL (see: Yu. A. Borisov, A. F. Kolomiets, A. V. Fokin, The Structure and CH-Acidity of  $\text{CF}_3$ -Substituted  $\beta$ -Thiolactones. A Theoretical Study, *Russ. Chem. Bull.* **1998**, 47, 1670-1676) and (b) (S)-BBL (calculated from Chem3D).

## References

- [1] a) Y. Lu, J. H. Swisher, T. Y. Meyer, G. W. Coates, *J. Am. Chem. Soc.* **2021**, *143*, 4119-4124. b) M. Cheng, A. B. Attygalle, E. B. Lobkovsky, G. W. Coates, *J. Am. Chem. Soc.* **1999**, *121*, 11583-11584. c) J. W. Kramer, D. S. Treitler, E. W. Dunn, P. M. Castro, T. Roisnel, C. M. Thomas, G. W. Coates, *J. Am. Chem. Soc.* **2009**, *131*, 16042-16044. d) E. Y. Tshuva, I. Goldberg, M. Kol, Z. Goldschmidt, *Organometallics* **2001**, *20*, 3017-3028. e) T. Toupance, S. R. Dubberley, N. H. Rees, B. R. Tyrrell, P. Mountford, *Organometallics* **2002**, *21*, 1367-1382. f) X. Liu, X. Shang, T. Tang, N. Hu, F. Pei, D. Cui, X. Chen, X. Jing, *Organometallics* **2007**, *26*, 2747-2757. g) A. Amgoune, C. M. Thomas, T. Roisnel, J.-F. Carpentier, *Chem. Eur. J.* **2006**, *12*, 169-179.
- [2] J. B. Zhu, E. Y.-X. Chen, *Angew. Chem. Int. Ed.* **2019**, *58*, 1178-1182; *Angew. Chem.* **2019**, *131*, 1190-1194.
- [3] M. Yuan, D. Zhitomirsky, V. Adinolfi, O. Voznyy, K. W. Kemp, Z. Ning, X. Lan, J. Xu, J. Y. Kim, H. Dong, E. H. Sargent, *Adv. Mater.* **2013**, *25*, 5586-5592.
- [4] a) M. G. Lin'kova, I. L. Knunyants, *Bull. Acad. Sci. USSR, Div. Chem. Sci.* **1968**, *17*, 1796-1797. b) H. B. Lee, H. Y. Park, B.-S. Lee, Y. G. Kim, *Magn. Res. Chem.* **2000**, *38*, 468-471.
- [5] J. W. Kramer, E. B. Lobkovsky, G. W. Coates, *Org. Lett.* **2006**, *8*, 3709-3712.
- [6] (a) A. Griesbeck, D. Seebach, *Helv. Chim. Acta* **1987**, *70*, 1326-1332. (b) R. Breitschuh, D. Seebach, *Synthesis* **1992**, 83-89.

## Author Contributions

J.-F. C and S. M. G. are co-leading this project. H. L. designed and conducted experiments related to monomer, catalysts, polymer synthesis, as well as polymer characterizations, and J. O. performed experiments related to mass spectrometry and thermal analysis. H. L. and J.-F. C. wrote the initial manuscript draft, S. M. G. revised subsequent versions of the manuscript, and all authors contributed to the revised manuscript.